

**The Potential neuroprotective effect of Manuka Honey in Sprague-Dawley rats with
Lipopolysaccharide induced neuronal injury**

By

Victoria Sue Verrall

15048200

Submitted in partial fulfilment of the requirements for the degree of

Master of Sciences

(MSc)

Department of Physiology

Faculty of Health Sciences

University of Pretoria

South Africa

Supervisor: **Dr J Bester**

Co-supervisor: **Dr J Serem**

2021

Abstract

Alzheimer's type dementia is the most common form of dementia and is a large contributor to mortality in the aging and geriatric populations. It is associated with amyloid plaque formation, neurofibrillary tangles, neuro-inflammation and memory loss. There appears to be a causal link between the neuro-inflammation and other pathological processes associated with the development of Alzheimer's type dementia and gastrointestinal presence of lipopolysaccharide (LPS), a component of the outer cellular membrane of Gram-negative bacteria. In addition to this, there is sufficient evidence suggesting honey as a possible treatment or preventative measure against inflammation and, therefore, against the neuro-inflammation associated with LPS and Alzheimer's type dementia.

In the current study, LPS derived from *Escherichia coli* (*E. coli*) was chosen based on the increased prevalence of *E. coli* infections in South Africa, and Manuka honey was chosen as a treatment against LPS due to its proven therapeutic use and wide use in scientific study. Thus, the aim of this study was to investigate the possible effects of systemic LPS administration on the behaviour and the hippocampal region of the brain as well as investigate the possible protective effect of Manuka honey in a Sprague-Dawley model.

This model was successfully implemented using a sample size of 40 over a thirteen-day period after which the animals were terminated, perfused and the intact brain removed and processed for light- and transmission electron microscopy. In addition to this, antemortem studies were conducted to assess the overall health status and possible memory decline of the test subjects.

The daily LPS administration of 0.01 mg per kilogram animal weight resulted in no significant weight loss or gain among the animals. In addition to this, no sickness behaviour was observed throughout the thirteen-day period. The LPS administration had no significant effect on the brain to weight ratio or antemortem behavioural studies. Additionally, the daily exposure to 0.5 mL of honey per kilogram animal weight resulted in no significant weight changes or sickness related behaviours among the animals.

The morphology analysis of the hippocampal tissue demonstrated some altered metabolic activity and amyloid formation in the LPS exposed groups. The ultrastructural analysis

indicated a decreased mitochondrial membrane integrity and enlarged rough endoplasmic reticulum in both exposed groups with these changes observed to a lesser extent in the honey exposed group.

In conclusion, this study suggests that LPS and honey exposure alone and in combination does produce some level of response in the dorsal hippocampal region of the Sprague Dawley rat brain. The response to LPS was not sufficient enough to produce statistically significant differences in behaviour amongst the groups; however, it was sufficient to produce differences in histological studies. This may be due to an insufficient exposure period or exposure concentration.

Keywords:

Alzheimer's disease, neuro-inflammation, Sprague-Dawley model, lipopolysaccharide, behavioural testing, neurodegeneration, amyloid formation

Declaration

I, Victoria Sue Verrall declare that this thesis entitled:

“The Potential neuroprotective effect of Manuka Honey in Sprague-Dawley rats with Lipopolysaccharide induced neuronal injury”

which I herewith submit to the University of Pretoria for the Degree Master of Science in Physiology, is my own original work and has never been submitted for any academic award to any other tertiary institution for any degree.

21 February 2022

Date



VS Verrall

Department of Physiology, Faculty of Health Sciences,
University of Pretoria
Pretoria
South Africa

Acknowledgements

I would like to dedicate this thesis to Dr Brittney Chapman for her unwavering support and love throughout this process and to Mr Clayton Roos, a true gentleman, a good friend and an unnecessary casualty of the Covid-19 pandemic.

Dr Janette Bester, I could not thank you enough for your guidance, understanding, motivation and especially your patience throughout my MSc study and for always being available to lend a hand or give advice. You are an incredible supervisor and this thesis would not be possible without you.

I would like to express my appreciation to the following people who made a valuable contribution to my study:

- Dr June Serem for her support and guidance as my co-supervisor
- Dr Helena Taute for her support, assistance and advice with the light microscopy preparation and analysis
- Prof Daniels from the University of Witwatersrand for his support and assistance with the behavioural studies
- All the members of the CAS unit for their assistance during the antemortem studies
- Dr James Wesley-Smith for his assistance with the transmission electron microscope and the entire microscopy unit at Sefako Makgatho Health Sciences University

I owe a huge thank you to both my parents, Mark and Sandy Verrall and the rest of my family including Sheena Roche, Michael Verrall and Jennifer Verrall for their love and support throughout my studies. I would not have been able to achieve this had it not been for your endless support, guidance and the countless cups of tea.

Lastly, I would like to thank Lyle Ireland for his love, patience, encouragement and support.

TABLE OF CONTENTS

Declaration	iii
Acknowledgements	iv
Figures, tables and diagrams Index	i
List of abbreviations and symbols	iv
INTRODUCTION	1
REVIEW OF LITERATURE	3
2.1 <i>Background on Alzheimer’s disease</i>	3
2.1.1 Subtypes of dementia	4
2.1.2 Diagnosis and prognosis of Alzheimer’s disease	5
2.2 <i>Pathogenesis and pathophysiology of Alzheimer’s disease</i>	10
2.2.1 Amyloid and tau protein	10
2.2.2 Neuroinflammatory Response	15
2.2.3 Atrophy in Alzheimer’s disease	19
2.3 <i>The influence of the gut microbiota on Alzheimer’s disease</i>	20
2.4 <i>Lipopolysaccharide model of Alzheimer’s disease</i>	22
2.5 <i>Existing treatment possibilities</i>	22
2.6 <i>Honey as a possible treatment for neuro-inflammation</i>	23
2.7 <i>Aims and objectives</i>	25
Objectives	25
IMPLEMENTATION OF THE SPRAGUE-DAWLEY RAT MODEL	26
3.1 <i>Introduction</i>	26

3.2	<i>Methods</i>	27
3.2.1	Ethical Considerations	27
3.2.2	Sprague-Dawley Rat Model	28
3.2.3	Administration	31
3.2.4	Termination	32
3.2.5	Collection of Nervous Tissue	33
3.2.6	Statistical analysis	34
3.3	<i>Results</i>	34
3.3.1	Analysis of body mass	34
3.3.2	Temperature reading	35
3.3.3.	Body weight to brain weight ratio	36
3.4.	<i>Discussion</i>	36
3.5.	<i>Conclusion</i>	38
	ANTEMORTEM STUDIES	39
4.1.	<i>Introduction</i>	39
4.2.	<i>Methods</i>	40
4.2.1.	Open field test	41
4.2.2.	Y-Maze test	42
4.2.3.	The Novel Object Recognition Test	43
4.2.4.	Statistical Analysis	45
4.3.	<i>Results</i>	45
4.3.1	Open-field test	45
4.3.2	Y-maze test	46
4.3.3	Novel object test	48
4.4.	<i>Discussion</i>	49
4.5.	<i>Conclusion</i>	51

MORPHOLOGY ANALYSIS	52
5.1 Introduction	52
5.2 Materials and Methods	53
5.2.1 Tissue collection for light microscopy	53
5.2.2 Paraffin wax embedding	53
5.2.3 Sectioning	55
5.2.4. Staining procedures	56
5.3 Results	58
5.3.1 General tissue morphology	58
5.3.2 Amyloid deposition	62
5.3.3 Nissl body staining	66
5.4 Discussion	70
5.5 Conclusion	72
ULTRASTRUCTURAL ANALYSIS	74
6.1 Introduction	74
6.2 Methods	75
6.3 Results	78
6.3.1 Mitochondrial Presence	78
6.3.2 Rough endoplasmic reticulum	80
6.4 Discussion	81
6.5 Conclusion	83
CONCLUSION	84
BIBLIOGRAPHY	87

APPENDIX	95
<i>Appendix 1</i>	95
Ethical Clearance	95
<i>Appendix 2</i>	96
MSC committee Approval Letter	96
<i>Appendix 3</i>	97
University of Witwatersrand Ethical Clearance	97
<i>Appendix 4</i>	98
Central Animal Services Competency certificate	98
<i>Appendix 5</i>	99
Ethics Renewal	99
<i>Appendix 6</i>	100
Animal Welfare Monitoring Sheet	100
<i>Appendix 7</i>	101
Plagiarism report	101

Figures, tables and diagrams Index

List of Figures

Figure 2.1 A schematic representation of the progression from a healthy brain to that of a Alzheimer's patient	7
Figure 2.2: A PIB PET scan of a normal control without A β deposition (NC-), a normal control with A β deposition (NC+), MCI with no A β deposition (MCI-), MCI with A β deposition (MCI+), MCI with substantial A β deposition (MCI++) and AD	9
Figure 2.3: A visualisation of the amyloid plaques, tau tangles, activated microglia and the atrophy consistent with AD pathology	10
Figure 2.4: Light microscopic view of AD pathology where the plaques are identified by the thick arrows, the tangles identified by dotted arrows and the neuropil threads identified by the thin arrows	12
Figure 2.5: The abnormal process of amyloid precursor protein (APP) cleavage as seen in Alzheimer's disease	13
Figure 2.6: The pathological Tau process as seen in Alzheimer's disease	15
Figure 2.7: The microglial cell has several important physiological functions, including immune surveillance and producing an inflammatory response, in response to certain stimuli and aggravators	16
Figure 2.8: MRI scans and illustrations demonstrating the differences between a healthy brain and an AD affected brain	19
Figure 2.9: An external view of the gross pathology observed in Alzheimer's disease (right) compared to a healthy control (left)	20
Figure 3.1 A flow diagram representing the experimental groups	29
Figure 3.2: A flow diagram representing the entire experimental procedure	30
Figure 3.3: A diagram representing the position of the cardiac puncture	32
Figure 3.4: Photographs of the superior view (left) and inferior view (right) of the removed, intact rat brain	34
Figure 3.5: Daily average weight (grams) from first day of experimental period until day of termination	35

Figure 3.6: Average weight gain ($\bar{x} \pm sd$) per group as measured over the entire 20-day period	35
Figure 3.7: Average brain to body weight ratio ($\bar{x} \pm sd$) for each treatment group	36
Figure 4.1 The setup and dimensions of the open field test	41
Figure 4.2: A schematic diagram showing the set-up of the Y-maze test during (a) the habituation period and (b) the testing period	43
Figure 4.3: An image of test subject 36 in the novel object testing arena taken after the completion of the testing phase	45
Figure 4.4: The measured parameters ($\bar{x} \pm sd$) during the open field test	46
Figure 4.5: The results of various parameters measured in y-maze test ($\bar{x} \pm sd$)	47
Figure 4.6: The measured parameters ($\bar{x} \pm sd$) during the novel object test	49
Figure 4.7: The number of test subjects within a group that visited each block first	49
Figure 5.1: A Sprague Dawley rat brain atlas according to the Waxholm model	56
Figure 5.2: A micrograph from the control group showing the areas of interest found in the dorsal hippocampal region	59
Figure 5.3: A micrograph of the CA1 region of the hippocampus proper from the control group (A), LPS treated group (B), the honey treated group (C) and the honey and LPS treated group (D)	60
Figure 5.4: A micrograph of the CA3 region of the hippocampus proper from the control group (A), LPS treated group (B), the honey treated group (C) and the honey and LPS treated group (D)	61
Figure 5.5: Collection of micrographs (A-C) of increasing magnification of the hippocampal region of the PBS treated group showing very little amyloid deposition (black arrows)	62
Figure 5.6: A collection of micrographs (A-E) of the hippocampal region of the LPS treated group showing increased presence of amyloid deposition (black arrows) as seen by the red shading	63
Figure 5.7: A collection of micrographs demonstrating the mild amyloid deposition (black arrows) in the PBS and Honey group	64
Figure 5.8: A collection of micrographs demonstrating mild amyloid deposition (black arrows) in the LPS and Honey group	65

Figure 5.9: A collection of micrographs of Nissl stained samples from the control group ___ 66

Figure 5.10: A collection of micrographs of Nissl stained samples from the honey administered group _____ 68

Figure 5.11: A collection of micrographs of Nissl stained samples from the LPS exposed group _____ 67

Figure 5.12: A collection of micrographs of Nissl stained samples from the LPS and honey exposed group _____ 69

Figure 6.1: The sagittal view of the right hemisphere of an LPS exposed Sprague Dawley rat 75

Figure 6.2: Image demonstrating the lifting of the cortex away from the midbrain _____ 76

Figure 6.3: Image of the separation of the midbrain from the hippocampal region _____ 76

Figure 6.4: Image of the lifted cortical region with the exposed hippocampus (indicated by red arrow)_____ 77

Figure 6.5: An intact hippocampus of an LPS exposed rat showing the head (1), body (2) and tail (3) as defined during sectioning _____ 78

Figure 6.6: TEM micrographs of mitochondrial presence among the groups _____ 79

Figure 6.7: TEM micrographs of the rough endoplasmic reticulum observed surrounding the pyramidal neuron nucleus.. _____ 81

Figure 7.1: Summary of results obtained from the histological and ultrastructural analysis. 86

List of Tables

Table 2.1: Different subtypes of dementia as well as a simple explanation of each subtype _ 5

Table 2.2: The stages and associated clinical signs of AD _____ 9

Table 3.1: Experimental group design _____ 28

Table 3.2: The treatment each experimental group received each day during the experimental period _____ 31

Table 3.3: Rectal temperatures obtained prior to termination _____ 36

Table 5.1: A table depicting the time (hours) and number of repeats each sample was immersed in each reagent _____ 54

List of abbreviations and symbols

α	Alpha
β	Beta
A β	Amyloid beta
AD	Alzheimer's disease
APP	Amyloid precursor protein
ATP	Adenosine triphosphate
CA	Cornu Ammonis
CAS	Central Animal Services
CCL	Chemokine (C-C) ligand
CNS	Central nervous system
COX-2	Cyclo-oxygenase 2
CSF	Cerebrospinal fluid
CXCL	Chemokine (C-X-C) motif ligand
DAMPs	Danger associated molecular patterns
ERK	Extracellular signal related kinase
FDG PET scan	fluoro-deoxy-D-glucose (FDG)-based PET scan
IL	Interleukin
LPS	Lipopolysaccharide
MAPK	Mitogen-activated protein kinase
MCI	Mild cognitive impairment
MGB axis	Microbiota-gut-brain axis
NF- κ B	Nuclear factor kappa-light-chain-enhancer of activated B cells
p-tau	Phosphorylated tau
PAMPs	Pathogen associated molecular patterns
PBS	Phosphate buffered saline
PET scan	Positron emission tomography scan
PHF-tau	Paired helical filament tau

PSEN	Presenilin
rER	Rough endoplasmic reticulum
ROS	Reactive oxygen species
SOP	Standard operating procedure
SSRI	Selective serotonin reuptake inhibitor
TEM	Transmission electron microscopy
TGF- β	Tumour growth factor beta
TLR	Toll-like receptor
TNF- α	Tumour necrosis factor alpha

INTRODUCTION

Alzheimer's disease (AD) is a prominent subtype of dementia worldwide with a significant presence in South Africa.^{1,2} In addition to or as a result of this increased prevalence, recent findings suggest AD to be the leading cause of morbidity and mortality worldwide in the geriatric population.³ The exact cause of non-hereditary AD is still largely unknown; however, there are scientific models currently used and accepted. One such model demonstrates that lipopolysaccharide (LPS) presence, either systemic or central, results in an increase in the formation of amyloid β in the hippocampus, a specific hallmark of Alzheimer's pathology as well as increased neuronal cell death.⁴ This model is the current study paradigm for both *in vivo* and *in vitro* research on Alzheimer's pathology where higher concentrations of LPS have been found in Alzheimer's affected nervous tissue compared to controls.^{5,6} A recognized and widely utilized *in vivo* model in biomedical research, especially in the study of neurodegeneration, is the Sprague Dawley rat model due to its relevance and applicability to human physiology.^{7,8}

The increased permeability of the basal intestinal layer as well as the differential microbiota composition observed in aged animals increases the risk of bacteria or bacterial component entry into systemic circulation.^{5,9} This is of specific interest as higher concentrations of LPS and *E. coli* K99 pili protein have been observed in the brain parenchyma and vasculature of Alzheimer's patients compared to controls.⁶ Honey has been demonstrated to be a potent antibacterial and anti-inflammatory agent and therefore has been nominated as a possible therapeutic agent against LPS pathology.¹⁰

A Sprague Dawley rat model, in which LPS was administered subcutaneously and honey was administered by oral gavage, was established in order to successfully evaluate the research objectives which governed this study.

This study made use of an already established model of systemic LPS administration to induce low level inflammation as well as a standardized behavioural testing apparatus in order to achieve these objectives. An altered version of tissue fixation was used in order to enable whole brain fixation.

It was hypothesized that LPS administration would result in systemic inflammation which would result in central inflammatory responses causing histological changes in the hippocampus. Additionally, honey was nominated for oral administration in order to provide a 'mopping' effect against this systemic inflammation and, therefore, provide a neuroprotective effect against the central changes observed. This may lead to a better understanding of the neuroinflammatory response, the exact neuronal injury caused by LPS exposure and the role of this response in neurodegenerative diseases such as AD.

It is clear that there is more investigation required into the pathophysiology of AD in order to develop more specific and effective treatment protocols. Therefore, the aim of this study was to evaluate the effect of LPS administration on the histology and morphology of cells within the hippocampal region of the brain as well as to observe any behavioural changes caused by the LPS. In addition to this, the effect of the consumption of honey was evaluated as a possible protective factor against these effects and changes.

REVIEW OF LITERATURE

“Cure will not be a silver bullet. A cure for us is either something that can prevent the someone from developing dementia in the first place, or stop dementia in its tracks before it has caused too much damage.”

– Doug Brown, the former chief of policy and research officer of the Alzheimer’s Society

Alzheimer’s Disease, a subtype of dementia, is a chronic neurodegenerative disease characterised by a progressive loss of cholinergic neurons in the basal forebrain and deposition of amyloid beta (A β) and hyperphosphorylated tau (p-tau) protein.^{11,12} The neuronal cell death and synaptic impairment found in AD patients is partially mediated by microglial and astrocyte activation, a key characteristic of neuro-inflammation.¹¹ This glial activation causes sustained pro-inflammatory cytokine and reactive oxygen species production resulting in chronic inflammation and an innate immune system activation. Therefore, the pathogenesis of AD is not only restricted to neuronal dysfunction but also includes certain immune mechanisms within the brain.¹³ There are also various other factors, such as systemic inflammation and lifestyle factors including stress exposure, diet and sleep-wake cycles, that may interfere with normal immune processes within the brain.¹⁴ This may escalate the disease progression. The factors that influence the immune response, as well as the cellular components and processes involved, may be important targets for therapeutic or preventative strategies in AD and its associated neuro-inflammation.

2.1 Background on Alzheimer’s disease

Although the knowledge of dementia and age-related memory decline has existed for centuries, AD was first classified by Dr Alois Alzheimer in the early 18th century.¹² This first identification of the disease included documentation of the severe cognitive disturbances, aphasia, delusions, unpredictable behaviour and progressive mental degeneration of a 51-year-old woman, Auguste D., over a period of four and a half years.¹⁵ Post-mortem studies of her brain tissue revealed brown-stained clumps of cells that were overrun by tangles of dark fibrils. These histopathological signs, known today as plaques and tangles, have

become the hallmark of the disease that was first identified and later named after Dr Alzheimer.¹²

Globally, there is one new case of dementia every three seconds.¹⁶ Worldwide prevalence of dementia in populations over the age of sixty is between 5-7% with incidence doubling every ten years thereafter.² Alzheimer's disease is currently the most common subtype of dementia, accounting for as many as 60-70% of all documented cases with approximately 33 million documented cases worldwide.^{3,12,16} The estimated lifetime prevalence for AD is one in ten for males and double that for females.¹⁷ Other types of dementia include vascular dementia, mixed dementia, Lewy body dementia or frontotemporal degeneration.¹⁶

In 2018, AD was found to be the leading cause of both morbidity and mortality in the geriatric population worldwide.³ Mortality is not a result of the AD pathology itself but rather as a result of associated infection, injury, malnutrition, dehydration or illness.¹² A localised study involving a low-income rural, Xhosa speaking community in South Africa found a dementia prevalence of 11% for those older than 65 years.¹⁸ Although research on the prevalence rates within South Africa has been limited and based on small, localised samples; the 2016 World Alzheimer's report estimated a 4,25% prevalence rate for dementia with a higher prevalence in urban areas.^{1,18} This prevalence rate is expected to double by the year 2030.¹⁸

2.1.1 Subtypes of dementia

As previously mentioned, AD forms only one subtype of Dementia. Each subtype of dementia has specific diagnostic criteria as well as different clinical assessments that allow for probable diagnosis.¹² The different subtypes of dementia are listed and simply explained in table 2.1.

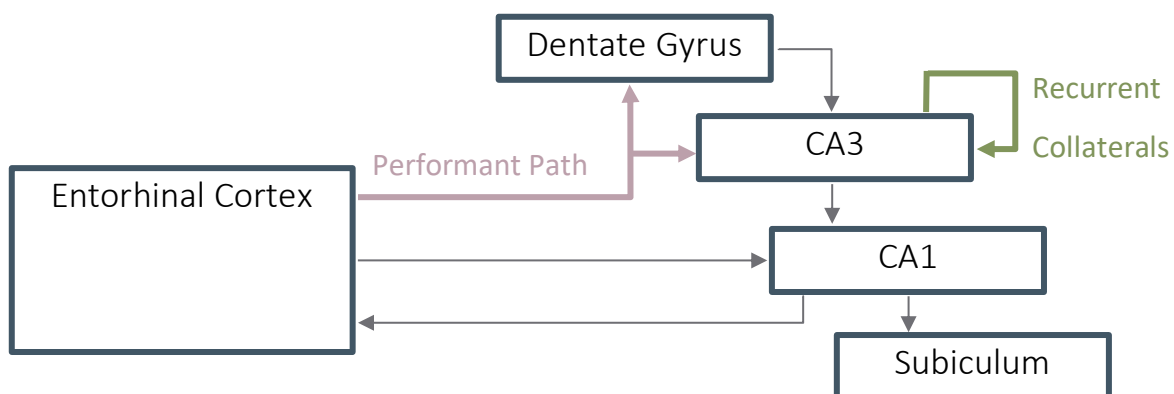
Table 2.1: Different subtypes of dementia as well as a simple explanation of each subtype¹²

Subtype	Description
Mild Cognitive Impairment	Syndrome of cognitive decline that falls between normal age-related cognitive changes and dementia
Dementia with Lewy bodies	Cognitive decline characterised by intraneural cytoplasmic Lewy body deposition and often associated spontaneous motor features of parkinsonism
Vascular dementia	Cognitive decline clinically similar to Alzheimer's disease caused by focal or diffuse cortical or subcortical brain damage as a result of cerebrovascular disease or injury
Alzheimer's disease	Progressive cognitive decline linked to amyloid- β and tau protein accumulation in the brain
Frontotemporal Dementia	A cluster of related dementias that have focal neuronal loss in the frontal/temporal lobes, cognitive impairment and associated disturbances in behaviour, language and personality
Dementia associated with medical conditions	Transient changes in mental status due to traumatic brain injury, HIV infection, Huntington's disease, Human prion disease and substance abuse

2.1.2 Diagnosis and prognosis of Alzheimer's disease

In order to understand the diagnosis and prognosis of AD, a disease that largely alters the way in which the patient learns and remembers, the typical pathways of learning and memory must be understood. Two prominent pathways exist in learning and memory, namely the direct and polysynaptic pathways.¹⁹ The direct pathway is important in episodic

and spatial memory whereas the polysynaptic pathway is important in semantic memory. These pathways involve a variety of different hippocampal and other regions of the brain. Input to different regions of the hippocampus is associated with different hippocampal roles.¹⁹ Entorhinal cortex input to the dentate gyrus plays an important role in pattern recognition and memory encoding. The performant path involves projections between the axons of the entorhinal cortex and the granule and pyramidal cells of Cornu Ammonis (CA) 3 as well as pyramidal cells of the CA1 and subiculum. This pathway is important in the pathogenesis of neurodegenerative disorders such as AD due to this being an early area of tau protein distribution and atrophy. Additionally, Alzheimer’s disease is associated with the loss of pyramidal neurons in the CA1 region of the hippocampus.²⁰ The pathway between the entorhinal cortex and CA3 area plays an important role in information retrieval. The Shaffer’s collaterals, axon collaterals projected from CA3 cells to the CA1 region, play an important role in memory formation and activity-dependent neuroplasticity. The recurrent



collaterals, which play an important role in working memory, send excitatory input to CA3 region.

Figure 2. 1: A schematic diagram of the memory pathways discussed above

The developmental progress of AD is progressive and usually begins with seemingly normal or otherwise age-related causes of decline in cognitive ability. For this reason, it is difficult to provide a definite diagnosis of AD without a histopathologic examination; however, many cases are defined based on clinical criteria with greater uncertainty in the diagnosis during the early stages.^{3,21} The neuropathology associated with AD can progress for over 20 years before the onset of the clinical presentation.^{22,23} This clinical presentation usually begins with impairment of the recent memory function and attention and later involves the loss of

multiple cognitive skills including language skills, abstract thinking, judgment and visuospatial orientation, behavioural and personality changes as well as the loss of bodily functions.¹¹ This cortical form of dementia typically lasts between eight and fifteen years after which it results in a vegetative state eventually culminating in death.¹²

There are three parameters on which the overall level of AD neuropathological change is based; where the level can be classified as either low, intermediate or high.³ These parameters include the A β plaque distribution score, neurofibrillary tangle distribution stage and the neuritic plaque density score. The neuritic plaques, that form one of the hallmarks of AD, are characterised by extracellular A β protein deposition and dystrophic neurites which often have p-tau immunoreactivity.³ This progression towards AD can be visualised in figure 2.1.

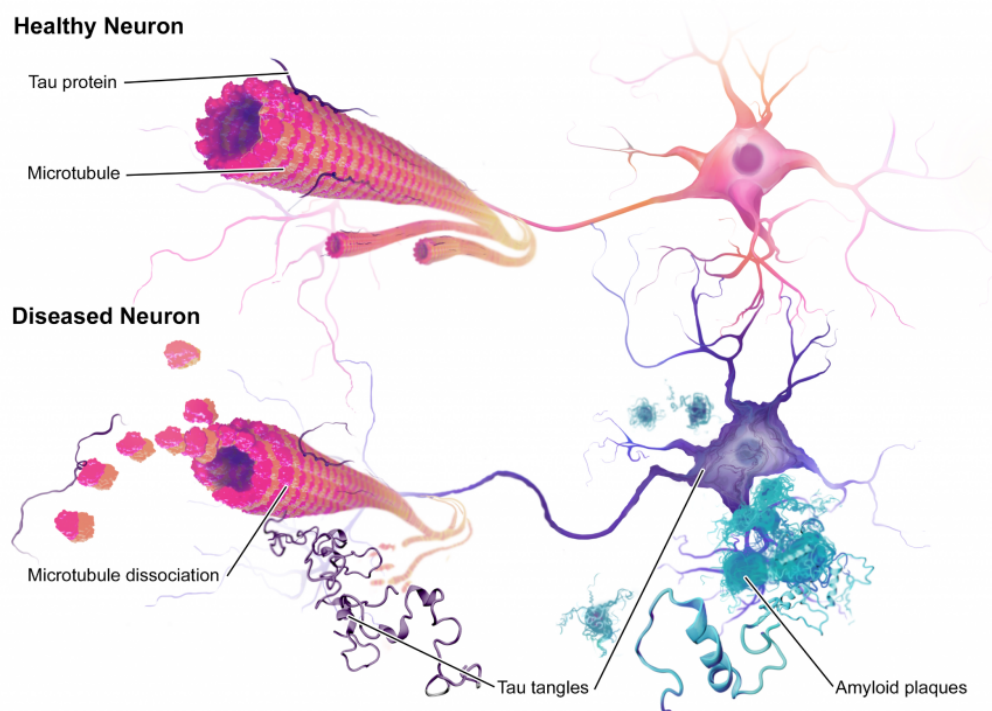


Figure 2.2 A schematic representation of the progression from a healthy brain to that of an Alzheimer's patient²⁴

Since AD is a slow, progressive disorder that has no fixed events that define its onset, it is easier to view AD as a continuum of symptoms.²¹ This continuum is further complicated by the pre-symptomatic stage that occurs between the biochemical changes in the brain and clinical presentation.³ As a result, AD has been subdivided into three phases; namely the

preclinical phase which is a construct used mainly for research, mild cognitive impairment (MCI) due to AD and lastly probable dementia due to AD.^{12,21}

The preclinical phase of AD is further divided into three stages where the first and second stages are asymptomatic.¹² Stage one involves the presence of A β in the cerebral spinal fluid (CSF) or on the amyloid-based positron emission tomography (PET) scan. Stage two includes evidence of neuronal injury based on MRI or fluoro-deoxy-D-glucose (FDG)-based PET scans as seen in figure 2.2. The FDG-based PET scan is largely a measure of synaptic activity based on the metabolism of glucose.²⁵ This AD FDG-PET profile shows severe hypometabolism in both the association and limbic cortex. These regions include the posterior-medial parietal, lateral parietal, lateral temporal, and medial temporal lobes. The last stage begins to involve subtle cognitive changes.

Between the preclinical phase and the dementia phase, MCI due to AD occurs. In this phase less subtle, more concerning impairments take effect with the degree of cognitive impairment not considered normal compared to the patient age standards.²¹ Mild cognitive impairment is a syndrome classified by clinical, cognitive and functional criteria.²¹ In this stage of disease progression, biomarkers, such as the Pittsburgh Compound-B, can be used to trace A β deposition.²⁶ However, these are not always present and core clinical criteria must be used in the diagnosis of MCI. These criteria include a change in cognition, decreased performance in one or more cognitive domains and mild impairment in their independence whilst performing tasks.²¹ It must be noted that, when these changes or impairments occur, there is no severe impairment in social or occupational functioning such as in the final stage of dementia.

Although it is challenging for clinicians to identify the transitions between the different stages of AD, a diagnosis of AD dementia is usually only made when there is sufficient cognitive impairment to cause interference in daily life.²¹ Figure 2.2 shows a comparison of the A β deposition seen in different populations of controls and patients with different severities of cognitive decline. The clinical signs and behavioural manifestations associated with each stage is summarised in table 2.2.

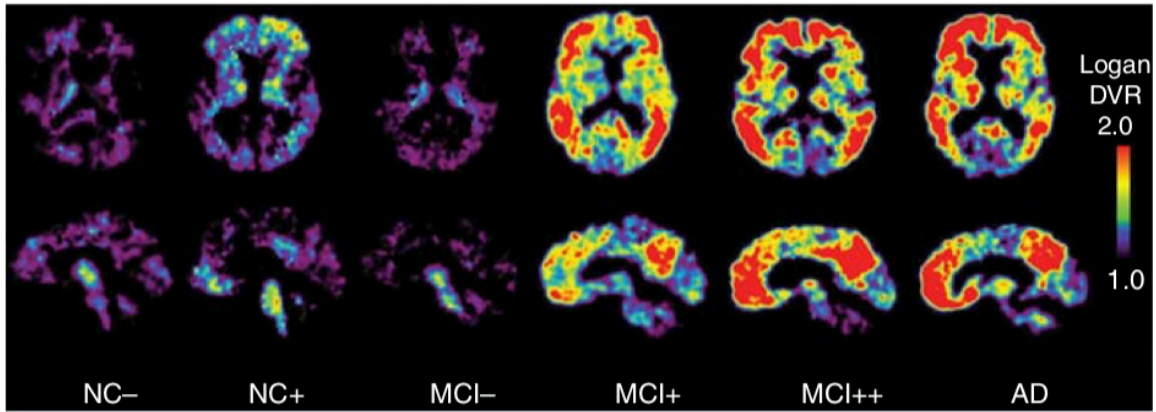


Figure 2.3: A PIB PET scan of a normal control without A β deposition (NC-), a normal control with A β deposition (NC+), MCI with no A β deposition (MCI-), MCI with A β deposition (MCI+), MCI with substantial A β deposition (MCI++) and AD²⁵

Table 2.2: The stages and associated clinical signs of AD²⁷

Preclinical, Mild Cognitive Impairment (MCI)	Mild Alzheimer's Disease	Moderate Alzheimer's Disease	Severe/Late-Stage Alzheimer's Disease
Very mild cognitive decline	Memory loss	Increasing memory loss	Inability to recognise family or communicate
Memory Loss	Confusion about location or familiar places	Confusion	Lost sense of self
Mild word-finding difficulties	Taking longer to accomplish normal daily tasks	Problems recognising friends and family	Weight loss
Decline in the ability to plan and organise; activities take longer	Trouble handling money and paying bills	Poor judgment leading to bad decisions	Groaning, moaning or grunting
	Poor judgement leading to bad decisions	Difficulty organising thoughts and thinking logically	Increased sleeping
	Loss of spontaneity and sense of initiative	Inability to learn new things or to cope with new and unexpected situations	Lack of bladder or bowel control
	Mood and personality changes, increased anxiety	Restlessness, agitation, anxiety, tearfulness, wandering	Seizures, skin infections, difficulty swallowing
		Repetitive statements or movements	Aspiration pneumonia
		Delusions, suspiciousness, paranoia	Death

2.2 Pathogenesis and pathophysiology of Alzheimer's disease

The pathology associated with AD includes the neuropathological alterations observed in A β and p-tau distribution as well as the correlation of these changes to clinical presentation, psychological functioning, neurological imaging and other data.

2.2.1 Amyloid and tau protein

The neuropathological hallmarks of AD consist of diffuse and neuritic plaques marked by amyloid beta and intracellular p-tau protein accumulation.³ This intracellular p-tau accumulation results in the formation of the neurofibrillary tangles. Additionally, there is increased levels of cell death due to A β accumulation in the cells surrounding the neocortical neuronal cells, causing an accumulation of neuropil threads formed by neurofibrillary tangle remnants.²⁷ These hallmarks, as well as the neural atrophy experienced by AD patients, can be visualised in figure 2.3 and 2.4.

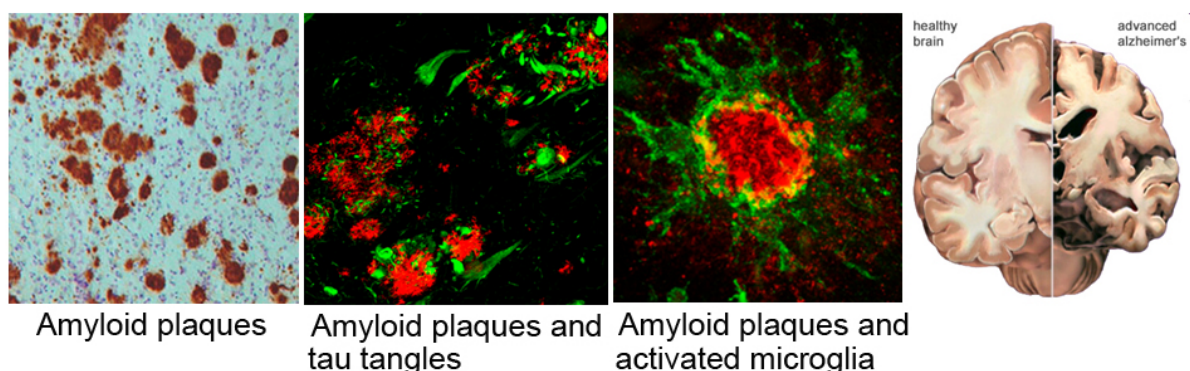


Figure 2.4: A visualisation of the amyloid plaques, tau tangles, activated microglia and the atrophy consistent with AD pathology²⁸

Amyloid- β is an abnormal form of amyloid protein that consists of either a 40 or 42 amino acid peptide chain. This chain is produced by the endoproteolytic cleavage of the amyloid precursor protein (APP) by β - and γ -secretase activity^{3,12,22} The 40 amino acid chain or A β 40 is the more common form; however, the 42 amino acid chain or A β 42 is more pathological.¹² β - and γ -secretase form a complex with Presenilin.³ Mutations in the Presenilin subtypes, Presenilin 1 (PSEN1) or Presenilin 2 (PSEN2), are related to both A β overproduction in general as well as the production of the more neurotoxic form A β 42.³ Mutations in the APP, PSEN1 or PSEN2 gene are related to familial or hereditary forms of AD.²² It then follows that familial forms of AD may be more likely due to an increased

production of A β as mutations in APP, PSEN1 or PSEN2 cause APP to be more readily cleaved to form A β .²² Additionally, when there are dominantly inherited genetic mutations in these genes, there is a longer pre-symptomatic period as well as a 100% risk for early onset AD with diagnosis usually between the ages of 35 and 50 years.³ In contrast to this, sporadic or non-inherited forms may be more likely caused by an impaired clearance mechanisms of A β .²²

When A β is formed, it aggregates to either soluble oligomers of up to six peptide chains or into fibrils. Both forms of A β , insoluble and soluble, can be pathogenic in two ways.¹² Firstly, accumulation of either A β protein is neurotoxic resulting in the death of surrounding neuronal cells. Secondly, these A β aggregates are viewed as foreign bodies in the brain causing an inflammatory response resulting in further neuronal cell damage and death. Under normal clinical circumstance, A β is cleared from the brain via a variety of processes; including endocytosis by astrocytes and microglial cells, enzymatic degradation (via neprilysin or insulin-degrading enzyme), clearance via the blood brain barrier and/or drainage along the periarterial spaces.²² In AD; however, there is an abnormal level of A β deposition and accumulation of insoluble beta-pleated sheets formed by these A β chains (figure 2.5).¹⁶ These β -pleated sheets aggregate and accumulate in clusters in the inter-neural spaces and small cerebral blood vessels thus disrupting and impairing their function. This neuronal functional impairment includes the reduced ability of neurotransmitter reuptake by the astrocyte. This is an important neuro-supportive function of the astrocyte and enables the conversion and recycling of the neurotoxic neurotransmitter, glutamate to glutamine.¹¹

There has been a surge of evidence suggesting that A β accumulation in clinically normal individuals created structural and functional alterations that are consistent with the patterns observed in AD.^{12,23} It can, therefore, be seen that although the complete picture of AD pathogenesis is not known, it is clear that an overproduction and/or reduced clearance of A β protein plays a large contributing role to the pathology of the disease.^{3,22}

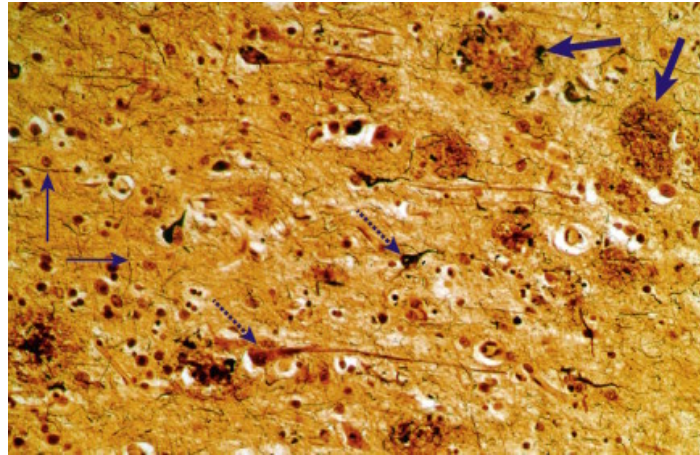
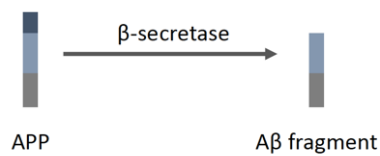


Figure 2.5: Light microscopic view of AD pathology where the plaques are identified by the thick arrows, the tangles identified by dotted arrows and the neuropil threads identified by the thin arrows²⁷

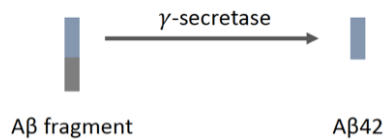
During the inflammatory response caused by $A\beta$ accumulation, activated leukocytes and microglial cells release cytokines and other mediators of inflammation. These mediators activate the surrounding astrocyte cells which results in lesion or plaque formation – the amyloid hallmark of AD. The plaque consists of a dense amyloid protein sheet core and damaged or dead neuronal constituents; including axons, dendrites as well as glial cells.¹² When viewed under a light microscope, these plaques appear to have a ‘fluffy’ central core surrounded by irregular processes (figure 2.4).

Stage 1:

i. APP is cleaved by β -secretase to form A β fragments

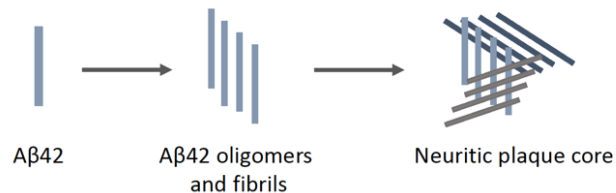


ii. The A β fragments are then cleaved by γ -secretase to form the toxic A β 42 protein



Stage 2:

The A β 42 aggregates into oligomers, β -pleated sheets and larger fibrils which form the insoluble core of the neuritic plaques



Stage 3:

The formation of the neuritic plaques causes an inflammatory response and subsequent destruction of neurons

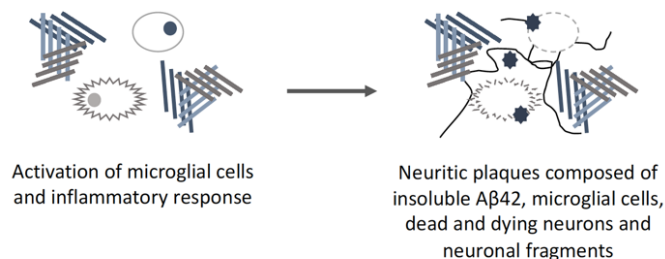


Figure 2.6: The abnormal process of amyloid precursor protein (APP) cleavage as seen in Alzheimer's disease (modified from Agronin¹²)

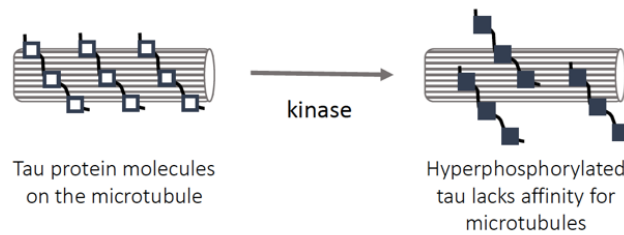
The activated microglia contribute to neuro-inflammation and neurodegeneration via the release of cytokines and antioxidants such as reactive oxygen species (ROS). This increased ROS production and release by the activated microglia which may cause oxidative-stress and further inflammation contributing to the neuronal cell death.²⁹ This is identified as a self-perpetuating cycle of inflammation as an initial damage to neurons that causes the activation of microglia which then results in more damage thus creating a prolonged inflammatory response.

As previously mentioned, there is a second major hallmark of AD: the hyperphosphorylation of the microtubule-associated protein, tau. Tau aids in the stabilization and assembly of microtubules. In the pathogenesis of AD, dissociated p-tau aggregates to form paired helical filament tau (PHF-tau) (figure 2.6).³ This form of tau protein is unable to aid in the stabilisation of the microtubule system and rather aggregates into clumps thus forming a major component of the neurofibrillary tangles observed in the neuronal cytoplasm.¹² These neurofibrillary tangles interfere with the neuron's normal transport system and are, therefore, toxic to neurons.¹⁶ The aggregates of tau may also be responsible for the spread of AD in the brain as a result of the transmission of pathological forms of tau between neurons.³

It is still unclear how these proteins interact or how they form a relationship in the pathology of AD.¹⁶ Alireza Atri, an internationally known cognitive neurologist and Senior Scientist with the Alzheimer's Prevention Institute, proposed a simple metaphor to explain the relationship between tau and A β proteins. He said that tau is like the fire in the brain compared to amyloid, which is more of a chemical toxin; if you spray a toxic chemical all over your house it will still cause damage, however, it's only when you light the match that the real damage occurs.¹⁶

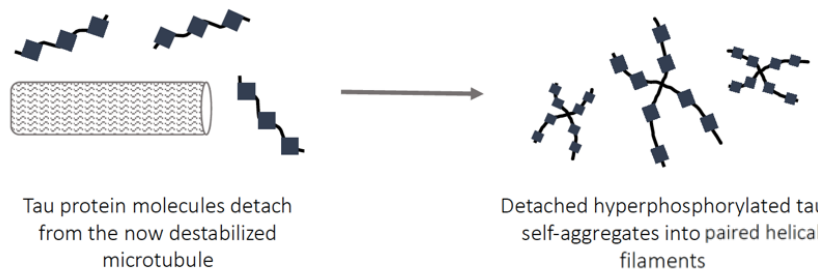
Stage 1:

Tau protein becomes hyperphosphorylated by kinase enzymes.



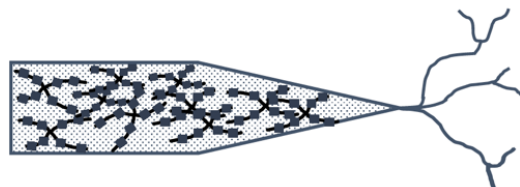
Stage 2:

Hyperphosphorylated tau detaches from microtubules, which become destabilized and are no longer able to provide normal axonal transport and cell structural integrity. The detached tau proteins form paired helical filament.



Stage 3:

Neurofibrillary tangles in the neurons are composed of insoluble aggregates of paired helical filaments of hyperphosphorylated tau protein. These cytotoxic tangles lead to the loss of metabolic and structural integrity of the neuron.



The neurofibrillary tangles 'clog' the cytoplasm of the neuron and are cytotoxic.

Figure 2.7: The pathological Tau process as seen in Alzheimer's disease (modified from Agronin¹²)

2.2.2 Neuroinflammatory Response

As previously mentioned, there is an increase in the activation of microglial and astrocyte activation in the nervous tissue of AD patients. This is known as neuro-inflammation and contrasts to the clinically normal brain where microglia do not produce proinflammatory molecules or ROS in abundance. Including the microglial cells and astrocytes already

mentioned, there are also different mediators, modulators and cellular components involved in this neuroinflammatory response.

The phagocytic microglial cells are distributed throughout the nervous tissue and form an important link between the peripheral immune system and the CNS.³⁰ In addition to their role as immune surveillance within the nervous tissue, the functions of these microglial cells include producing factors responsible for tissue maintenance support and the maintenance and protection of neural plasticity via synaptic remodelling.¹³ These functions are mediated in part by the microglial ability to release trophic factors including brain-derived neurotrophic factor. Brain derived neurotrophic factor plays an important role in memory. These functions can be seen in figure 2.7.

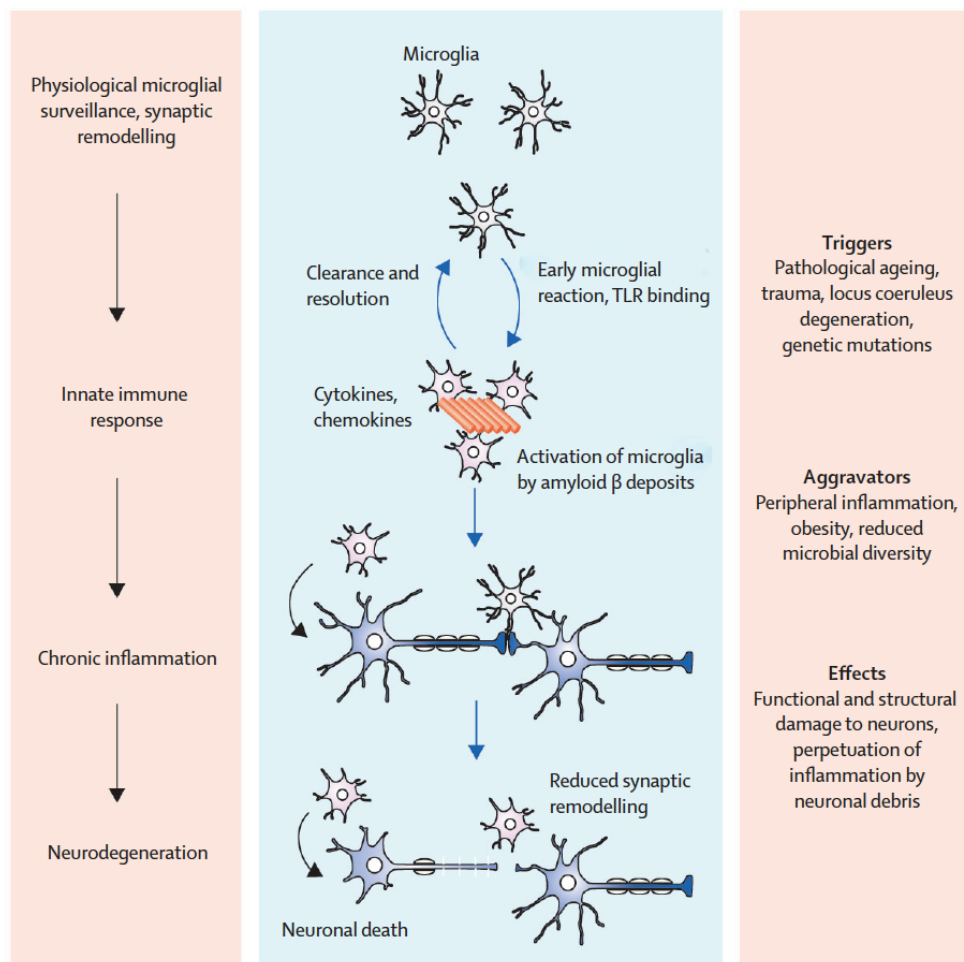


Figure 2.8: The microglial cell has several important physiological functions, including immune surveillance and producing an inflammatory response, in response to certain stimuli and aggravators¹³

Pathological trigger detection; such as the detection of neuronal cell death, pathogen invasion, cellular debris or protein aggregates, is mediated by receptors that identify danger associated molecular patterns (DAMPs) or pathogen-associated molecular patterns (PAMPs).¹³ This detection results in the extension of the microglial processes to the site of injury or invasion allowing migration and the activation of the innate immune system.¹³ This process can be visualised in figure 2.7.

In AD, A β deposition is detected by microglia via cell surface receptors, including SCARA1, CD36, CD14, α 6b1 integrin, CD47 and Toll-like receptors (TLR2, TLR4, TLR6 and TLR9).¹³ In addition to this 'normal' activation of microglia, the microglia in the ageing nervous tissue show an increased sensitivity to inflammatory stimuli due to years of priming.³⁰ The binding of A β 42 and CD36, TLR4 or TLR6 causes both microglial activation and the production of proinflammatory cytokines and chemokines thus aiding in the clearance of the protein via phagocytosis or degradation.¹³

Contrary to a normal microglial inflammatory response, there are various processes (such as the unrelenting production of A β or the reduced phagocytic ability of the microglial cells) that prevent the cessation of inflammation in AD resulting in a chronic state of inflammation. In AD, the down regulation of the A β phagocytosis receptors on microglia are suspected to be the cause of the insufficient microglial phagocytic activity.¹³

The microglial activation is a major source of cytokines production in the tissue of the AD brain.¹³ Cytokines are proinflammatory molecules that play an important role in almost all aspects of neuro-inflammation. Various proinflammatory molecules are present in increased concentration in the AD brain including interleukin-1 α (IL-1 α), interleukin-1 β (IL-1 β), interleukin-6 (IL-6) and tumour necrosis factor- α (TNF- α) as well as the enzyme cyclooxygenase 2 (COX-2).¹¹

Elevated concentrations of IL-1 have been documented in the serum, cerebrospinal fluid and brain of AD patients.¹¹ This increased concentration of IL-1 may be due to increased production by astrocytes, microglia or neurons in the CNS. In addition to this, there are high concentrations of IL-1 β in the astrocytes of the cortex and hippocampus. This dramatic increase is associated with increased levels of A β in these regions.¹¹ Interestingly, the

astrocytes and neurons that produce A β seem to be induced by IL-1 which leads to the deposition of amyloid fibrils. IL-1B plays an important role in the neuronal degeneration and astrogliosis by binding to receptors and stimulating the production of APP and neurotoxic A β .¹¹ IL-1 β also induces other cell types to release cytokines and nitric oxide synthase activity resulting in neurotoxicity. These signals are cell type specific. In glial cells, IL-1 β induces nuclear factor kappa-light-chain-enhancer of activated B cells (NF- κ B) which leads to increased cytokine production.¹¹ In neurons, the IL-1 β induces the mitogen-activated protein kinase (MAPK)-p38 signalling cascade which leads to an increased APP fragment secretion and thus the formation of A β . This is especially seen in the AD brain where IL-1 β is overexpressed at neuroinflammatory sites.¹¹ The activation of the MAPK-38p pathway in neurons is also involved in the hyperphosphorylation of tau protein. As previously noted, the hyperphosphorylation of tau causes in a loss of axonal integrity resulting in the decline of connectivity and synapses; both of which are associated with AD. Therefore, it can be noted that IL-1 plays an important role in the development and pathology of AD.

Another cytokine produced by the astrocytes, microglia, neuronal and endothelial cells of the brain, IL-6, has an additive effect on the inflammatory response initiated by IL-1 β . The increased concentrations of IL-6 in the entorhinal cortex and superior temporal gyrus in AD affected brains supports the relationship between the increase of these cytokines and AD pathology.¹¹

This proinflammatory environment in the AD brain is pathological to both the functioning and the structure of the neuronal tissue. IL-1 β , TNF α and various other cytokines may cause functional impairment prior to the structural changes as demonstrated by the suppression of long term potentiation of synaptic transmission.¹³

As previously mentioned, the activation of astrocytes is an important contributor to neuroinflammation; however, this activation may also be an important contributor to AD pathology. This is due to the production of low amounts of A β in response to chronic stress causing overexpression of β -secretase 1.¹¹

2.2.3 Atrophy in Alzheimer's disease

Although the plaques and fibrils form the hallmarks, these are not the only pathologic changes observed in AD. Neural atrophy is also a common pathological consequence of AD. This atrophy results in a brain weight reduced by 100-200 grams.²⁷ It is suspected that the major contributor to atrophy is neuronal and dendritic cell losses.²⁵ The atrophy seen in AD can be visualised in figure 2.8.

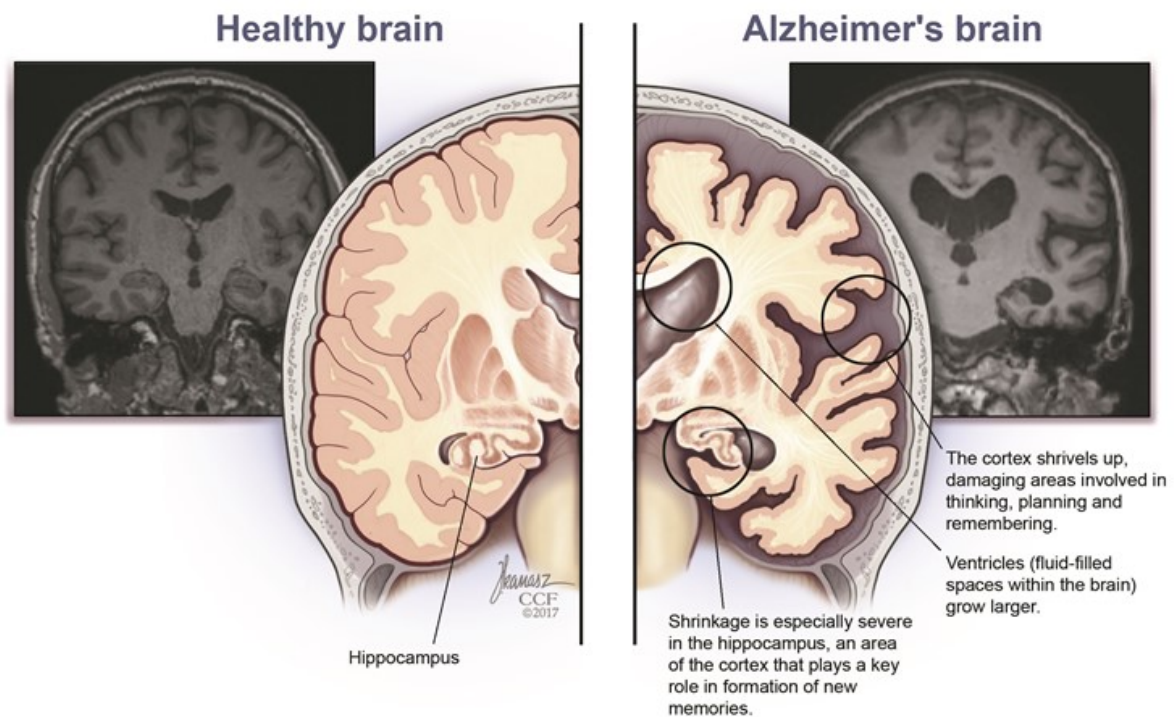


Figure 2.9: MRI scans and illustrations demonstrating the differences between a healthy brain and an AD affected brain³¹

The atrophy observed in AD first manifests in the medial temporal lobe, usually beginning with the entorhinal cortex, closely followed by bilateral atrophy in the hippocampus, amygdala and parahippocampus.^{25,27} Hippocampal sclerosis that is disproportionate to AD neuropathologic change is also observed in AD patients.³ This involves pyramidal cell loss and gliosis in the hippocampal formation. This progressive atrophy in the hippocampal region can be seen in figure 2.8. In addition to medial atrophy, there is also severe cortical atrophy on the surface of the temporal, parietal, and frontal lobes (figure 2.9).²⁷ This figure demonstrates the more prominent meningeal vessels present in an AD brain as a result of the shrinking of the gyri.

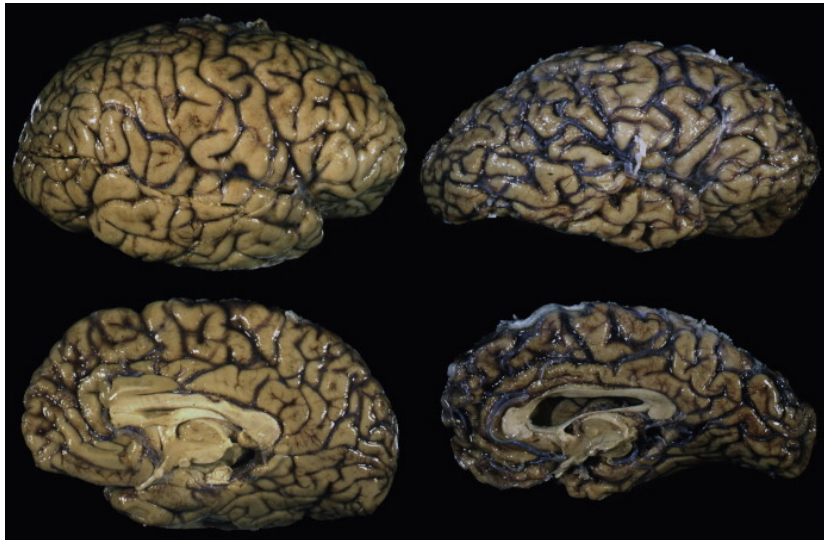


Figure 2.10: An external view of the gross pathology observed in Alzheimer's disease (right) compared to a healthy control (left)²⁷

2.3 The influence of the gut microbiota on Alzheimer's disease

The human gastrointestinal tract is inhabited by more than 10^{14} microorganisms forming the microbiota of the gut.³² The bidirectional communication between the gastrointestinal system and the central nervous system, known as the microbiota-gut-brain (MGB) axis, plays an important role on the key brain processes including neuro-inflammation.^{9,33} The gut microbiota also play a role in the permeability of the blood-brain-barrier during gestation; the effect of which remains throughout life.³²

Aged animals possess a different microbiota composition with the changes in the phyla previously associated with inflammation.⁵ These animals also display an increased basal intestinal permeability.⁹ This increased permeability likely increases the risk for entry of bacteria or bacterial components (e.g. LPS) into circulation from the gut lumen where an inflammatory response may result.

This has led to extensive research on the role of the gut microbiota in all aspects of health and disease. Much of this research has focussed on the influence of the gut on brain health. Microbiota dysfunction has been reported in many mood, neurodevelopmental and neurodegenerative diseases including depression, autism, stroke, Parkinson's disease and Alzheimer's disease.⁹ The bacteria in the gut are able to influence these central processes

via the production of neurotransmitters and metabolites with neuroactive properties as well as immune activation.³³

Therefore, an important intermediary between the gut microbiota and the brain is the immune system. The cytokines produced by the immune system can signal the brain from the periphery via the vagus nerve or directly through regions in the blood-brain-barrier that are relatively permeable.³³ For example, Gram-negative bacteria stimulate the production of pro-inflammatory cytokines through the binding of the LPS component of their cell walls with toll-like receptors (TLRs) expressed on monocytes, macrophages and microglia.³³ The inflammation response associated with pro-inflammatory release has been linked to cognitive decline in AD.³²

This has led to the interest in the role of the MGB-axis in AD. Studies have shown an increase in Gram-negative bacteria associated with increased inflammation (including *Escherichia* and *Shigella* bacterial genera) in faecal samples obtained from AD patients compared to controls.⁹ This increase was correlated to an increase in proinflammatory expression of interleukin 1 beta (IL-1 β) and chemokine (C-X-C) motif ligand (CXCL) 2 in whole blood suggesting a causal link between dysregulation in the gut microbiota and systemic inflammation. This systemic inflammation may initiate or exacerbate the neurodegeneration in AD.

Alzheimer's patients have a greater level of LPS and *E. coli* K99 pili protein in the brain parenchyma and blood vessels when compared to normal controls.⁶ In addition to the increased LPS levels, this LPS also colocalised with A β in the amyloid plaques and around blood vessels.⁶ This suggests that, in AD, bacteria or bacterial components do in fact leave the gut lumen, enter systemic circulation and reach the brain. Since the presence of LPS in the gut lumen initiates an immune response, the microbiota may influence neurodegeneration through similar processes due to the presence of LPS in the brain.

Disruption in the gut microbiota has also been implicated in many of the risk factors of AD. Hyperglycaemia, such as that seen in diabetes, causes an increase in the intestinal barrier permeability and is thus associated with intestinal barrier dysfunction.³² The bacteria that play a role in the regulation of blood pressure via their fermentation products have decreased levels in AD patients.³²

2.4 Lipopolysaccharide model of Alzheimer's disease

Lipopolysaccharide is an endotoxin that forms part of the outer membrane of Gram-negative bacteria found commonly in the gut.³⁴ It binds to the CD14 receptor on microglial membranes forming the LPS-CD14 complex. This complex then interacts with the TLR-4 activating microglia thus initiating the release of proinflammatory cytokines (such as IL-1, IL-6, IL-12, p40, TNF- α), chemokines (such as CXCL8, (chemokine (C-C) ligand (CCL) 2 and CCL5), and complement system proteins.³⁴ The proinflammatory cytokines produced activate both the neuroendocrine and neuroimmune systems.⁴ In addition to this, the LPS may interact with the brain via peripheral nerve induction, the more permeable regions in the blood-brain-barrier called the circumventricular organs, area postrema or via the hypothalamus.⁴

Some of the inflammatory cytokines released as a result of LPS-CD14 complex interaction with TLR-4, such as IL-1 β , IL-6, TNF- α and transforming growth factor beta (TGF- β), have been shown to increase APP expression, A β formation and β -secretase activity.⁴ The administration of LPS causes an increase in hippocampal A β expression as it alters the A β transport across the blood-brain-barrier and decreases central clearance of A β .⁴

The neuronal cell death induced by LPS may be related to COX2 and extracellular signal-related kinase (ERK) activation.⁴ The presence of COX2 is increased by proinflammatory cytokines and mitogenic stimuli, thereby mediating the deleterious effects seen in neurodegenerative disorders.⁴ In agreement with this, COX2 is upregulated in AD, associated with A β plaque formation and linked to A β -induced apoptosis.⁴

2.5 Existing treatment possibilities

Although an incurable disorder, there is an increasing school of thought demonstrating that AD is a preventable disorder. Most prevention strategies, including supplements, specific diet and improved lifestyle choices, are aimed at reducing the risk of the development of AD and once clinical presentation occurs, treatment options become more limited.¹² The treatment possibilities aimed at the behavioural and psychological symptoms of clinical presentations can be grouped as either non-pharmacological or pharmacological.

Non-pharmacological treatments involve providing care, adhering to a strict daily routine, managing the environment to ensure status-quo and using behavioural techniques to monitor depression.³⁵ The general approach of management, commonly known as the three-Rs, includes reassuring the patient that they will be okay, reconsidering the situation from the patients point of view and redirecting the patient to avoid confusion and confrontation.³⁵

Pharmacological treatments are used to improve cognition, medical complications, depression, anxiety, psychosis, and agitation.³⁶ These include cholinesterase inhibitors and memantine to treat cognition and selective serotonin reuptake inhibitors (SSRIs) for depression and anxiety.³⁶ Cholinesterase inhibitors not only improve cognition, but assist in other areas of cognition including memory, general functions, behavioural problems and neuropsychological symptoms.²⁷ The functional and neuropsychiatric symptoms prominent in patients with moderate to severe pathology are aided by memantine.²⁷

The medication mentioned above are used to stabilize and manage the symptoms of AD. In addition to these medications, there have been numerous studies on treatments to slow the course of the disease; however, these drugs have not yet been approved by the FDA.¹² It is clear that an easily accessible and relatively cheap treatment or preventative measure is required to treat this disease. It is also notable that these treatment options are not specific to the cellular changes or molecular defects present in these patients but represent a symptomatic approach to treatment.

2.6 Honey as a possible treatment for neuro-inflammation

As previously mentioned, one of the hallmarks of the neurodegeneration, as seen in AD, is the presence of activated microglia. These microglia may contribute to the neurodegeneration and inflammation via the release cytokines.²⁹ In addition, individuals with degenerative disorders are more susceptible to both oxidative stress and damage due their unbalanced antioxidant/oxidant ratio.¹⁰ Therefore, the release of cytokines combined with the excess of ROS leads to the oxidative and nitrosative stress associated with AD. Oxidative stress is caused by an imbalance of oxidants to antioxidants and often results in oxidative damage to cellular components.¹⁰ This can lead to impaired physiological functioning. The antioxidant defence system is responsible for scavenging excess reactive

species or oxidants. This system is comprised of endogenous antioxidants including enzymatic antioxidants (superoxide dismutase, catalase and glutathione peroxidase) and non-enzymatic antioxidants (glutathione, Vitamin C and Vitamin E) as well as exogenous antioxidants.¹⁰ Due to these hallmarks and the processes described above, it has been proposed that honey may be a viable measure to reduce the extent of these processes.

Honey is comprised of glucose, fructose, sucrose, maltose and oligosaccharides; as well as enzymes such as glucose oxidase, diastase, catalase, peroxidase and invertase.³⁷ It has been shown to have health benefits; including gastroprotective, hypoglycaemic, antioxidant, antihypertensive, antibacterial and anti-inflammatory effects.¹⁰ It can, therefore, be seen that honey may have a direct protective effect in AD or an indirect protective effect by minimising risk factors associated with oxidative stress as well as other potential risk factors for AD.

There is also evidence that honey has the potential to decrease oxidative stress in the brain as it produces a strong scavenging activity against free radical and oxidative stress.¹⁰ Tualang honey was shown to have therapeutic potential against kaonic acid induced oxidative stress and neurodegeneration in the cortex of rats as a result of its antioxidant effect.³⁸ In addition to this antioxidant potential in the brain, Candiracci et al. (2012) identified honey flavonoid extract as potent inhibitor for microglial activation. These findings demonstrate the potential for honey to be used as a therapeutic agent in neurodegenerative diseases that involve neurodegeneration and neuro-inflammation, such as AD.²⁹

It can, therefore, be seen that there is ample evidence suggesting a causal link between LPS in the human gut and the events that result in the neuro-inflammation associated with the development of AD. Due to the composition of honey as well as previous research conducted, honey appears to be a possible preventative measure for AD as well as for the associated neuro-inflammation. It is also easily accessible, relatively cost effective and natural. Therefore, the potential use of honey as a natural, easily accessible and relatively cost-effective treatment method for AD requires further investigation. As a result of these findings, it is clear that the potential neuroprotective function of honey in the LPS model of Alzheimer's disease requires further investigation.

2.7 Aims and objectives

The aim of this study was to investigate the effect of systemic LPS on the hippocampal formation and behaviour as well as the effect of oral Manuka honey administration on these identified changes by using antemortem behavioural studies and post-mortem analysis of the hippocampal formation using light- and transmission electron microscopy.

Objectives

1. Establishment of the Sprague-Dawley rat model exposed to subcutaneous LPS administration in the absence and presence of oral manuka honey administration.
2. Antemortem analysis of anxiety or sickness behaviour and memory alterations of the Sprague Dawley rats using standardised testing.
3. Post-mortem histological analysis of possible alterations in general tissue morphology in the dorsal hippocampal region using light microscopy
4. Post-mortem histological analysis of possible alterations in amyloid accumulation in the dorsal hippocampal region using light microscopy
5. Post-mortem histological analysis of possible alterations in Nissl body formation in the dorsal hippocampal region using light microscopy
6. Post-mortem ultrastructural analysis of the possible alteration of the shape, size and presence of different organelles within the dorsal hippocampal region using transmission electron microscopy

IMPLEMENTATION OF THE SPRAGUE-DAWLEY RAT MODEL

Chapter objectives:

- Substantiate the use of the Sprague-Dawley animal model
- Initiation of LPS induced neuro-inflammation via subcutaneous injection of LPS in two groups
- Introduction of Manuka honey as a neuroprotective agent via oral gavage in two groups
- Description of the nervous tissue collection
- Analysis of weight gain/loss, body temperature, brain to body weight ratio and overall health

3.1 Introduction

The use of the animal model forms a valuable tool in the evaluation of the pathogenic factors, the mechanisms involved in disease initiation and progression as well as the related therapeutic strategies. These models enable limited influence of confounding factors on the investigation of different infectious and therapeutic agents due to the high level of control over other factors such as environmental and genetic contributors. This has resulted in a large contribution of animal models to scientific discoveries and understanding. The most notable and applicable disease model is that of the laboratory rat which has largely contributed to research in the field of neuroscience. Although the popularity of the rat model in Alzheimer's research diminished in the last decade due to the advancements made in the genetic manipulation techniques of mice, there are still many useful applications of the model.⁷ In addition to this, the Sprague-Dawley animal model is an extensively studied and commonly used animal model in biomedical research, specifically in neurodegeneration and aging, due to the intelligence of the rat and the relevance of the model to human physiology.^{7,8}

An idealistic version of a disease model would recapitulate the symptoms, causes and lesions in a chronological order similar to that of the actual disease. In this version, therefore; the inflammation model of Alzheimer's should include early chronic neuro-inflammation, secondary memory and cognitive impairment and then A β and tau pathology development. The use of LPS is the current study paradigm for both *in vivo* and *in vitro*

models of neuro-inflammation and is considered as a good fit for these predetermined criteria.^{4,34} In addition to meeting the predetermined criteria, LPS is also associated with AD neuropathology with higher concentrations found in Alzheimer affected brains compared to normal controls.⁶

The route and duration of LPS administration was selected based on existing research.⁴ These parameters were selected based on the prolonged low concentration systemic exposure to LPS in humans, thus creating an applicable model. Substantial research has been conducted on chronic neuro-inflammation in rats where the neuroinflammatory processes that last seven or more days are considered chronic and capable of causing sufficient memory decline.^{4,39} Systemic LPS administration has shown to result in selective hippocampal impairment in context-object discrimination.⁴⁰

Current research suggests that the inhibition of microglial-mediated neuro-inflammation may be a reliable protective strategy against neurodegenerative disorders.¹¹ The identification of the possible therapeutic target for AD as well as the shift toward more sustainable treatment options for disease has led to the search for a natural compound that may hinder the effects of neuro-inflammation in disease pathology. Although honey is becoming popular as a functional food and as a therapeutic agent for disease, there is a major limitation with regards to the existing knowledge of its possible neuroprotective function and this is the major focus of this *in vivo* research. The study of the effects of orally administered honey in *in vivo* research of honey is important due to the digestive processes that occur and the first-pass metabolism to which the honey is exposed.

The aim of this chapter includes the implementation of the Sprague-Dawley model, the evaluation of the effect of LPS and honey alone and in combination on the rat weight and the weight of the intact brain. In addition, the intact brain was prepared for further histological study. It should be noted that the antemortem observations that were conducted are discussed in *Chapter 4*.

3.2 Methods

3.2.1 Ethical Considerations

Ethical considerations included reducing the number of animals required, limiting the discomfort experienced by the animals by refining the treatment protocols, and ensuring educated handling of the animals. Ethical clearance and Animal Ethical clearance was obtained from the University of Pretoria (Reference number: 182/2020) and the University of Witwatersrand (Reference number: 2109/07/44/C). These certificates can be seen in Appendices 1 and 3 respectively. Additionally, training for proper murine animal treatment and handling was provided by the Central Animal Services unit at the University of Witwatersrand (appendix 4).

3.2.2 Sprague-Dawley Rat Model

Twelve to thirteen-week-old male Sprague-Dawley rats, with an average weight of 410-430 grams, were maintained at the Central Animal Service (CAS) at the University of Witwatersrand. The rats were housed conventionally with feeding and enrichment according to the CAS standard operating procedures. The room temperature was maintained between 25°C and 27°C with a relative humidity of 50% (\pm 20%) and a twelve-hour night/dark cycle throughout the study. A total of 40 rats were used with ten rats assigned to each experimental group. The rats were divided into the four experimental groups at random, as indicated in Table 3.1.

Table 3.1: Experimental group design

Groups	Number of Rats per Group
Vehicle Control	10
GH	10
GL	10
GL+H	10
Total	40

Key: GH = honey only, GL = LPS only, GL+H = LPS and honey

Due to time constraints on the day of termination, as well as advice given by the CAS unit, the total number of rats were halved and two separate experimental runs were conducted with five rats in each group therefore a total of 20 rats were used per run. Both runs were conducted under the same circumstances with all environmental and other contributing factors controlled.

Following a seven-day acclimatization period, neuro-inflammation was induced in the experimental group using a subcutaneous (SC) injection of LPS extracted from *E. coli* 055:B5;σ (Sigma Aldrich, L6529-1MG). Phosphate buffered solution (PBS) was used as a vehicle control. Manuka honey (Advancis Medical, CR3830) was administered to randomly selected rodents from the experimental and control groups via oral gavage. The experimental groups can be visualised in Figure 3.1.

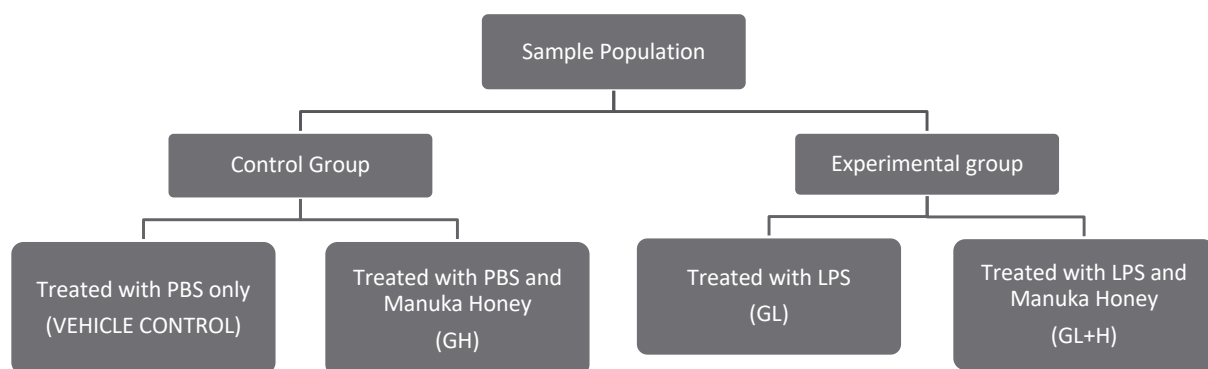


Figure 3.1 A flow diagram representing the experimental groups

An outline of the entire experimental procedure can be seen in figure 3.2. This will act as a guide to the progression of the chapters.

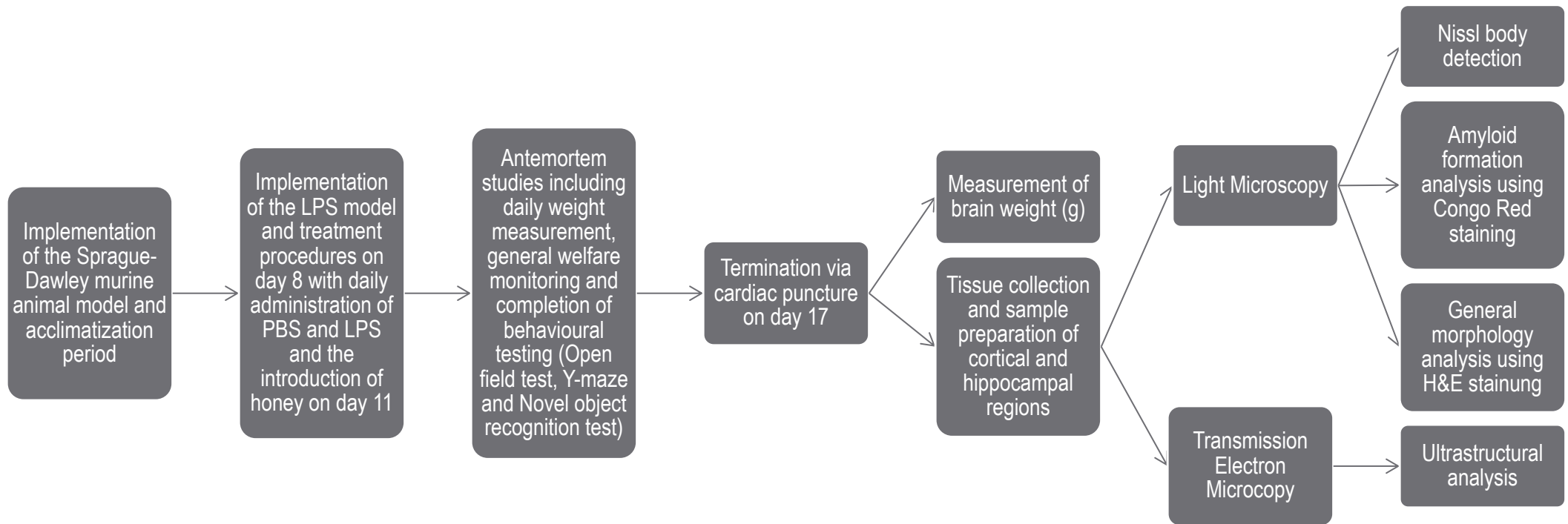


Figure 3.2: A flow diagram representing the entire experimental procedure

3.2.3 Administration

The control group was administered a daily subcutaneous (SC) injection of 0.1 M PBS at a volume of 0.1 mL per kg of rat for ten days.

Group GH was administered a daily SC injection of PBS at a volume of 0.1 mL per kg of rat for seven days in combination with administration of 0.5 mL honey per kg of rat via oral gavage from day four until day ten. The honey was mixed 50% v/v with water to enable a comfortable consistency for the rats.

According to the protocol, group GL were meant to be administered a daily SC injection of LPS dissolved in PBS at a concentration of 0.1 mg/mL at a volume of 0.1 mL per kg of rat for ten days. However, due to the inability to administer such small quantities, the LPS was administered with a concentration of 0.01 mg/mL at a volume of 1.0 mL per kg of rat. This maintained the dose given to each animal as well as ensured a volume that could be accurately administered.

Group GL+H were administered a daily SC injection of LPS dissolved in PBS at a concentration of 0.01 mg/mL at a volume of 1.0 mL per kg of rat for ten days in combination with administration of 0.5 mL honey per kg via oral gavage from day four until day ten.

The administration for each group is summarised in Table 3.2.

Table 3.2: The treatment each experimental group received each day during the experimental period

Group	Day in Experimental Period										Treatment received	
	1	2	3	4	5	6	7	8	9	10		
Vehicle Control	PBS	PBS	PBS	PBS	PBS	PBS	PBS	PBS	PBS	PBS	PBS	
GH	PBS	PBS	PBS	PBS & Honey	PBS & Honey	PBS & Honey	PBS & Honey	PBS & Honey	PBS & Honey	PBS & Honey	PBS & Honey	
GL	LPS	LPS	LPS	LPS	LPS	LPS	LPS	LPS	LPS	LPS	LPS	
GL+H	LPS	LPS	LPS	LPS & Honey	LPS & Honey	LPS+ Honey	LPS & Honey	LPS & Honey	LPS & Honey	LPS & Honey	LPS & Honey	

Key: GH = honey only, GL = LPS only, GL+H = LPS and honey

Observations were made during the experimental period regarding weight as well as memory deficits. These observations will be discussed in *Chapter 4: Antemortem Studies*.

3.2.4 Termination

Euthanasia of the animal test subjects was used to enable post-mortem studies of the cardiovascular, hepatic and nervous tissue as part of a larger study performed on the groups.

Cardiac puncture was used as a means of euthanasia to prevent the effect of chemicals on the clotting cascade and therefore effect the results of the coagulability status of the rats as well as specific metabolite interference in the liver. This was done as the rats were used as part of other studies as well. Before euthanasia, general anaesthetic was administered to each animal to limit discomfort during the euthanasic procedures. Each animal was briefly exposed to Isofor for approximately 30 seconds in a designated box until sedation and loss of consciousness occurred. After sedation was achieved, they were provided with additional Isofor to ensure sedation was maintained and prevent discomfort during the procedure. The euthanasia of the animals was carried out by qualified personnel from the CAS unit according to their approved standard operating procedure (SOP).

In order to perform the cardiac puncture, the sedated rat was placed in dorsal recumbency. A needle was then inserted inferior and slightly to the left of the xiphoid cartilage of the sternum at angle between 20 and 30 degrees. The needle was advanced slowly with small amounts of negative pressure applied to the barrel of the syringe. As the needle tip entered the heart, blood flowed into the hub of the needle. The syringe was aspirated gently until blood flow ceased.

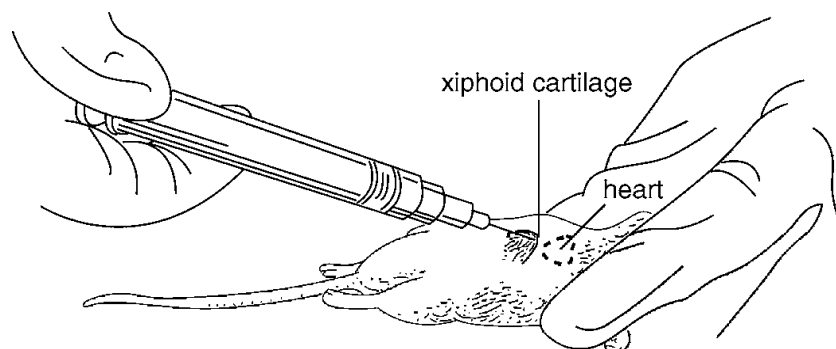


Figure 3.3: A diagram representing the position of the cardiac puncture⁴¹

Once euthanasia was confirmed, an external examination was performed for verification of the animal's identification number and visual inspection and palpitation of the animal's appearance. The skin was checked for abnormal colour, subcutaneous neoplasms ulceration, traumatic wounds, ectoparasites, general fur condition as well as any other external anomalies. The presence of nasal, ocular and/or aural discharge was assessed. Both the anus and perineal region were assessed for diarrhoea or lesions. An examination of the urethra and external genitalia were examined for blood, purulent discharge, neoplasms or abnormalities. Any abnormalities or anomalies found would have been photographed; however, none were present.

After euthanasia, the animals were perfused with saline to clear the tissue of additional blood and enhance the histological view of the tissue samples. Additionally, the animals were perfused with 4% paraformaldehyde to ensure complete penetration of the fixative solution. This was done according to the CAS SOP.

3.2.5 Collection of Nervous Tissue

After completion of the external examination and perfusion, the animal was decapitated at the atlantico-occipital joint via guillotine.

The skull was exposed by cutting and removing the skin beginning at the atlantico-occipital joint and moving toward the frontal bone. The brain was then collected by carefully removing the calvaria using bone-cutting forceps so as to not damage the brain tissue. This was done by bilaterally cutting the occipital, parietal, and frontal bones beginning at the foramen magnum dorsal to the occipital condyle and ending at the frontal bones between the orbits. The opened brain cavity was then turned upside-down to enable the extraction of the intact brain. This was carried out by pulling the brain gently away from the ventral aspect with a small spatula or scalpel blade starting at the foremen magnum and moving toward the olfactory bulbs. During this process, the nerve roots were sectioned.

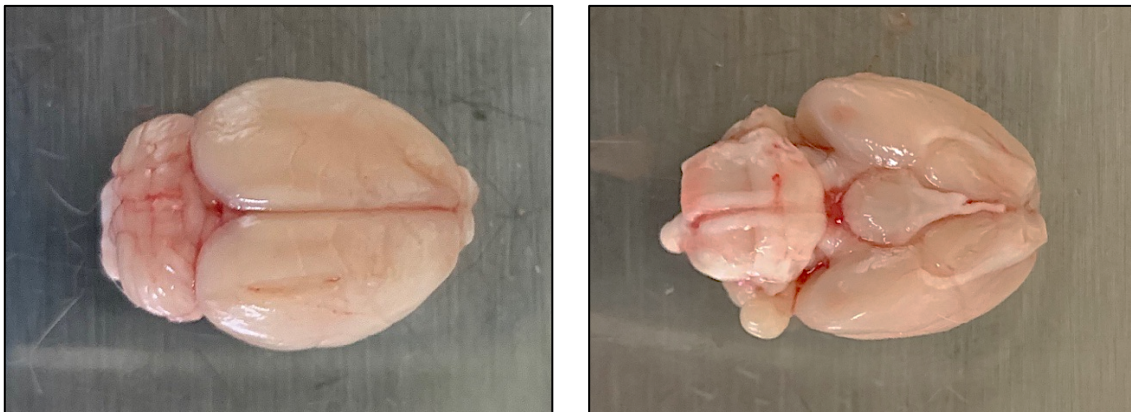


Figure 3.4: Photographs of the superior view (left) and inferior view (right) of the removed, intact rat brain

The entire, intact brain sample was then weighed. This overall brain weight was used to calculate a ratio of brain weight to total animal weight taken on the last day of life.

The intact brain was then placed in a 4% paraformaldehyde fixative as sectioning before fixation causes severe histological distortion of the tissue. The brains remained suspended in the fixative for at least three days at 4°C.

3.2.6 Statistical analysis

Statistical analysis of the animal weight, temperature and brain to body weight ratio were performed on GraphPad Prism Version 9.0.2 using one-way analysis of variance (ANOVA) and Tukey' multiple comparisons test, where a p-value of ≤ 0.05 was considered significant.

3.3 Results

3.3.1 Analysis of body mass

During the experimental period, the weights of the rats were recorded daily. As shown in the figures 3.5 and figure 3.6, there were no significant differences in final weight between the groups or change in weight over the experimental period.

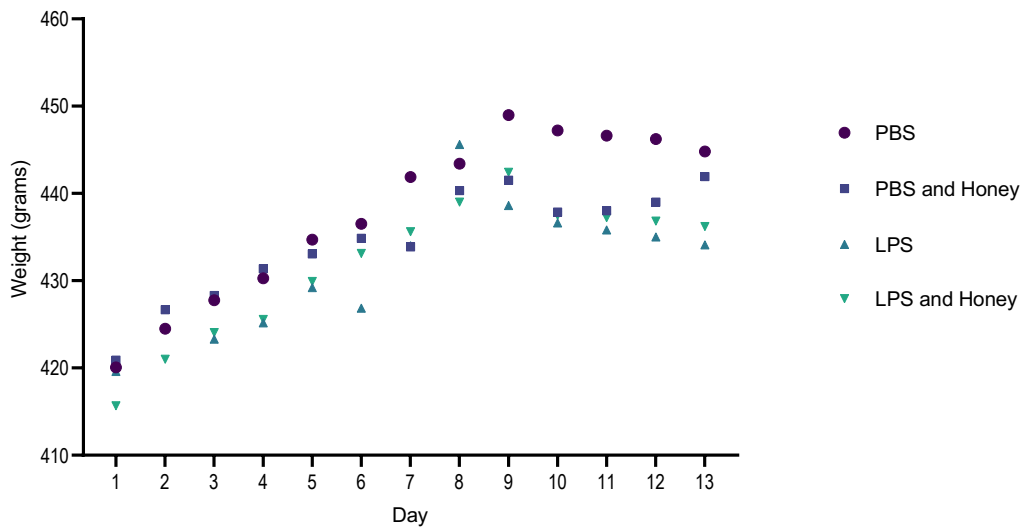


Figure 3.5: Daily average weight (grams) of 40 male Sprague Dawley rats from first day of experimental period until day of termination. Significant differences between groups were evaluated at p-value: ≤ 0.05 .

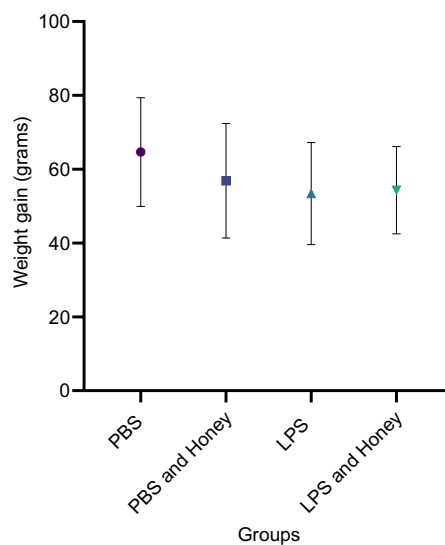


Figure 3.6: Average weight gain ($\bar{x} \pm sd$) per group as measured over the entire 20-day period. Significant differences between groups were evaluated at p-value: ≤ 0.05

3.3.2 Temperature reading

During the Isoflor sedation induced prior to termination, rectal temperature readings were obtained. The readings obtained identified no significant difference between the groups. Additionally, the readings were within the confines of the normothermic range for male Sprague-Dawley rats ($36.99 \pm 0.42^\circ\text{C}$).

Table 3.3: Rectal temperatures obtained prior to termination of 40 male Sprague Dawley rats

Group	Mean Temperature \pm Standard deviation ($^{\circ}$ C)
PBS	36.72 \pm 0.68
PBS and Honey	36.85 \pm 0.41
LPS	36.45 \pm 0.65
LPS and Honey	36.74 \pm 0.73

3.3.3. Brain weight to body weight ratio

Brain and body weight were measured post- and perimortem respectively. These measurements were used to calculate a brain to body weight ratio. As shown in the figure below, there was no statistical difference observed between these ratios.

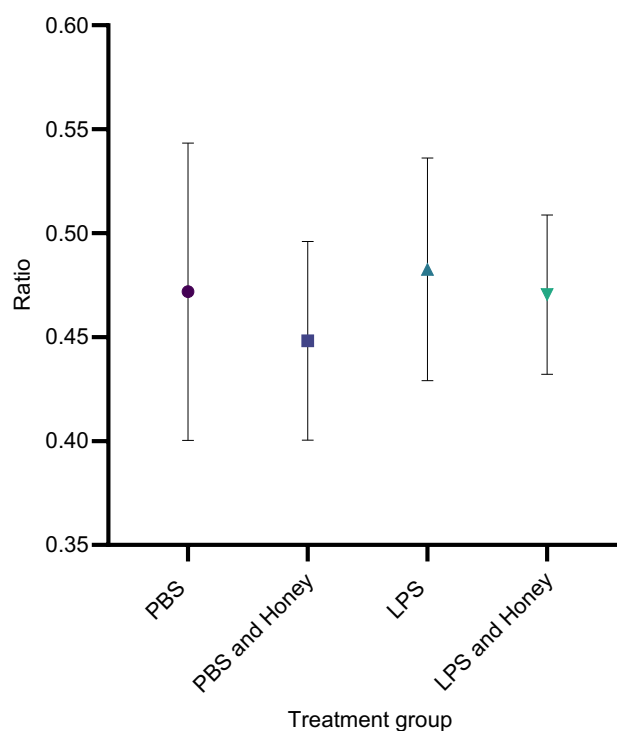


Figure 3.7: Average brain to body weight ratio ($\bar{x} \pm sd$) for each treatment group of 40 male Sprague Dawley rats. Significant differences between groups were evaluated at p-value: ≤ 0.05

3.4. Discussion

The Sprague-Dawley model was utilised in this study as it is an extensively studied model of neurodegeneration and enables the empirical investigation of memory changes due to the establishment of behavioural tests as well as the intelligence level of the rat.^{7,8} Rats aged

12-13 weeks at experimental period initiation were used, as this is the age that represents the beginning of adulthood.⁴² This age was chosen as the neuropathology associated with AD can begin more than 20 years before the onset of the clinical presentation.^{22,23} This clinical presentation usually begins with an impairment of the recent memory function.¹¹ Additionally, it has been shown that younger animals present with fewer age related histological variations, improved cell visibility and identification.⁴² The exposure period of LPS was selected based on both the prolonged systemic exposure to LPS in humans and research conducted on rats where neuroinflammatory processes that last seven or more days are considered chronic and capable of causing sufficient memory decline.^{4,39} The dose of LPS was selected so as to mimic chronic low dose exposure to LPS in humans. The dose and route of administration of honey were chosen based on a real-life application. An achievable daily human consumption of honey was considered to be seven teaspoons or rather approximately two heaped tablespoons. The adaption of this to the animal model was based on the average South African male weight of 71,9kg.⁴³

There were no significant changes in weight across all groups throughout the duration of the study. The weights showed a steady increase comparable to that of the control and to expected weight gain as outlined by the guidelines of the CAS unit. This steady increase can be seen in figure 3.5. Therefore, LPS administration did not cause decrease in appetite or weight-loss. Additionally, the consumption of the additional sugar found in the honey did not cause noticeable weight gain. The rectal normothermic temperature readings showed no indication of fever or sickness at the time of termination.

There was no statistically significant difference in the brain to body weight ratio as seen in figure 3.7. Though not significant, the honey groups showed lower ratios compared to their respective exposure groups. Additionally, the LPS groups demonstrated higher ratios compared to their respective PBS counterparts. These small, insignificant differences may be indicative of a greater mobilisation anti-inflammatory, pro-inflammatory molecules or an increase in hippocampal A β presence respectively.^{4,34} This is however speculation and the non-significant difference between groups suggests that further investigation of histology is required in order to form an argument in this regard.

3.5. Conclusion

In this study, the Sprague-Dawley model was successfully established over a seven-day acclimatisation period and a thirteen-day experimental period. Additionally, the literature has shown the LPS model to be a reliable model for neuro-inflammation. Administration of LPS and honey alone and in combination did not result in any significant weight loss or gain. No fever or sickness behaviours were reported across the groups. The non-significant trends observed in the brain to body weight ratios will be further evaluated in the peri-mortem studies as well as in the histological and ultrastructural analysis of neural structures in the chapters to follow.

ANTEMORTEM STUDIES

Chapter objectives:

- Evaluation of general well-being using animal weight and general welfare monitoring
- Evaluation of sickness behaviours using behavioural testing
- Implementation of open field testing, novel object recognition testing and y maze testing
- Identification of trends in memory decline or behavioural changes

4.1. Introduction

In order to demonstrate a behavioural application of the LPS model as well as the possible neuroprotective properties of honey, behavioural antemortem studies were conducted. This included the open field test, novel object recognition test and the Y-maze test. Additionally, as a marker of overall health, the animals were monitored using a general welfare monitoring sheet and weighed daily during the experimental period.

In animals, infectious agents can lead to a collection of behaviours, known as sickness behaviours, which serve the purpose of facilitating recovery.⁴⁴ These behaviours include decreased locomotor activity, weight loss, disrupted sleeping patterns, a decrease in social and environmental exploration, and a reduction in sexual interest as well as decreased grooming. The loss of weight during infection is mainly a result of decreased food ingestion or anorexia; however, adult rodents demonstrate less significant anorexic behaviours compared to middle-aged or aged rodent populations when exposed to LPS.⁴⁴ The exposure to pathogens as well as novel environments can also increase anxiety and stress. Anxious and stressed animals show abnormal locomotor activity with research showing mixed results as to whether anxiety and stress increase or decrease locomotor activity.⁴⁵ These non-specific symptoms demonstrate an important interplay between the peripheral immune system, the general organisation of the central nervous system and central cytokine production.⁴⁶ In addition to this, LPS administration has been demonstrated to induce several behavioural changes in rats; including general malaise, decreased locomotor activity and decreased social and environmental exploration.^{4,47} It is, therefore, evident that the presence of extreme sickness behaviours would influence the overall performance of the animals in the behavioural tests. For this reason, the open field test is used as a measure

of activity, anxiety-like behaviour and exploratory behaviour to ensure that any differences observed in the other behavioural tests were not significantly influenced by these parameters.

Chronic exposure to LPS has been shown to impair spatial memory as well as induce memory decline and learning deficits similar to the cognitive decline observed in AD pathology.⁴ This is further demonstrated by the hippocampal impairment observed following systemic administration of LPS in rats.³⁴ Evaluation of cognition and memory is complex as the process of cognition and memory is complex itself. In order to evaluate the short-term or working memory of rats, two valuable measures of cognition are commonly used: the Y-maze test and the novel object recognition test. The Y-maze test has two variants where the recognition memory test version is used to evaluate spatial reference memory and the spontaneous alteration version is used to evaluate exploratory behavior.⁴⁸ The brain areas involved in this test include the prefrontal cortex, septum and basal forebrain with special emphasis of involvement of the hippocampus. The novel object recognition test, a type of behavioural test that evaluates the ability of the rat to recognize familiar stimulus, forms part of the core of the animal model tests of human amnesia and memory.⁴⁹

The aim of this chapter includes the evaluation of any sickness or anxiety behaviours exhibited by the animals as well as the identification of trends and differences in behaviour observed in the different experimental groups as identified by the open field test, novel object recognition test and Y-maze test. Additionally, well-being will be assessed using weight-loss assessment and welfare monitoring.

4.2. Methods

The animals were weighed daily to monitor any weight loss during the experimental period. Weight-loss of more than 15% was considered significant and would have resulted in the removal of these animals from the study; however, this did not occur in this study. Welfare was monitored daily during the experimental period in order to ensure that overall health and wellbeing was maintained at a level acceptable according to CAS regulations. The welfare monitoring sheet can be found in Appendix 6.

Behaviour was analysed using the open field test, the novel object recognition test and the Y-maze test. The behaviour was scored using the AnyMAZE software. Additionally, observations were also recorded using a non-professional camera to enable later viewing and, if required, third-party observations by a party blind to the experimental protocol to ensure a limitation of bias.

The evening before the testing commenced, the home-caged test subjects were placed in the testing room which allowed acclimatisation to the sounds, smells and temperature change associated with the room change in order to minimize the effects of stress on observations made during the behavioural tests.

4.2.1. Open field test

The open field test was used as a measure of locomotor activity, anxiety-like behaviour and exploratory behaviour to ensure that these parameters were not significantly attributable to the possible differences observed in the other tests.

The open field test was comprised of a three-minute observational period which was recorded using a non-professional camera and analysed using the AnyMaze software. Additionally, to counteract any possible inaccuracies in the data, the videos were played back and the data was manually verified.

The apparatus for this test consists of a 1 m X 1 m plexiglass arena with walls 50 cm in height. The plexiglass apparatus formed the 'field'. The field was divided into an outer zone (1 m X 1 m) and an inner zone (80 cm X 80 cm). Additionally, the centre block and the corner blocks were demarcated as blocks of interest. The field was further divided into 20cm X

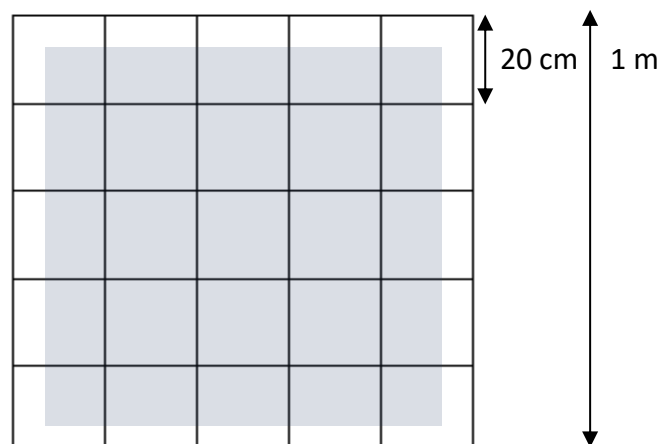


Figure 4.1 The setup and dimensions of the open field test

20cm blocks. This setup can be seen in Figure 4.1.

At the start of the observational period, the animal was placed in the arena facing the wall. During the observational period, various parameters were measured including the number of squares crossed, entry into the inner zone, rearing, average speed, time spent in the zones and grooming behaviours. After the three-minute observational period, the animals were returned to their cages and the field was cleaned with 70% ethanol. This was done in order to prevent the animal's scent and pheromones from influencing the next test subject.

The number of squares crossed in the arena served as the measure of locomotor activity. Additionally, exploratory behaviour was assessed by monitoring entry into the inner zone and rearing which is where the rat rises onto his hind limbs. Animals that are stressed or anxious usually demonstrate a decrease in exploratory behaviour as indicated by the open field test. Lastly, time spent grooming was measured as either an indication of relaxed behaviour or otherwise an attempt at self-soothing. The decision as to which will be made by looking at the other parameters.

4.2.2. Y-Maze test

The Y-maze test has two variants: (1) the recognition memory test which is used to evaluate spatial reference memory and (2) the spontaneous alteration version which is used to evaluate exploratory behaviour. The first variant was chosen as trends in the spatial reference memory were of specific interest.

The recognition memory Y-maze test consists of a three-minute habituation phase and a three-minute testing phase separated by a one-and-a-half-hour retention interval. Both phases were recorded using a non-professional camera and analysed using the AnyMaze software. Additionally, to counteract any possible inaccuracies in the data, the videos were played back and the data was manually verified.

The apparatus consists of a Y-shaped maze with walls 50 cm in height.

During the habituation phase, the third arm of the Y-maze was closed off using an opaque Perspex divider so that only two arms could be explored. This can be seen in figure 4.2(a). In this phase, each test subject was placed in ARM 1 facing the wall. The test subject was then

given a three-minute period to explore the two open arms. The number of entries into each arm was counted as well as the time spent in each arm measured. The animal was then removed from the maze and placed into its home cage for a one-and-a-half-hour retention period. The maze was then cleaned with 70% ethanol to prevent the interference of previous scents and pheromones on future testing periods.

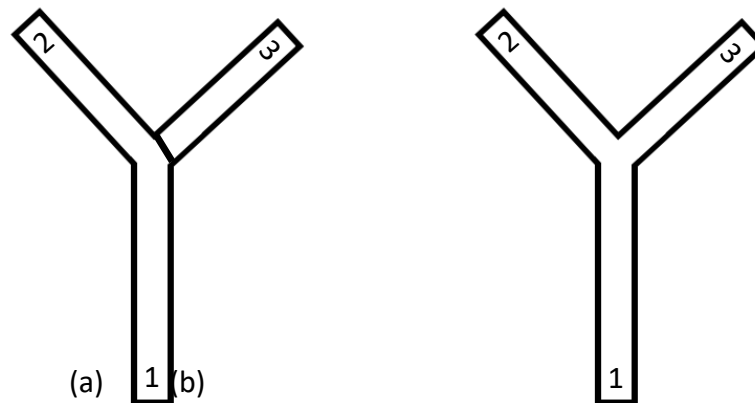


Figure 4.2: A schematic diagram showing the set-up of the Y-maze test during (a) the habituation period and (b) the testing period

After the one-and-a-half-hour period had passed, the testing phase began. In this phase, the Perspex divider was removed and ARM 3 was opened. This can be seen in figure 4.2(b). The test subject was then placed in the ARM 1 facing the wall and given a further three-minute period for exploration. During this period the number of entries into each arm was counted and the time spent in each arm measured. Additionally, other parameters such as freezing time, average speed and time spent in the periphery of the arms was noted.

It was expected that test subjects that had good working and spatial memory would spend more time exploring the new arm compared to the arms previously explored.

4.2.3. The Novel Object Recognition Test

The novel object recognition test is used in the evaluation of the ability of the animal to recognize familiar stimulus.

The novel object recognition test procedure consisted of three phases, each with a specific time frame for analysis. These phases included the habituation phase (45 seconds), the familiarization phase (two minutes) and the testing phase (two minutes). Only the

familiarisation phase and the testing phase were recorded using a non-professional camera and analysed using the AnyMaze software. Additionally, to counteract any possible inaccuracies in the data, the videos were played back and the data was manually verified.

The apparatus for the test consisted of a 44 cm by 53 cm arena with walls 10 cm in height as well as two identical orange rectangular shaped blocks and one green cylindrical shaped block. The orange blocks were given the denotation of A and the green block the denotation of B.

In the habituation phase, the test subject was placed in the arena facing the wall and given a 45 second period to freely explore the open field area where the testing procedure would take place. The animal was then removed from the arena so that two identical objects (A + A) could be placed for the familiarization phase. The animal was then released against the centre of the opposite wall with its back to the objects. The test subject was then given a two-minute period to explore the identical objects. The test subject was then removed from the arena and placed in its home cage. The arena and the objects were then cleaned with 70% ethanol in preparation for the next test subject.

Each test subject remained in their home cage for a retention period of one hour and 45 minutes prior to the commencement of the testing phase. For the testing phase, two objects were placed in the arena: the first object was identical to the sample object and the second object was a novel object (A + B). After the retention period, the animal was released against the centre of the opposite wall of the arena and given a two-minute period to explore the objects. The amount of time that the animal spent in a 1cm radius of the sample object and the novel object was recorded. The apparatus, as seen during the testing phase of subject 36, can be seen in the figure 4.3.

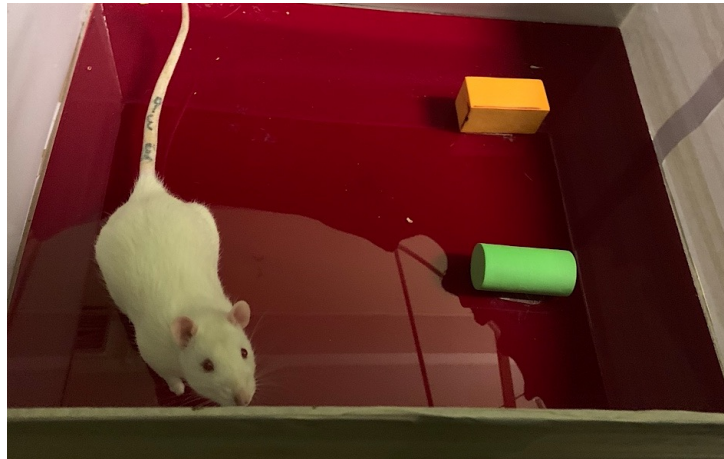


Figure 4.3: An image of test subject 36 in the novel object testing arena taken after the completion of the testing phase

It was expected that the animal would spend more time with the novel object compared to the familiar object.

4.2.4. Statistical Analysis

Statistical analysis of the parameters measured in the behavioural tests were performed on GraphPad Prism Version 9.0.2 using one-way analysis of variance (ANOVA) and the Bartlett's test, where a p-value of ≤ 0.05 was considered significant.

4.3. Results

4.3.1 Open-field test

During the open field test, several parameters were observed. Included in these were the total distance travelled by the test subject over the duration of the test, the time spent in the centre zone, the time spent immobile and the percentage of time spent mobile. The results obtained from the open field test can be viewed in figure 4.4 (A-D). As shown in this figure, there was no significant difference in the parameters measured.

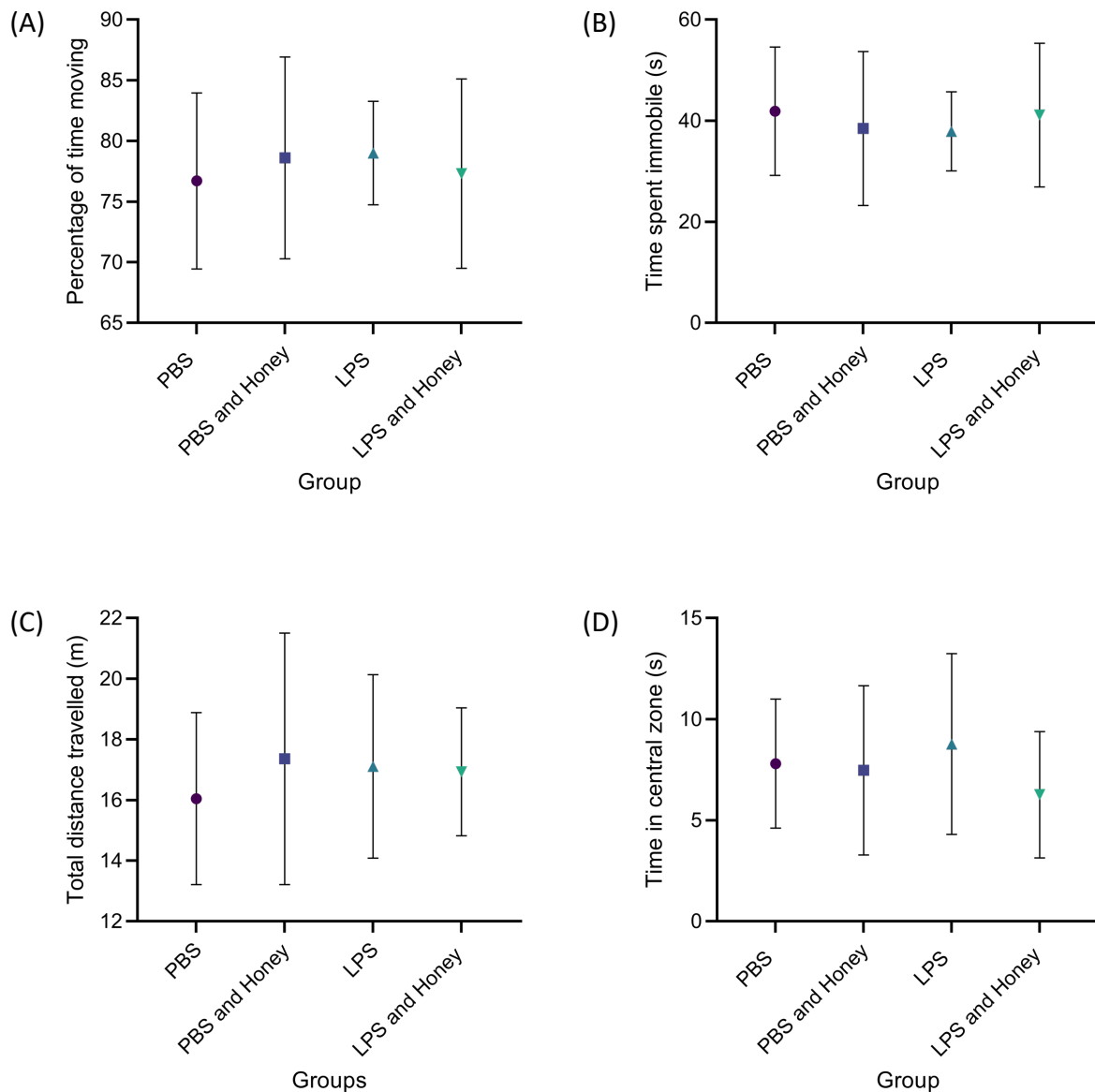


Figure 4.4: The measured parameters ($\bar{x} \pm \text{sd}$) during the open field test of 40 male Sprague Dawley rats include the percentage of time spent moving (A), the total time spent immobile in seconds (B), the total distance travelled in meters (C) and the time spent in the most central zone in seconds (D). Significant differences between groups were evaluated at p-value: ≤ 0.05

4.3.2 Y-maze test

The Y-maze consisted of two separate stages, an acclimatization phase and a testing phase. No recorded parameters are stated during the acclimatization period as this was to enable the test subject to explore the two open arms of the apparatus freely. During the testing phase of the Y-maze test, several parameters were observed. These parameters included the percentage of time spent in the new arm, the proportional ratio of time spent in the new arm compared to the old arms, the amount of time spent in the radial part of the new

arm and the percentage of the total distance travelled that was travelled in the new arm. These results can be seen in figure 4.5 (A-D). No significant differences were observed between the means of the groups; however, a significant difference was observed in the standard deviation of the two treatment groups compared to the control groups in one of the parameters measured. According to the Bartlett's test, the calculated standard deviations of the new arm to old arm ratio are considered statistically significant with a P-value of 0.0196.

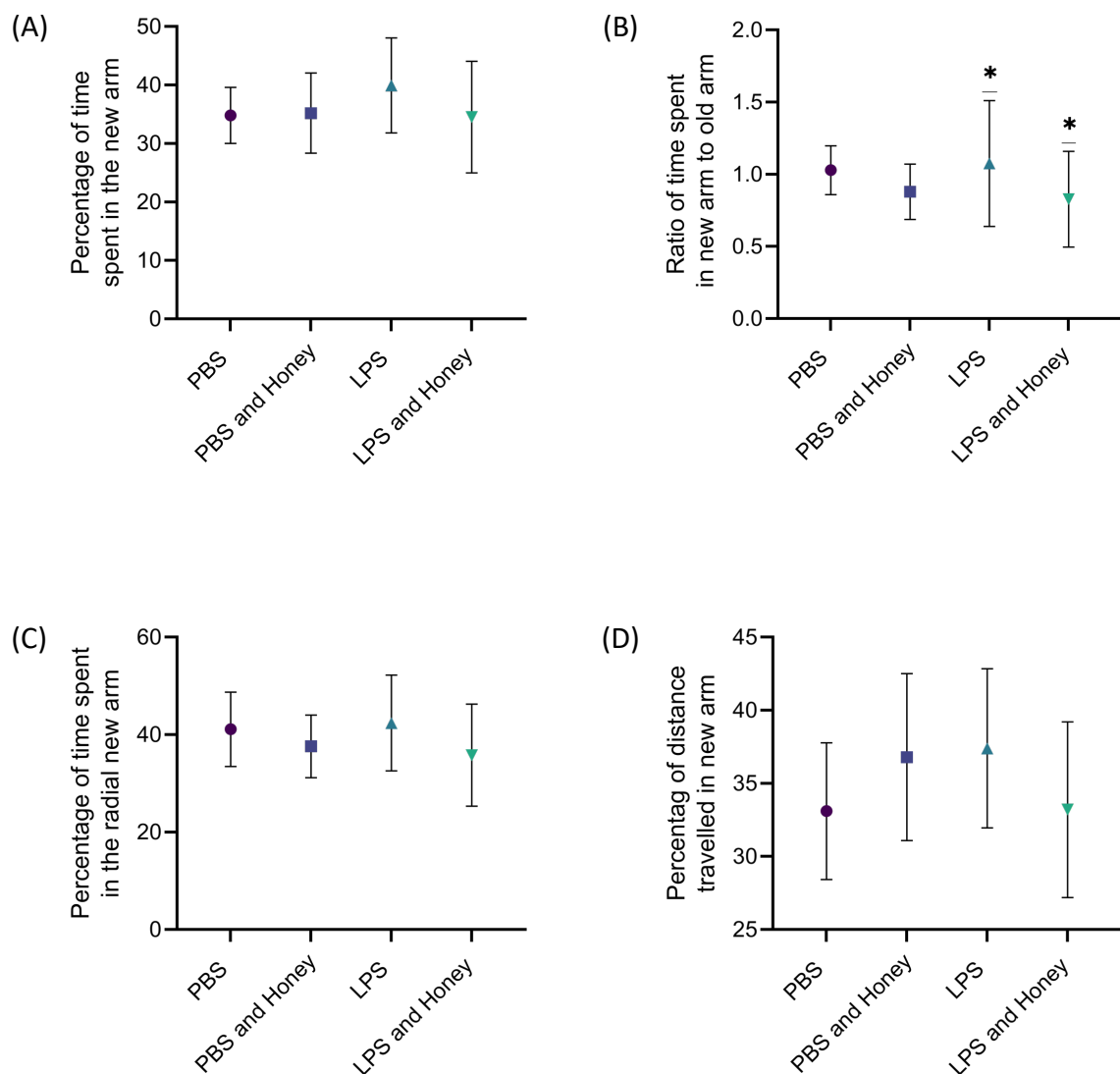
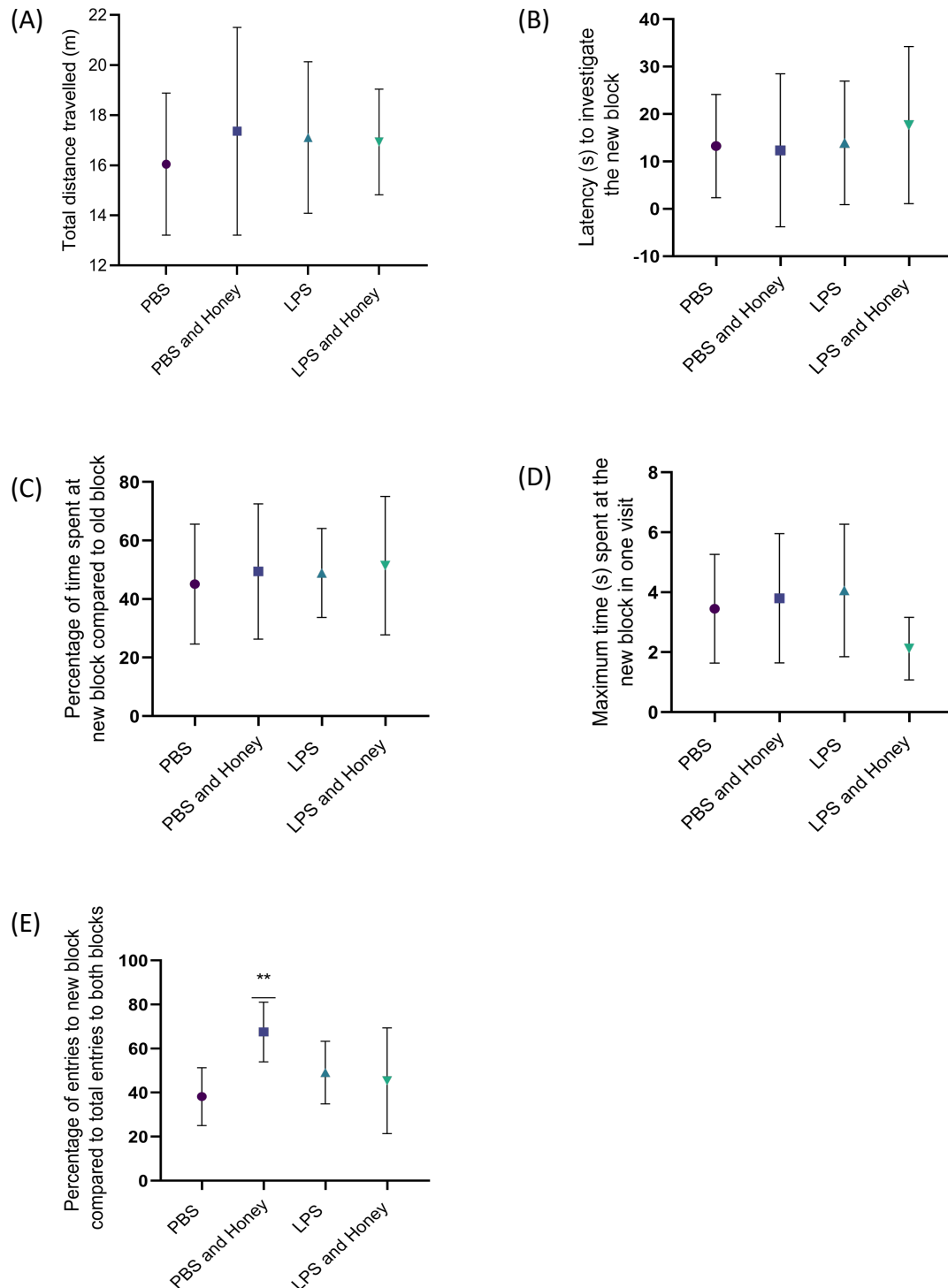


Figure 4.5: The results of various parameters measured using 40 male Sprague Dawley rats in y-maze test ($\bar{x} \pm sd$): percentages or ratios of the time spent in the new arm (A), time spent in new arm compared to the average time spent in the other two arms (B), the time spent in the radial part of the new arm compared the time spent in the radial part of the old arm (C) and the percentage of the

total distance travelled in the new arm (D). Significant differences between groups were evaluated at p-value: ≤ 0.05

4.3.3 Novel object test

Several parameters were observed in the novel object test. The results obtained can be seen in figure 4.6 (A-E). There was no significant difference in the means obtained from the



parameters A to D.

Figure 4.6: The measured parameters (mean \pm SD) of 40 male Sprague Dawley rats during the novel object test: the total distance in meters covered during the testing phase (A), the latency of the test subject in seconds to investigate the new block (B), the percentage of time spent at the new block compared to the old block (C), the maximum amount of time in seconds spent at the new block in one visit (D), and the percentage of entries the block zones that occurred at the new block site. Significant differences between groups were evaluated at p-value: ≤ 0.05

There was a significant difference observed between the mean number of visits to the old versus the new block. This was demonstrated by a significant difference with regards to the ANOVA test with a P-value of 0.0033.

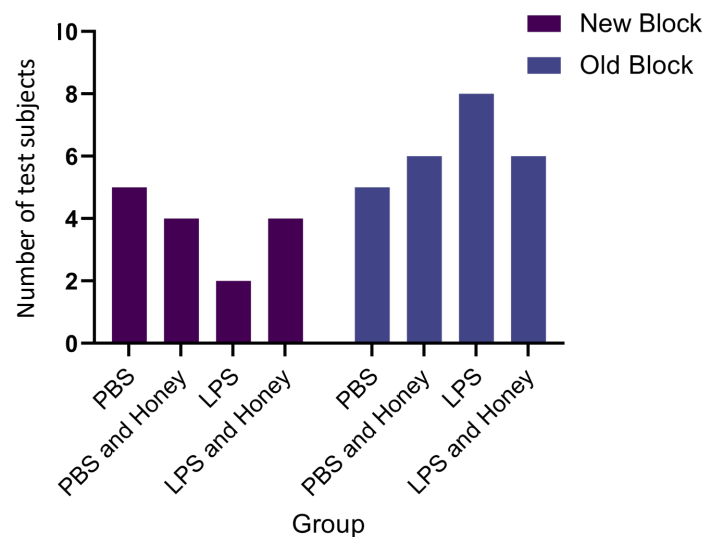


Figure 4.7: The number of test subjects within a group that visited each block first

4.4. Discussion

The behavioural tests utilised in this study are extensively used models to observe possible anxiety-like or sickness behaviours, changes in spatial memory and changes in the ability to recognise novel objects. In addition to the extensive use of these models in the study of neurodegeneration and other behavioural changes or abnormalities internationally, the apparatus available at the CAS unit has had considerable use in research conducted by the University of Witwatersrand and is standardized according to international operating protocols.

The open field test was used as a measure of possible sickness or anxiety-like behaviours. Since LPS administration has been shown to induce several behavioural changes in rats

including general malaise, decreased locomotor activity and decreased social and environmental exploration, the open field test was required to discount these behaviours as possible confounding factors in the other behavioural tests conducted.^{4,47} In addition to the LPS administration, the use of an oral gavage can be seen as an anxiety-inducing procedure and therefore, the open field was also useful in this regard. No significant differences were reported in the open field test with regards to exploratory behaviour, freezing and all parameters observed during this period. The results obtained in the open field test, as seen in figure 4.4, were substantiated by the daily welfare monitoring sheets as grooming was maintained throughout the experimental period, no test subjects were considered to be displaying symptoms of sickness or sickness behaviours while in their home cages and all test subjects remained social throughout the experimental period. This is an important finding as it discounts these behaviours as possible confounding factors in the findings in the rest of the behavioural and histology testing procedures.

The spatial memory variation of the Y-maze test produced no statistically significant differences between the means of the groups as seen in figure 4.5. However, the two groups that were administered LPS produced significantly larger standard deviations in the amount of time spent in the new arm compared to the old arms (0.436 and 0.332 for LPS and LPS and honey respectively) than the two groups that were administered PBS (0.170 and 0.192 for PBS and PBS and honey respectively). This demonstrates that there was a much larger deviation in measured values which may lean toward a differential effect of the LPS administration on different test subjects. This is an interesting observation to make as not all members of society present with Alzheimer's pathology and this may lean toward future investigation on the epigenetic factors involved in LPS induce pathology.

The first four parameters measured in the novel object test seen in figure 4.6 A-D produced no statistical differences between the groups. The difference observed in the mean number of visits to the new block was statistically significant ($p=0.0033$). This result, demonstrated in figure 4.6 E, showed that the PBS and honey group visited the new block the most times compared to the other groups. Although the least number of mean visits was contributed by the PBS only group. This result is interesting since the least number of visits was attributed to the control group, the significance of this result is limited. Although no applicable significance was found in the groups, there is a trend demonstrated by figure 4-6. This trend

shows that the PBS group had the most test subjects to visit the new block first, followed by the two honey groups and lastly the LPS group. Although not incredibly apparent, this result may allude to a trend in the effect of LPS on immediate novel object recognition.

The statistics provided by this section did not produce statistically significant results; however, looking closely at the data may show some clinical relevance of the data. This information may have been more statistically sound if a larger number of test subjects were used in order to decrease the standard deviation of the results and enable the exclusion of outliers. Additionally, a longer exposure period or slightly higher concentration of LPS could have been used to induce a higher prevalence of clinical symptoms or pathology. The testing itself may have some flaws due to the human element of test subject placement or other possible areas of human error. This was limited to the best of the research team's ability (i.e. the animals were handled by the same person, the apparatus was cleaned by at least two people and the testing was started by the same person) but unfortunately, small errors are unavoidable. These errors could have been decreased by further automation of the system; however, this would have come at an extreme financial cost.

4.5. Conclusion

The results from the behavioural tests indicated that the LPS exposure did not seem to have a significant effect on the behavioural changes of the test subjects. This could be attributed to the short time of exposure or the low concentration of the LPS introduced. Although the literature had shown that low levels of systemic LPS administration would be adequate to demonstrate behavioural and memory changes in the test subjects, this was not observed to a large extent in this study. There were; however, trends in the data which will be investigated in the future chapters observing the histological and ultrastructural changes between the groups. The purpose of the low concentration of LPS and honey administration was not to cause immediate change but rather mimic the change that might occur over long-term exposure. Therefore, these subtle changes between the groups may be the beginning signs of symptomatic presentation of histological pathology. This will be examined and investigated in *Chapter 5: Morphology Analysis*.

MORPHOLOGY ANALYSIS

Chapter objectives:

- Method development for tissue embedding
- Identification of the dorsal hippocampus during sectioning
- Staining of the dorsal hippocampal region using haematoxylin and eosin, Nissl body and Congo red staining techniques
- Critical evaluation of histological differences between groups

5.1 Introduction

The aim of this chapter was to determine the effect of systemically introduced LPS and the oral administration of honey alone and in combination on the dorsal hippocampal region of the brain. This area of the brain was chosen based on its unique function in memory and learning as well as the specific neurodegeneration of this area associated with the memory decline observed in Alzheimer's disease. Since this chapter makes use of light microscopy to conduct a histology analysis, the normal anatomy and histology of the hippocampus will be discussed as well as the changes expected due to Alzheimer-related neurodegeneration.

Nervous tissue is comprised of two types of cells, namely neurons and supporting cells; whereas, the hippocampus is comprised primarily of pyramidal cells, a type of multipolar neuron.⁵⁰ These cells have both afferent (dendrites) and efferent (axons) processes.

The hippocampus consists of two distinct parts; the dentate gyrus and the hippocampus proper (CA regions).¹⁹ Additionally, there is a region known as the subiculum which acts as a transitional zone between the two former zones and connects the hippocampus with the entorhinal complex.^{19,20} The CA formation is a sea-horse shaped structure divided, based on histology, into four fields, the CA1, CA2, CA3 and CA4 regions.²⁰

The changes in histology of the dorsal hippocampal regions were analysed using three different staining techniques; namely, Haematoxylin and Eosin for general histology, Cresyl violet for Nissl body identification and Congo red for amyloid deposition.

5.2 Materials and Methods

5.2.1 Tissue collection for light microscopy

Samples were obtained as described in Chapter 3.

5.2.2 Paraffin embedding

For the analysis of the samples using light microscopy, whole brains were used to produce coronal sections and the left hemisphere was used to produce both sagittal and coronal sections. This method was used in order to reduce the number of animals sacrificed. This was possible by first separating the right and left hemispheres by means of cutting with a scalpel. As will be described in the following chapter, the right hemisphere was used in the transmission electron microscopy analysis.

In order to cut thin sections of nervous tissue, paraffin embedding is an ideal method to use. This also ensures non-distortion of the tissue histology, increased wax penetration to the centre of the tissue and limited tissue shrinking or hardening. The use of the formalin-fixed paraffin-embedding is a commonly used protocol for wax embedding; however, the use of xylene as a clearing agent is not recommended for large tissue embedding due to shrinking and hardening after long-time exposure. Therefore, due to the size of the tissue that needed to be fixed, a modified version of the fixation protocol was required. This led to the process of method development to find a more suitable clearing agent to ensure the most appropriate sample preparation. The paraffin-embedding method developed by Zhanmu et al., (2020) was used as a general outline.⁵¹

5.2.2.1 Methods and materials

Two separate trials were conducted to determine which clearing agent, xylene or tert-butanol, produced better results.

Both trials consisted of the same steps with the exception of the clearing methods. The whole brain sample was removed from the 4% paraformaldehyde solution and placed in a 0.01 M PBS for 24 hours. The whole brains were then placed in two changes of each concentration of ethanol solution beginning at 50% and moving to 70%, 80% and 90% for a duration of three hours each. The whole brains were then placed in three changes of 100%

ethanol for a duration of two hours each. This process is illustrated in table 5.1. The times used for each step were adapted from Zhanmu et al., (22 in which the method for whole rat brain fixation was optimized.⁵¹

Table 5.1: A table depicting the time (hours) and number of repeats each sample was immersed in each reagent

Reagent	Time (hours)	Number of repeats
4% paraformaldehyde	24	1
0.1 M PBS	24	1
50% (vol/vol) ethanol	3	2
70% (vol/vol) ethanol	3	2
80% (vol/vol) ethanol	3	2
95% (vol/vol) ethanol	3	2
100% (vol/vol) ethanol	2	3
100% tert-butanol (>25°C)	48	1
50:50 paraffin wax to tert-butanol maintained at 60°C	48	1
100% paraffin wax maintained at 60°C	24	1

The samples prepared in the xylene trial were placed in two separate changes of a 50:50 xylene to 100% ethanol solution for one hour each. The samples were then placed in 100% xylene for one hour and 30 minutes. Post clearing, the samples were placed in a 30:70 paraffin wax to xylene solution maintained at 60°C for eight hours, then a 70:30 paraffin wax to xylene solution maintained at 60°C for eight hours and then finally 100% paraffin wax maintained at 60°C for eight hours.

The samples prepared in the tert-butanol trial were placed in 100% tert-butanol maintained above 25°C for 48 hours. The samples were then placed in a 50:50 paraffin wax to tert-butanol solution maintained at 60°C for a further 48 hours. The samples were then placed in 100% paraffin wax maintained at 60°C for 24 hours.

The paraffin that was used for the embedding process was first stored in the moulds for a period of 12 hours at 60°C to decrease the presence of bubbles. These moulds will be referred to as the embedding moulds from here on out. After the clearing process for both trials was completed, an optimized embedding process was used to decrease the presence of air bubbles, the probability of rupturing of the block and/or difficulty in the sectioning process.⁵¹ This involved the placement of the samples in the embedding moulds for four hours at 60°C. During this period, the moulds were shocked gently to rid the specimen of bubbles. The embedding moulds were then placed at room temperature until the surface of the wax began to solidify. At this point, the embedding moulds were carefully placed in an ice bath to enable fast solidification.

5.2.2.2 Results

During sectioning, it was evident that the samples cleared with xylene were more fragile and had an almost crystalized texture due to the hardening of the sample. It was difficult to produce ribbons with the microtome and therefore challenging to get slides without excessive artefacts. Additionally, one-week post-embedding, the samples retracted from the wax, had a dry appearance and were impossible to section.

The sections cleared with tert-butanol sectioned well and produced ribbons enabling easy slide retrieval with fewer artefacts compared to the xylene cleared samples. The samples had a longer 'shelf-life' as the wax completely penetrated the samples thus preventing the tissue from separating from the wax.

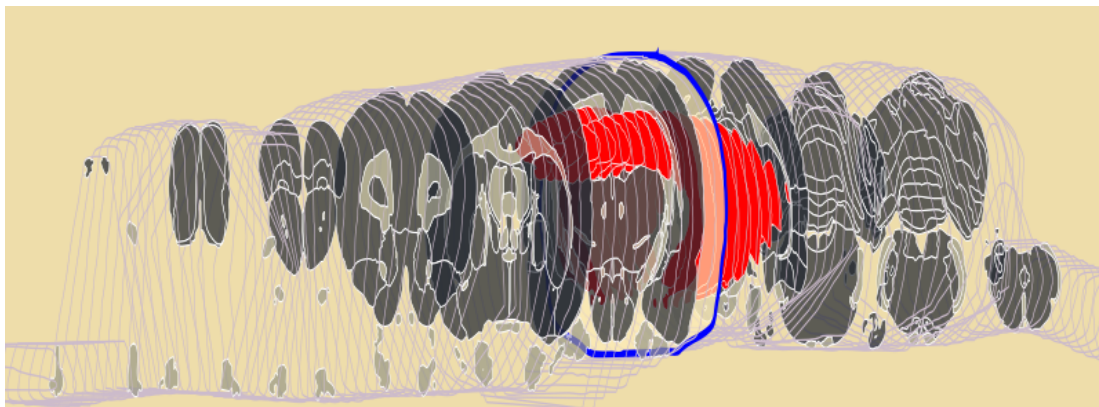
During the histological analysis, the samples were stained with haematoxylin and eosin. A comparison of samples from each clearing agent were compared with little to no difference observed in the staining efficacy. The samples cleared with xylene; however, had more tears and artefacts present.

Therefore, from these results, the method using tert-butanol as a clearing agent was deemed preferential over xylene clearing when specifically using large nervous tissue samples.

5.2.3 Sectioning

The samples were sectioned using a rotary wax microtome (Reichert-Jung, Ultracut E, Leica) into ultra-thin sections. For Congo Red and H&E staining the ideal thickness for the sections was stated as 5-10 μm . For Nissl staining the ideal thickness for the sections was stated as 5-30 μm . Therefore, all sections were sliced at 6 μm . The sections were then placed in the ThermoScientific Section Flotation Bath and collected with a glass slide. The glass slides were then placed on a hot plate to allow for the sample to dry.

The Waxholm Sprague Dawley rat brain atlas was used to determine the correct region to



section.⁵² Figure 5.1 makes use of the Waxholm model to visualise the sections of interest.

Figure 5.1: A Sprague Dawley rat brain atlas according to the Waxholm model⁵²

5.2.4. Staining procedures

5.2.4.1 General Tissue Morphology: Haematoxylin and Eosin Staining

The samples were stained using the haematoxylin and eosin method in order to evaluate general tissue morphology.

The slides were cleared in two changes of xylene for 10 minutes each. The slides were then rehydrated using descending ethanol concentrations. These steps consisted of two separate changes of 100% ethanol for two minutes each, one change of 90% ethanol for one minute and a further change of 70% ethanol for one minute. The sample slides were then placed in distilled water for one minute. The sample was then placed in haematoxylin solution (1 g/L haematoxylin, 0.2 g/L sodium iodate, 50 g/L potassium aluminium sulphate, 1 g/L citric acid and 50 g/L chloral hydrate) for 15 minutes in order to stain the cell nucleus and RNA-rich

portions of the cytoplasm of the cells. The slides were then transferred into Scott's Buffer (2 g/L potassium bicarbonate, 20 g/L magnesium sulphate) for eight minutes. This enabled the colour change of the stained sample from reddish-purple into a blueish-purple. The slides were then rinsed in distilled water and dipped in a 0.01 g/L eosin solution as a counterstain. After this, the tissue was dipped in ascending ethanol concentrations (70% ethanol, 90% ethanol, 100% ethanol) to dehydrate the tissue and ensure excess stain was removed. Finally, the slides were dipped in xylene and mounted with entellen and a cover slip.

After the samples had dried for a few minutes, the samples were examined with a Zeiss AXIO Imager.M2 (Carl Zeiss Microscopy, Munich, Germany).

5.2.4.2. Amyloid formation Analysis: Congo Red Staining

The samples were stained using the Congo Red method in order to evaluate the formation and deposition of amyloid in the tissue sections.

The slides were cleared in two changes of xylene for ten minutes each. The slides were then rehydrated using descending ethanol concentrations. These steps consisted of two separate changes of 100% ethanol for two minutes each, one change of 90% ethanol for one minute and a further change of 70% ethanol for one minute. The sample slides were then placed in distilled water for one minute.

The working Congo red staining solution comprised of 100 mL of stock solution A (0.05 grams of Congo red and 0.25 grams of Sudan Black in 0.1 litre of saturated NaCl 80% ethanol solution) and 1 mL of stock solution B (1% sodium hydroxide solution). This solution was viable for 20 minutes and therefore, a fresh solution was required for each staining cycle.

The rehydrated slides were placed in 50% ethanol for one minute. The slides were then transferred to a 50:50 solution of 50% ethanol and stock solution B for five minutes. The slides were then placed in the working Congo red solution for 20 minutes and then rinsed in distilled water. The sample was then rapidly differentiated (5-10 dips) in alkaline alcohol solution (0.1 g/L sodium hydroxide, 50% ethanol). After which, the sample was rinsed in running tap water for five minutes and then counterstained with haematoxylin for 10 minutes. The slides were then differentiated in Scott's buffer for eight minutes. After this, the sample was rinsed under running tap water for two minutes. The slide was then dipped

in ascending ethanol concentrations (70% ethanol, 90% ethanol, 100% ethanol) to dehydrate the tissue and ensure excess stain is removed. Finally, the slides were dipped in xylene and mounted with entellen and a cover slip.

After the samples had dried for a few minutes, the slides were examined with a Zeiss AXIO Imager.M2 (Carl Zeiss Microscopy, Munich, Germany). This staining procedure produced red stained amyloid deposits, elastic fibres and eosinophil granules and blue nuclei.

5.2.4.3 Nissl Body detection

The samples were stained using the Nissl staining method in order to detect the presence of Nissl bodies in the neurons of the brain tissue sections.

For this process to occur, the sample was cleared in xylene three times for 10 minutes each to remove the paraffin wax. The samples were then rehydrated using descending ethanol concentrations. This series consisted of placing the slides in two separate containers containing 100% ethanol for five minutes each, then in 95% ethanol for three minute and then in 70% ethanol for three minutes. The sample slide was then rinsed in running tap water and placed in distilled water for one minute. After which, the sample was stained in a 0.1% cresyl violet solution for seven minutes at 40°C. The higher temperature was used to improve stain penetration. The sample was then rinsed in distilled water. After this, the sample was differentiated in 95% ethyl alcohol for 15 minutes and checked microscopically for best result. The sample was then dehydrated in two changes of 100% alcohol for five minutes each and cleared twice in xylene for five minutes each. Finally, the samples were mounted with entellen and a cover slip.

After the samples had dried for a few minutes, the samples were examined with a Zeiss AXIO Imager.M2 (Carl Zeiss Microscopy, Munich, Germany). This staining procedure produced pink-violet stained Nissl bodies in the neurons.

5.3 Results

5.3.1 General tissue morphology

Histological examination of the H&E stained sections revealed the characteristic areas of the hippocampus and hippocampal formation. These include the hippocampus proper, dentate gyrus and subiculum. The specific areas of interest included the CA1 and CA3 regions (Figure 5.2).

The CA1 and CA2 regions are formed by a zone of small pyramidal cells whereas the CA3 and CA4 regions are formed by large pyramidal cells. The CA4 region projects into the concave structure formed by the two arms of the dentate gyrus. The dentate gyrus is formed of small granule cells.

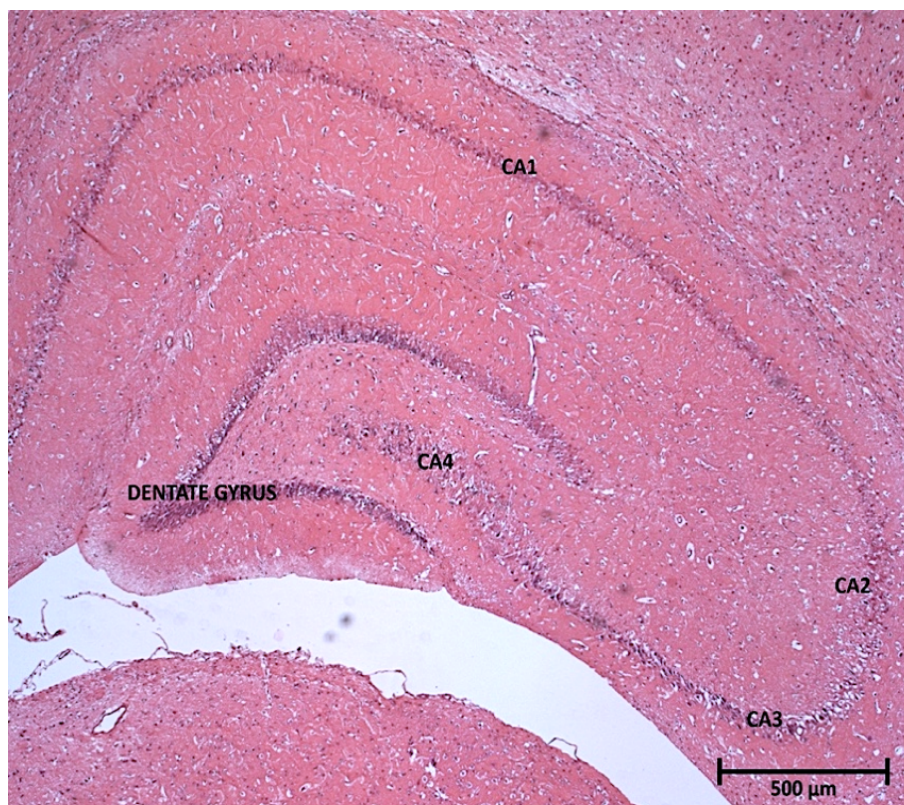


Figure 5.2: A micrograph from the control group showing the areas of interest found in the dorsal hippocampal region. The regions labelled include the CA1, CA2, CA3 and CA4 regions as well as the dentate gyrus. The dentate gyrus is seen surrounding the CA4 region by its upper and lower extensions. Areas not labelled include the molecular layer found between the concavity of the dentate gyrus and CA regions and the subiculum which is found to the left of the CA1 region.

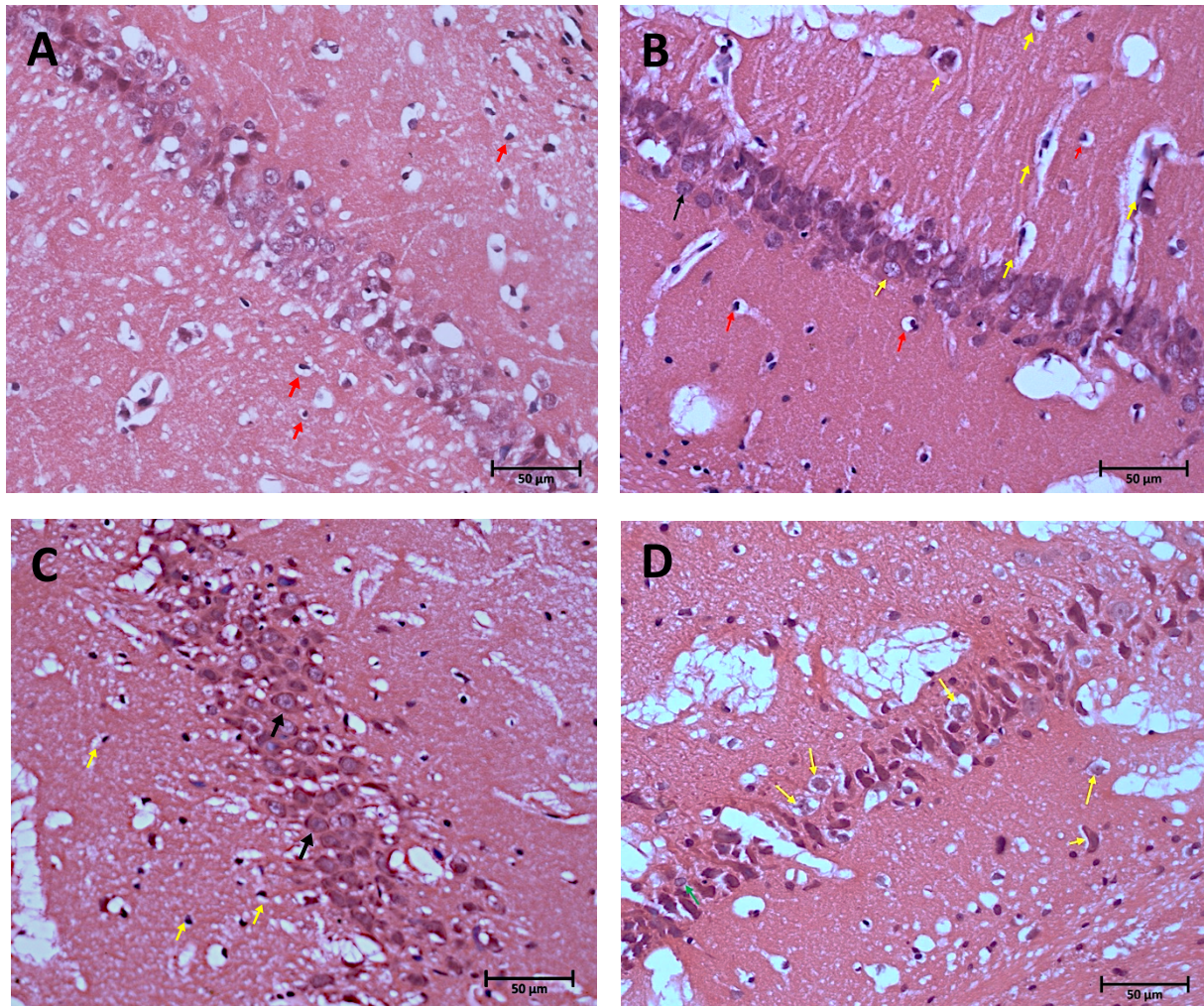


Figure 5.3: A micrograph of the CA1 region of the hippocampus proper from the control group (A), LPS treated group (B), the honey treated group (C) and the honey and LPS treated group (D). Black arrows indicate cells with visible nuclei. The green arrow indicates Alzheimer's type astrocytes. Red arrows indicate glial cells. Yellow arrows indicate degeneration neurons.

The glial cells in the LPS group appear enlarged compared to the other groups. The molecular layer in each of the images can be identified by the presence of large number of glial cells among the neuronal processes. The pyramidal layer appears to be thicker in the honey control group compared to the other groups.

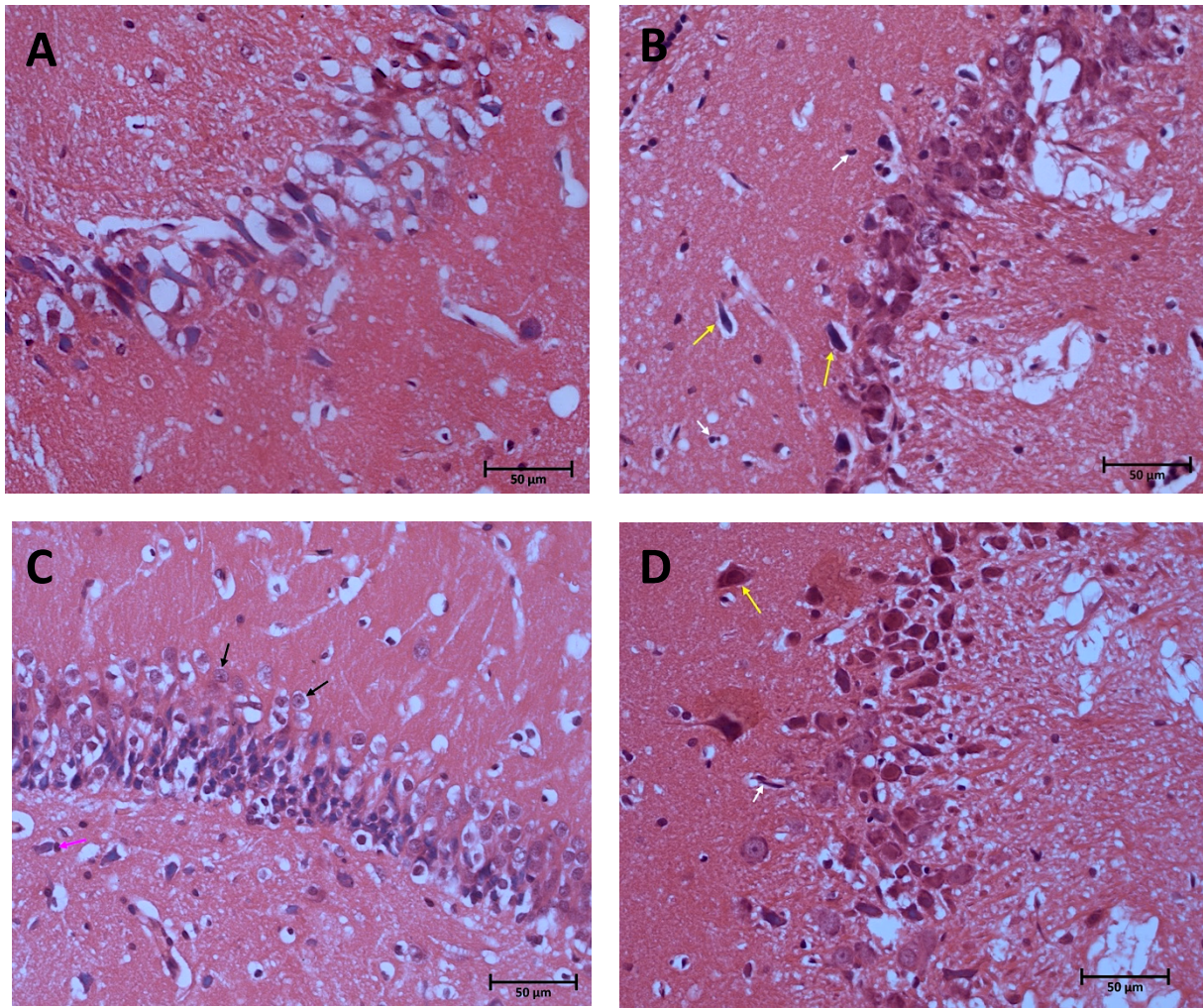


Figure 5.4: A micrograph of the CA3 region of the hippocampus proper from the control group (A), LPS treated group (B), the honey treated group (C) and the honey and LPS treated group (D). Black arrows indicate cells with visible nuclei. Yellow arrows indicate degeneration neurons. The pink arrow indicates an oligodendrocyte in close proximity to neuron. The white arrow indicates a microglial cell.

5.3.2 Amyloid deposition

There was some red pigment deposited in all four groups; however, the LPS group demonstrates a high incidence of positive amyloid detection using the Congo red staining method described above.

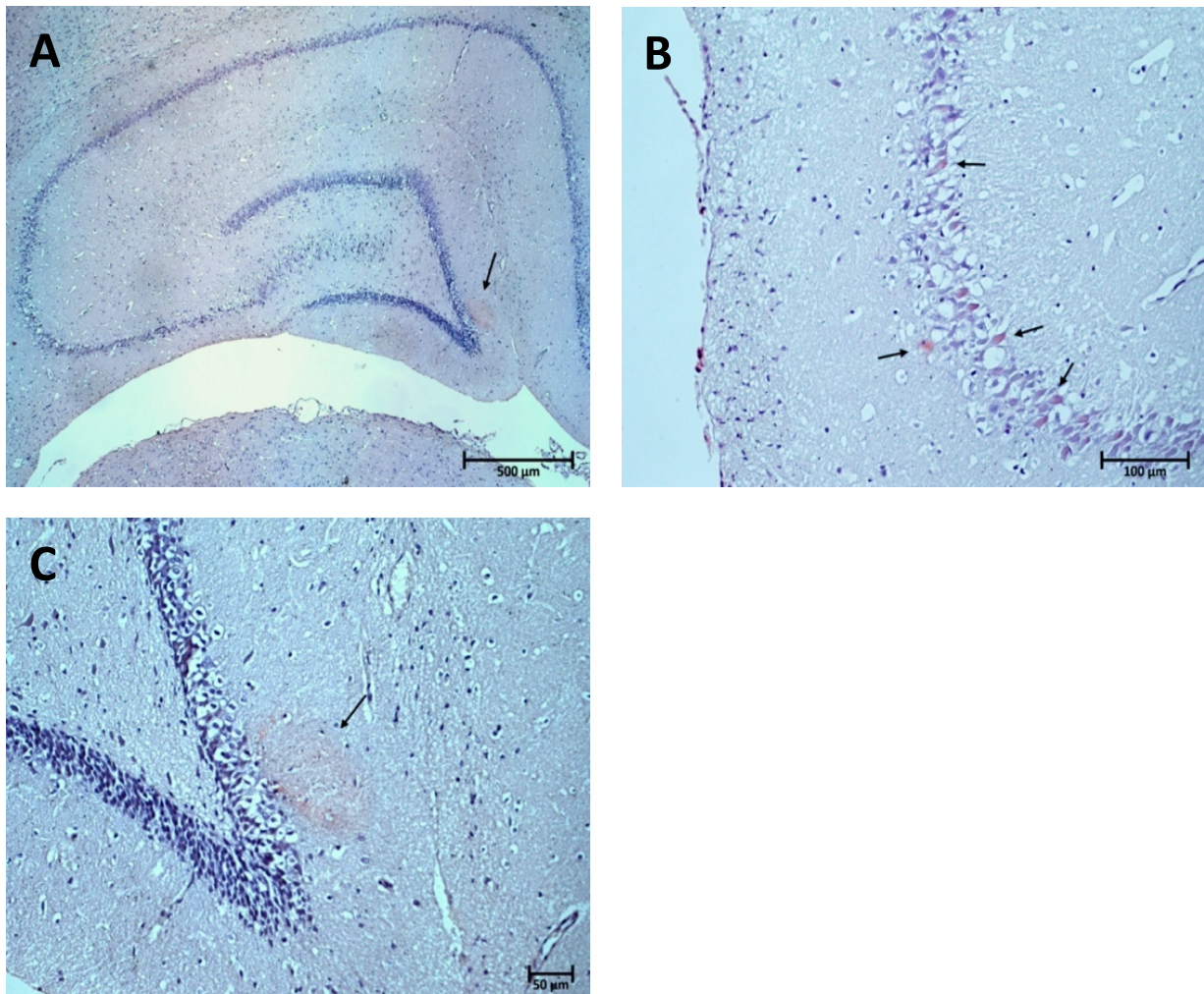


Figure 5.5: Collection of micrographs (A-C) of increasing magnification of the hippocampal region of the control group showing very little amyloid deposition (black arrows). Micrograph A shows the right hippocampus. Micrograph B and C are magnified sections of the hippocampus captured in A.

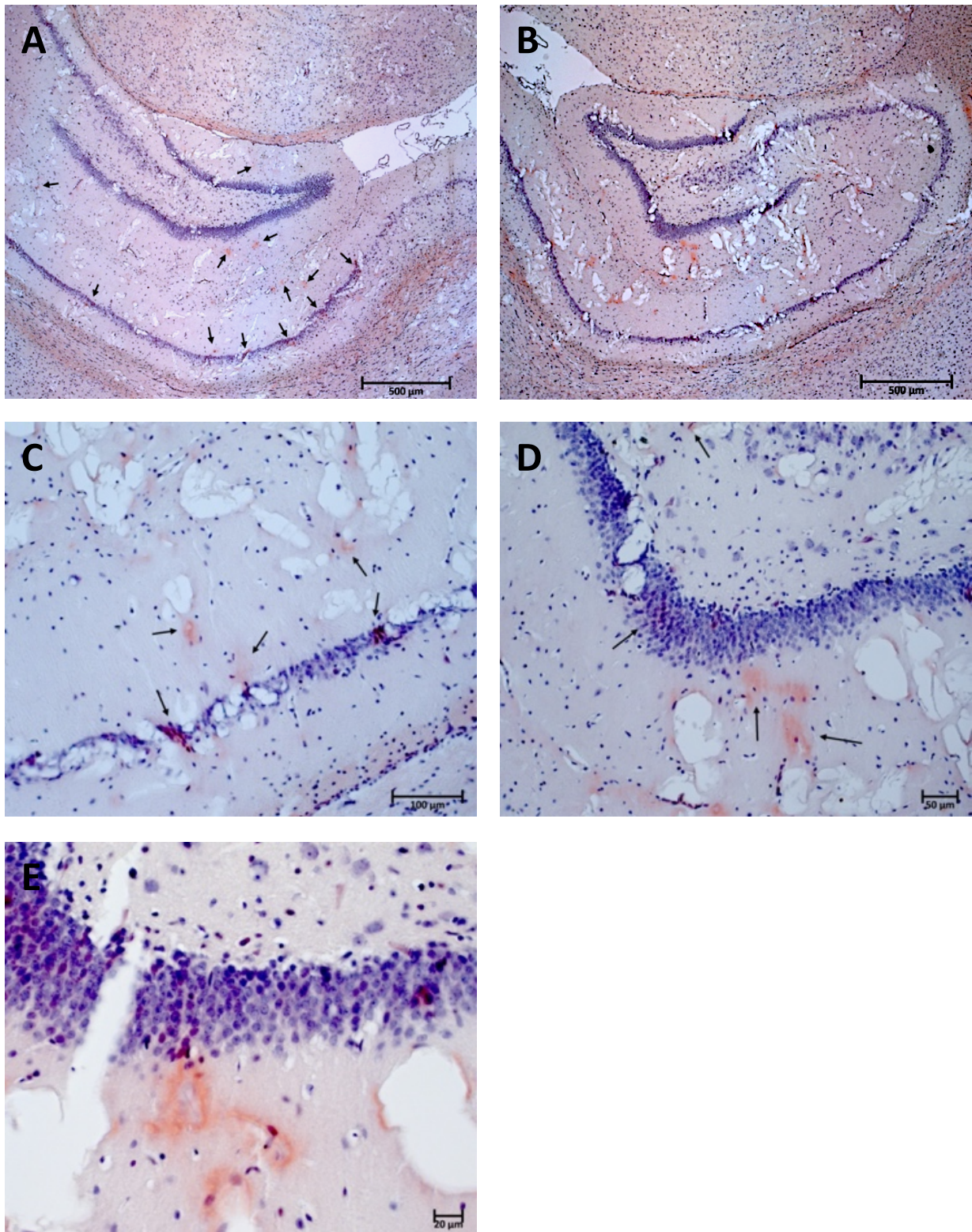


Figure 5.6: A collection of micrographs (A-E) of the hippocampal region of the LPS treated group showing increased presence of amyloid deposition (black arrows) as seen by the red shading. Micrograph A and B show the left on right hippocampal formations of different test animals. Micrographs C-D show increased magnification of regions within micrograph B.

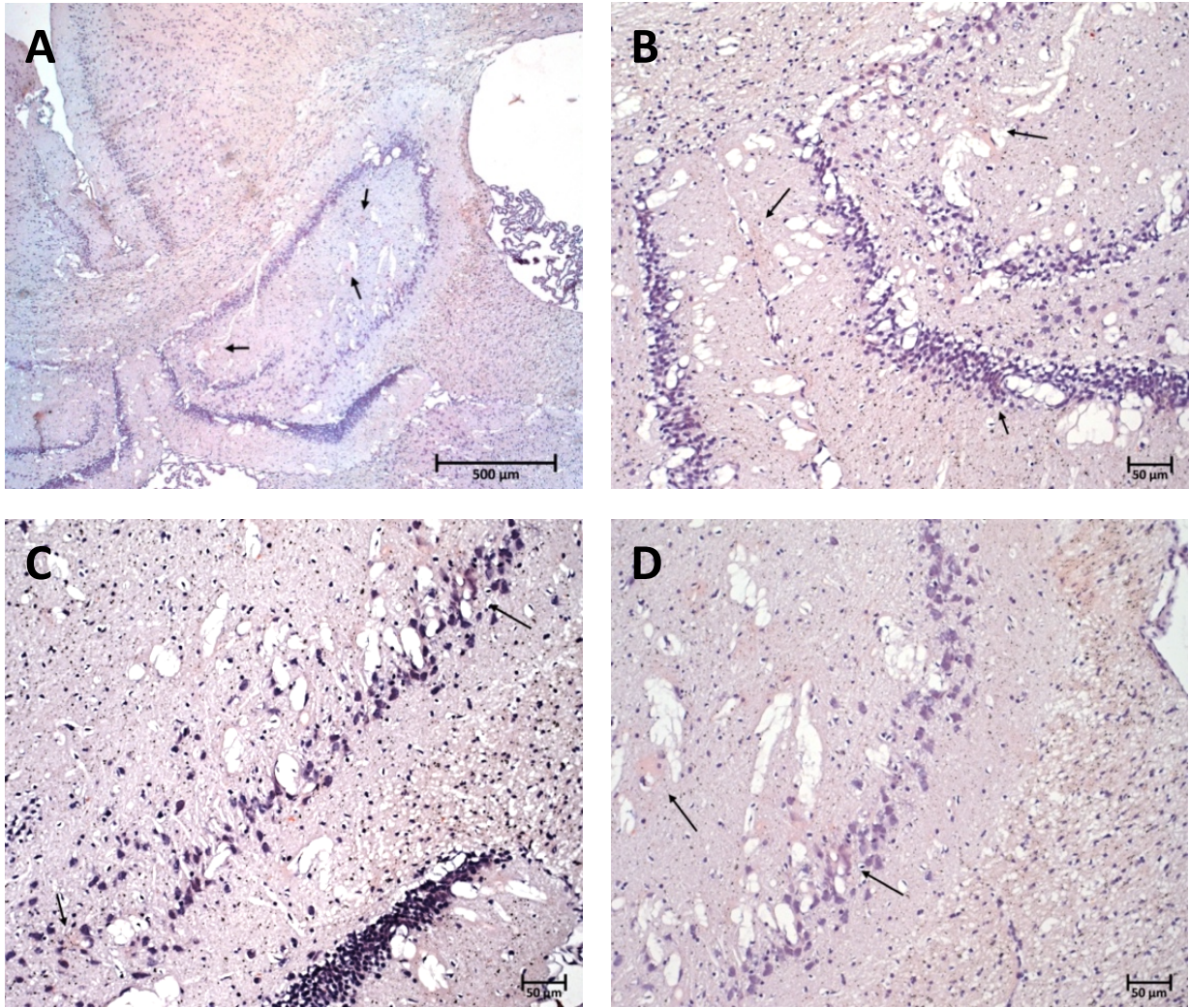


Figure 5.7: A collection of micrographs (A-D) demonstrating the mild amyloid deposition (black arrows) in the PBS and Honey group. Micrograph A shows an image of the entire right hippocampus and part of the left hippocampus. Micrograph B-C show magnified sections of the right hippocampus captured in A.

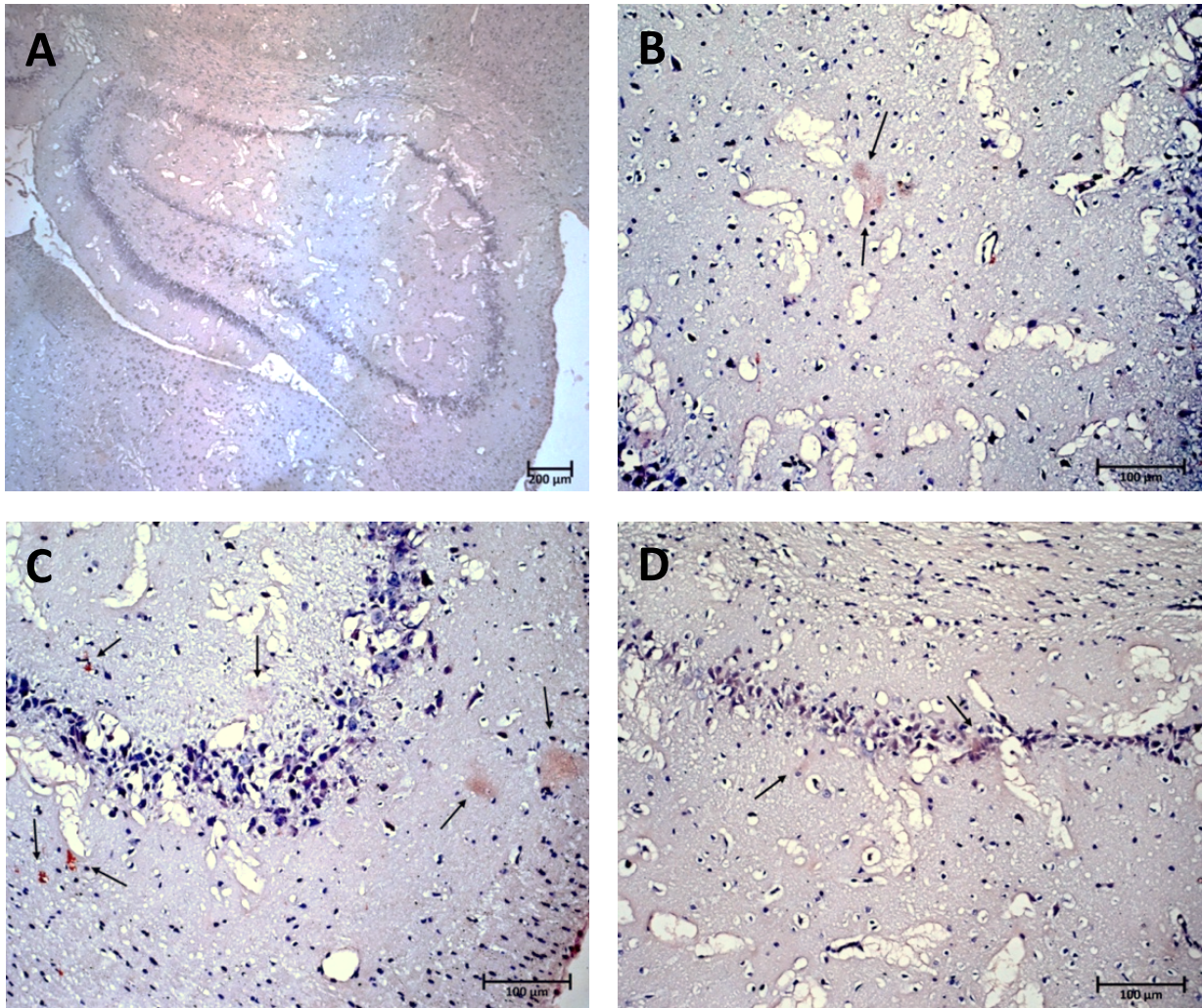


Figure 5.8: A collection of micrographs (A-D) demonstrating mild amyloid deposition (black arrows) in the LPS and Honey group. Micrograph A is of the right hippocampus. Micrographs B-D are magnified sections of the hippocampus captured in A.

5.3.3 Nissl body staining

There was a decreased density in Nissl stain observed in the LPS exposed groups; however, due to tissue tearing during the tissue processing procedures, the results obtained and the relevance thereof are limited.

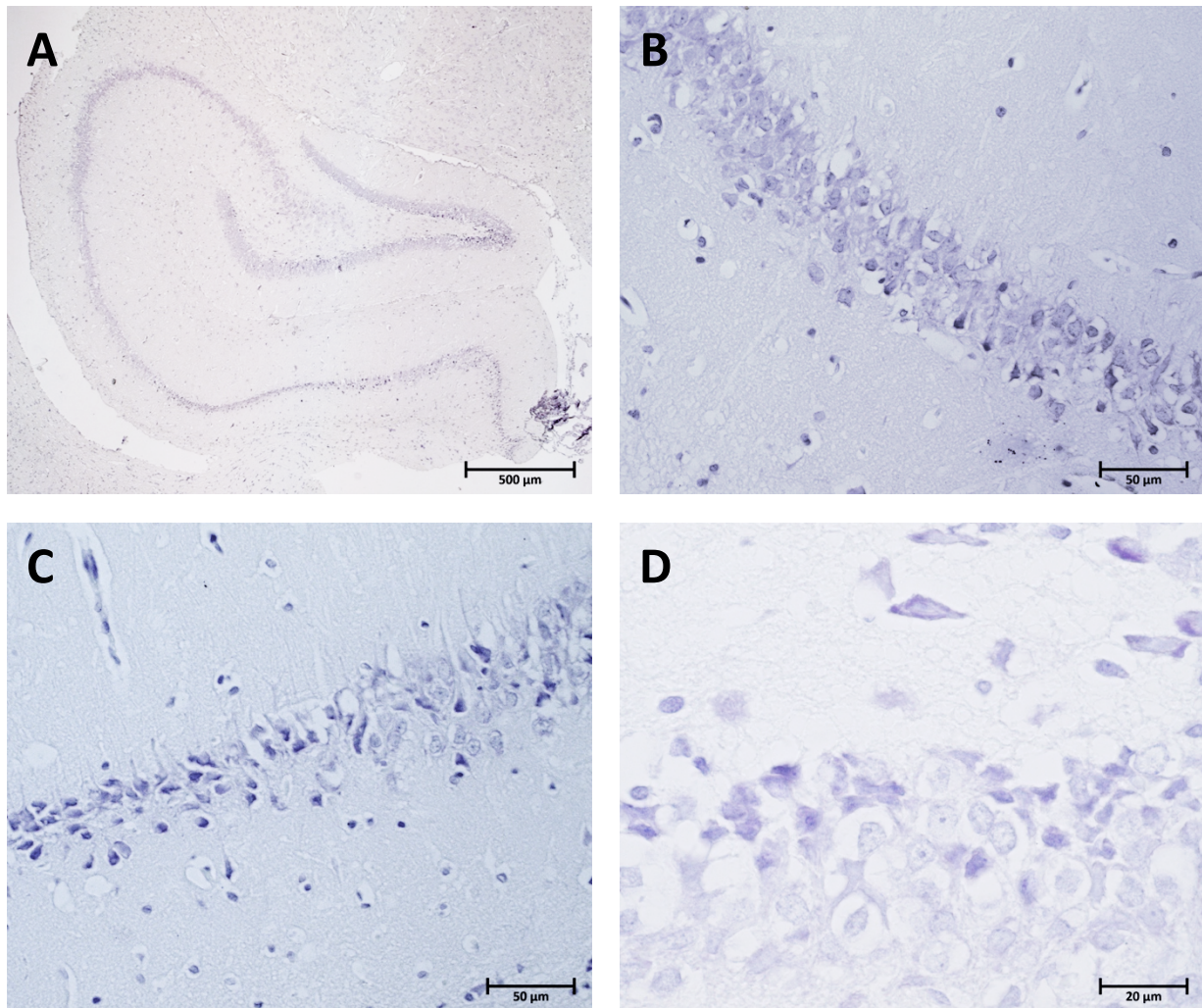


Figure 5.9: A collection of micrographs (A-D) of Nissl stained samples from the control group. Micrograph A shows the left hemisphere. Micrograph B-D shows images of the CA1 region with higher magnification.

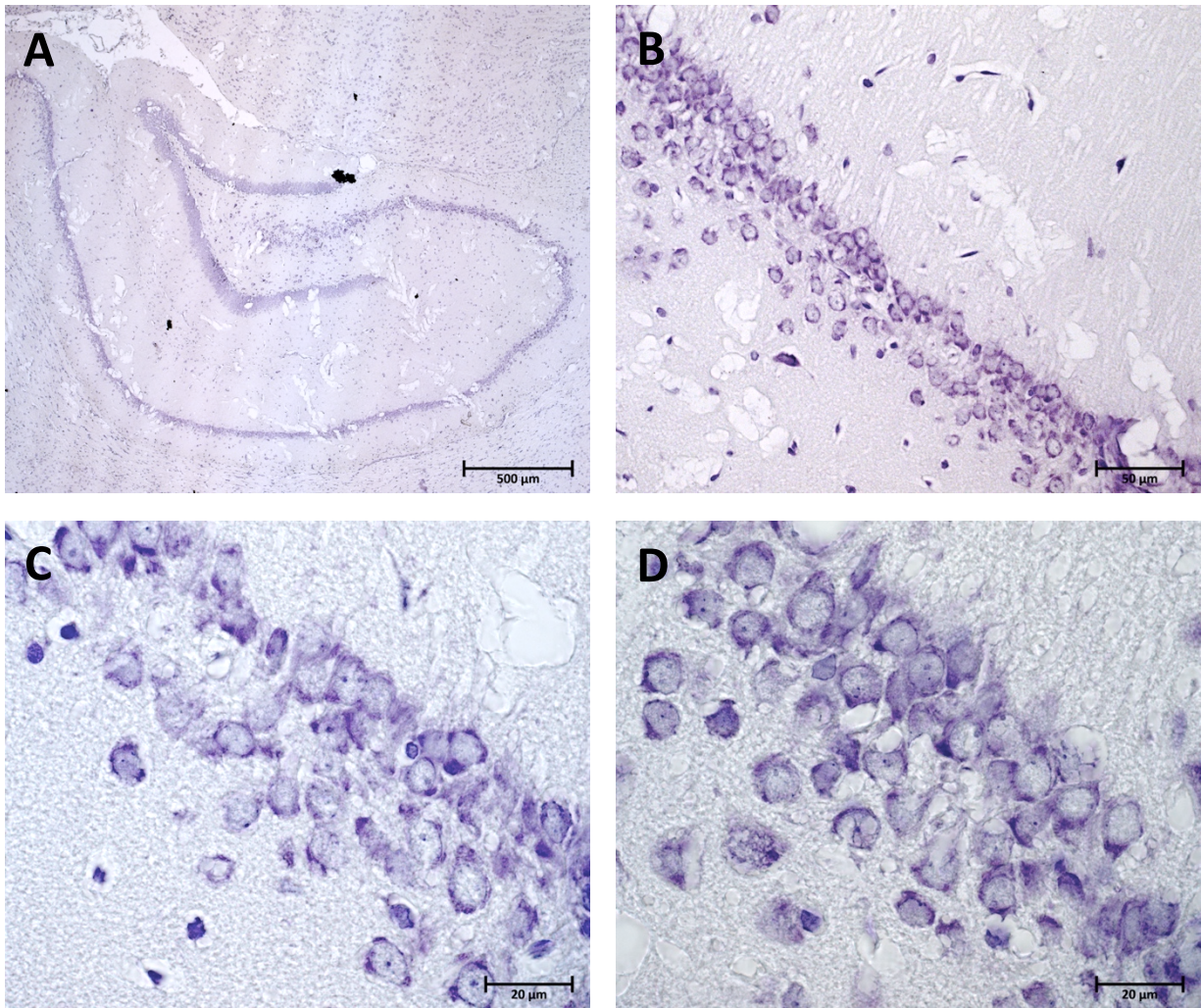


Figure 5.10: A collection of micrographs of Nissl stained samples from the LPS exposed group. Micrograph A shows the entire right hippocampal region. Micrograph B-D are images of increased magnification of the CA1 region.

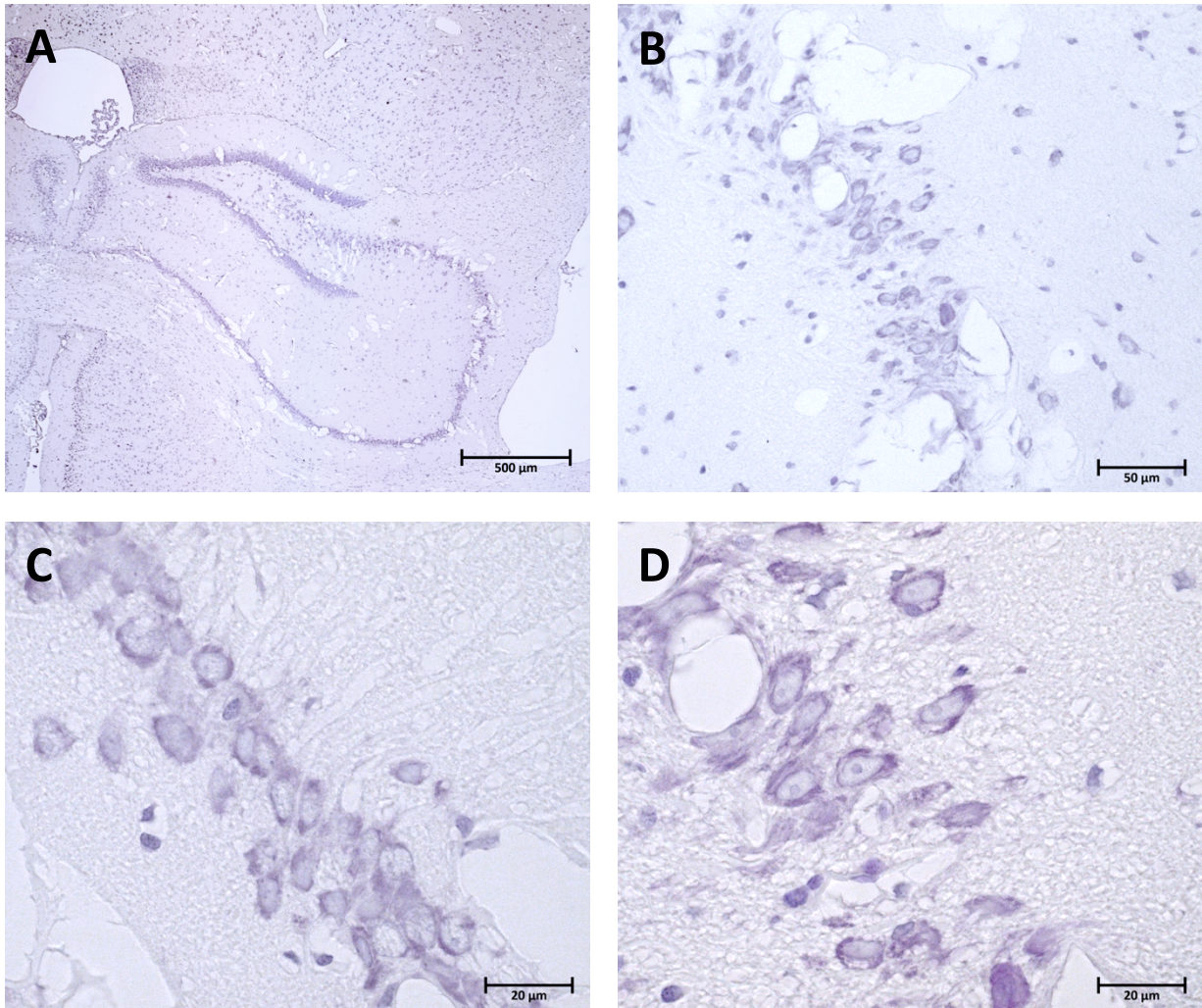


Figure 5.11: A collection of micrographs of Nissl stained samples from the honey administered group. Micrograph A shows the entire right hippocampal region. Micrograph B-D are images of increased magnification of the CA1 region.

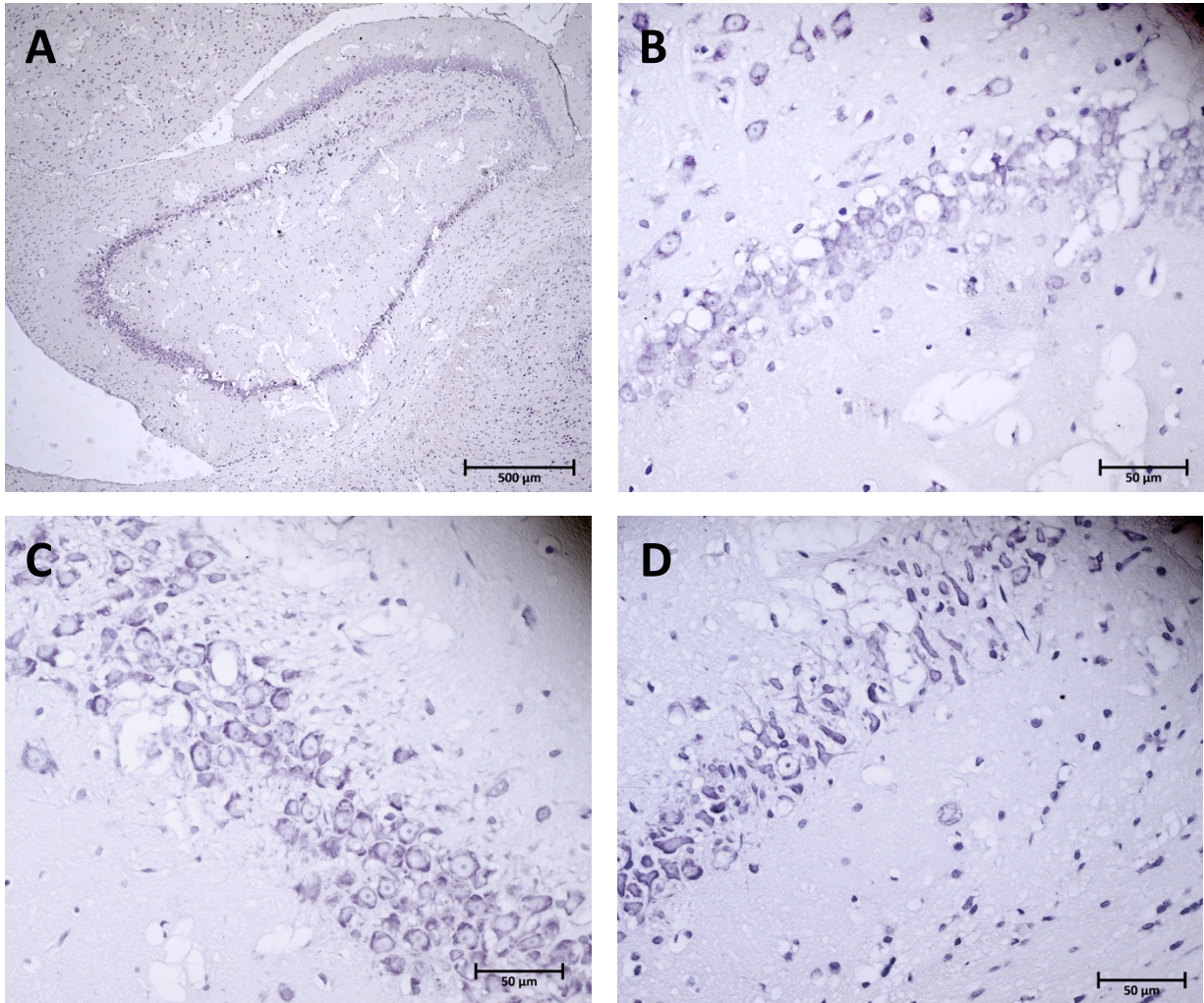


Figure 5.12: A collection of micrographs of Nissl stained samples from the LPS and honey exposed group. Micrograph A shows the entire left hippocampal region. Micrograph B-D are images of increased magnification of the CA1 region.

5.4 Discussion

Haematoxylin and Eosin (H&E) staining was used to investigate the general tissue structure of the CA1 and CA3 regions. In these regions, the monomorphic pattern of the dark neurons within the pyramidal layer of the hippocampus was examined. The presence of the neuron swelling and vacuolation, degenerating neurons, Alzheimer's type and other astrocytes, oligodendrocytes and microglial cells was also examined.

The examination of the H&E stained slides revealed the effects of LPS administration in the form of cell death, enlarged glial cells and disruption of normal layer organisation. The enlarged glial cells may be the earliest indication of some response to the presence of systemic LPS.

In both the CA1 and CA3 regions, the pyramidal layer in the LPS group appeared the thinnest. This is associated with the clumping of neuronal processes (appearing as excess eosinophilia) which is indicative of damage to these neurons. This is an important observation as the CA1 region plays an important role in the monosynaptic circuit and both these regions play an important role in the trisynaptic circuit.⁵³ These circuits are associated with the maintenance or strengthening of memories and the formation of new memories, respectively. This correlates to alterations in both granule cell neurons and the atrophy of CA1 pyramidal cells observed in AD affected brains and the decreased efficiency in these circuits as observed by Llorens-Martin et al., (2014). They also noted that the variable atrophy or neuronal loss resulted in variable symptomatic presentation. This may explain why the observed atrophy did not have clinical presentation in the behavioural testing as it may not have caused an impairment in the behavioural parameters that we were testing but some other immeasurable feature. Additionally, it may not have resulted in a behavioural impairment to a sufficient extent so as to produce a measurable behavioural change in the parameters that were tested. This is further substantiated by the lack of quantitative correlation between neuronal cell loss and behavioural impairment where clear atrophy and neuronal cell death is present in those with only mild symptomatic presentation.⁵³ This demonstrates that atrophy can predate moderate to severe clinical presentation.

Dark neurons are a common artefact in H&E staining of the hippocampus.⁵⁴ This artefact can be differentiated from degenerating neurons by examining cell body shrinkage, loss of Nissl substance, intensely stained eosinophilic cytoplasm, and pyknotic nucleolus. Degenerating neurons are also heterogenous in appearance and can be found in various stages of degeneration compared to the monomorphic appearance of the dark neuron artefact. Degenerating neurons were present in all groups with the highest concentration in the LPS group and then the LPS + honey group.

The observed increase in degenerating neurons demonstrate how the processes that maintain healthy neurons have become impaired. These processes include communication, metabolism and repair.⁵⁵ When the neurons in the CA1 region and other regions of the hippocampus experience a reduction in activity, lose their connections with other neurons and eventually die, the destruction and death of these cells results in memory failure, personality changes, difficulty with daily tasks and other key features of the disease. Although sufficient cell death has not occurred in the current study to result in clinical presentation, the cell death that has occurred is indicative of the early stages of this pathophysiological change.

The Congo red test for amyloid detection showed an increased presence of amyloid deposition in the LPS treated group compared to the other groups. This indicates that systemic LPS leads to some form of increased amyloid presence; whether by increased production or decreased clearance mechanisms. This links to the increased size of the microglial cells found since these cells are responsible for the release inflammatory cytokines, complement components, chemokines and free radicals which are known to contribute to the formation of amyloid β production and accumulation.⁵⁶ The increased level of amyloid deposition in the exposed groups is similar to that observed in groups exposed to a single dose intraperitoneal injection in a study conducted by Wang et al., (2018). The LPS and honey treated group did not display the widespread amyloid deposition displayed in the LPS alone group. This indicates that the administration of honey provided relief to the mechanisms involved in the amyloid accumulation experienced by the LPS group.

The increase in A β in the exposed groups may be a response to the oxidative injury caused by exposure to LPS.⁵⁷ This response may serve a protective function by inducing mitochondrial dysfunction. The analysis of possible mitochondrial dysfunction requires alternative methods of tissue preparation and viewing and, therefore, will be examined using transmission electron microscopy in the next chapter.

The limited presence of A β in the controls plays an important role within the CNS as A β at physiological levels reduces the excitatory activity of potassium channels of neuronal cells as well as reduces neuronal cell death.⁵⁸ Therefore, low concentrations of A β provide a neuroprotective effect and play an important role in the release of specific neurotransmitters that aid in the improving synaptic plasticity and memory. However, high concentrations have the opposite effect by resulting in inhibited memory formation and increased neuro-inflammatory processes. This demonstrates that A β is a hormetic protein and, once it reaches a critical level, it becomes inhibitory in memory formation. Although there is an increased level of amyloid deposition in the LPS exposed groups, this deposition may not have reached this critical level. This may be due to the short exposure time to LPS or small LPS exposure concentration.

The Nissl body stain demonstrated a decreased density of Nissl stain. The Nissl body represents the protein synthetic machinery of the cell and is, therefore, representative of the cell activity and sensitivity to damage of the neuron.⁵⁹ Damaged neurons may appear as vacuolated, swollen, shrunken or dark when staining with indistinct Nissl substance. Therefore, the decreased density or distinctiveness of the Nissl stain in the LPS exposed group may be indicative of a loss of Nissl substance due to degeneration of neurons. The results obtained from the Nissl staining technique are limited due to the decreased quality of the images obtained due to tissue tearing during sample preparation.

Although, light microscopy is a good technique to provide information on the structure and distribution of cells, a major limitation of this technique is that the staining methods do not provide information on the membrane and organelle structure.

5.5 Conclusion

The subtle differences observed between the groups in the light micrographs indicates that there is some altered hippocampal activity, pyramidal cell death and amyloid accumulation between the groups.

In order to get a more comprehensive view of these processes, the cells need to be examined in more depth and at a higher magnification. Additionally, the possibility that mitochondrial dysfunction has occurred as part of a protective mechanism against oxidative damage requires further exploration.

ULTRASTRUCTURAL ANALYSIS

Chapter Objectives:

- Discussion on the relevance of ultrastructural changes in the hippocampal tissue
- Preparation of the tissue for transmission electron microscopy analysis
- Critical analysis of the changes in the tissue

6.1 Introduction

There is a link between altered central nervous system and systemic inflammation.⁶⁰ In order to provide insight into the possible alterations in the nervous tissue that were not detectable by the previous methods, the microglial cells and their interaction with synapses were evaluated. The microglia were of specific interest as previous research conducted by Savage et al., (2019) demonstrated that LPS treated mice displayed larger cell bodies as well as less complex cellular processes. The area of specific interest was the CA1 area of the hippocampus as this region, responsible for learning and memory, is often impacted by peripheral LPS administration.⁶¹

Peripheral inflammation and the increase of circulating levels of proinflammatory cytokines results in the increased activity of microglia and therefore the increased expression of inducible nitric oxide producing enzymes which remain elevated for several days. This high level of nitric oxide serves the purpose of destroying the invading bacteria. Unfortunately, a consequence of this high level of nitric oxide is the apoptosis of nearby neurons.⁶¹

The mitochondrion is also an important organelle to observe due to its function in adenosine triphosphate (ATP) synthesis. The mitochondria differ in size, shape and number based on the requirements of the tissue. There are, however, similarities in mitochondrial structure. The mitochondrion has two membranes. The outer membrane plays an important role in the transport of small molecules as well as the conversion of lipid containing compounds into useable compounds for the mitochondria. The inner membrane folds into structures known as cristae which project into the mitochondrial matrix, the area between the two membranes. The mitochondrial matrix and the region within the inner membrane, the intramembranous space, both contain enzymes, minerals and DNA/RNA important in

the production of ATP. The mitochondria were evaluated for possible loss of membrane integrity and irregular shape which may indicate impaired mitochondrial function.

The rough endoplasmic reticulum (rER) functions to produce proteins. It consists of stacks of flattened interconnected membranous sacs known as cisternae. The rough appearance of the rER is caused from the attachment of ribosomes to the membrane. The rER was examined for dilation or increased size as this could indicate increased water uptake by the cell or increased protein production respectively.

In this chapter, the possible ultrastructural changes in the CA1 region of the hippocampus after exposure to LPS and honey, either alone or in combination, were investigated. Special interest was placed on the microglia; however, the shape, size and number of mitochondria and endoplasmic reticulum was also examined.

6.2 Methods

Tissue was collected for analysis with transmission electron microscopy (TEM) as described in chapter 3. In order to perform an ultrastructural analysis, the hippocampus was removed from the intact right hemisphere. The sagittal view of right hemisphere can be seen in figure 6.1. The hippocampus is located in the medial temporal lobe, below the cortical regions and therefore careful removal is required.

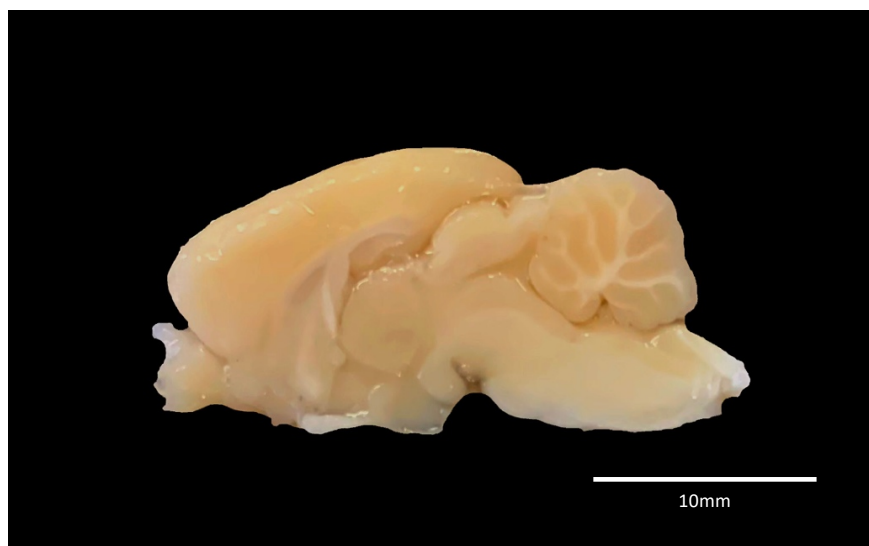


Figure 6.1: The sagittal view of the right hemisphere of an LPS exposed Sprague Dawley rat

This process began with the removal of the cerebellum and the prefrontal cortex by means of a scalpel. Once the middle section of the brain was acquired, the cortex was gently lifted using a pair of fine tweezers (figure 6.2).



Figure 6.2: Image demonstrating the lifting of the cortex away from the midbrain

The cortex separated easily from the midbrain to reveal the hippocampus (indicated in figure 6.3). The cortex was then cut away using a scalpel. Once the hippocampus was visible, the rest of midbrain was gently separated from the hippocampus using the tweezers (figure 6.4). The remaining non-hippocampal tissue was also removed using tweezers leaving the intact hippocampus.

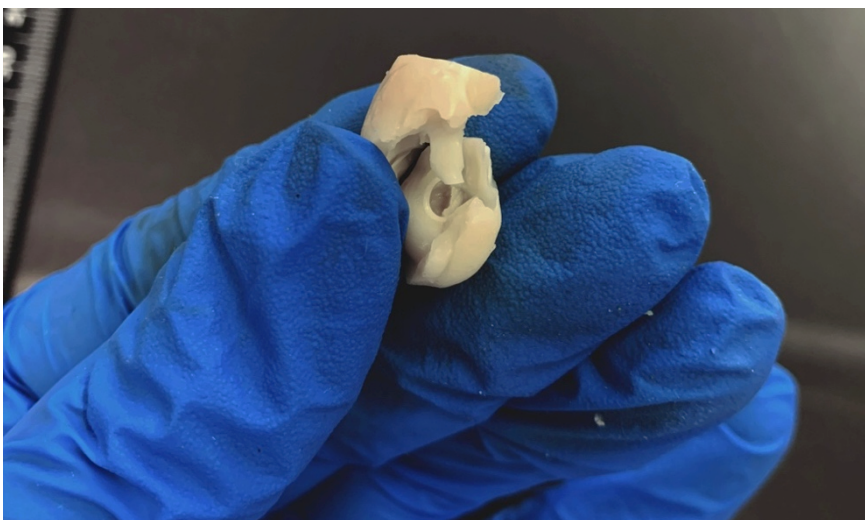


Figure 6.3: Image of the separation of the midbrain from the hippocampal region

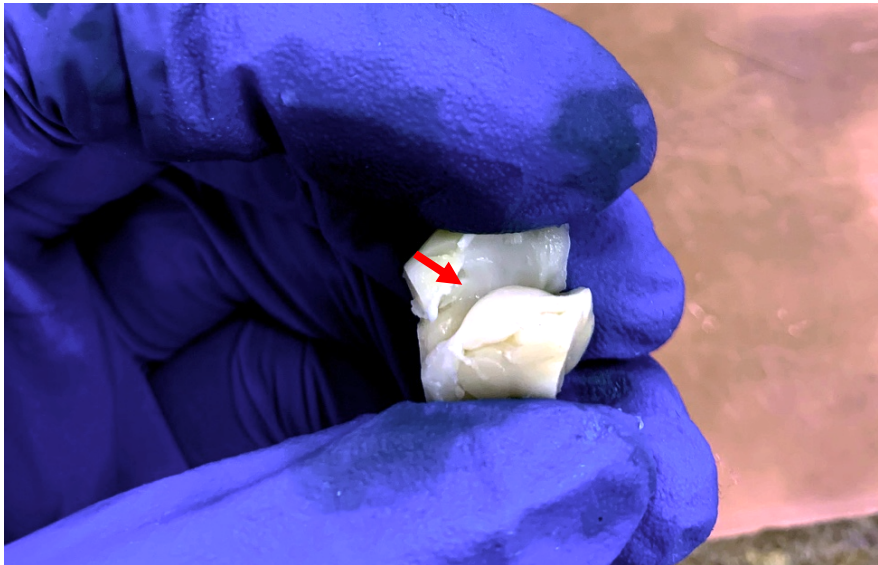


Figure 6.4: Image of the lifted cortical region with the exposed hippocampus (indicated by red arrow)

The intact hippocampus was then separated into a head, body and tail using a scalpel. This division is demonstrated in figure 6.5. This was to enable the specific comparison of lateral regions of the hippocampus between groups. Each section was then divided into three separate slices and further cut into four equal cubes to separate the CA1, CA2, CA3 and dentate gyrus. This resulted in approximately 1mm³ sections. All areas were embedded in resin; however, only the CA1 areas of the head portion were examined.

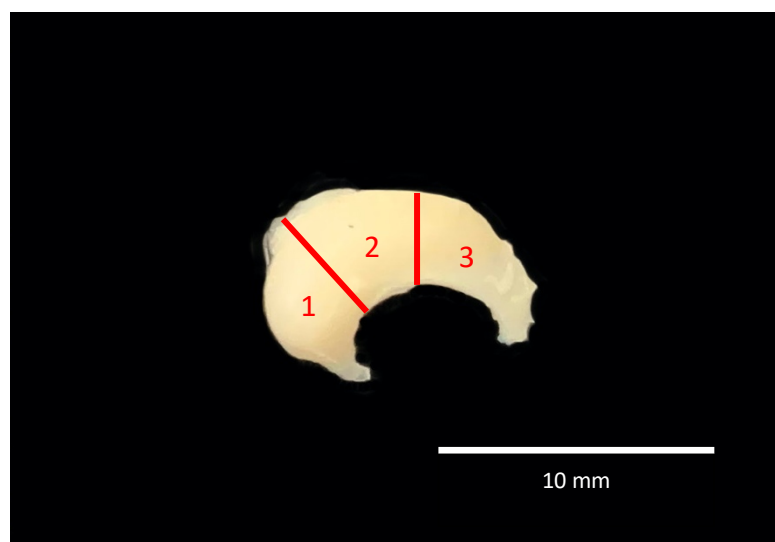


Figure 6.5: An intact hippocampus of an LPS exposed rat showing the head (1), body (2) and tail (3) as defined during sectioning

These sections were placed in 2.5% glutaraldehyde-formaldehyde (GA/FA) fixative (1 mL glutaraldehyde, 1 mL formaldehyde, 3 mL distilled water, 5 mL buffer) for one hour. The sections were then washed three separate times, for 15 minutes each, in a 50:50 phosphate buffer. Following washing, the section was placed in the fume hood with osmium tetroxide for one hour. The section was then rinsed for 15 minutes in 50:50 sodium phosphate buffer in the fume hood and twice more outside the fume hood. Dehydration of the tissue was then carried out using a single change of 30%, 50%, 70% and 90% ethanol solutions and three changes of 100% ethanol for 15 minutes each. The samples were then left in new 100% ethanol overnight.

The following morning, the samples were placed in new 100% ethanol. The sample was then placed in a 50:50 resin ethanol mixture and spun for 30 minutes. The sections were then placed in a 100% resin mixture and spun for a further four hours. The resin mixture and allocated sample numbers were then transferred to the moulds. The moulds were placed in the oven at 60°C for 38 hours to polymerize.

Once polymerization occurred, the samples were shaped using a minora blade and trimmed using the ultramicrotome glass knife. The sample was then cut with a DiATOME diamond knife, picked up with a copper grid and placed in the grid holder. The sample was contrasted with uranyl acetate for five minutes and lead citrate for two minutes. After the samples had dried for a few minutes, the samples were examined with a JEOL JEM 2100F transmission electron microscope (JEOL Ltd., Tokyo, Japan).

6.3 Results

6.3.1 Mitochondrial Presence

The TEM micrographs of the samples obtained from the control group revealed normal cellular ultrastructure, with mitochondria presenting with normal shape and size as well as intact mitochondrial membranes.

The TEM micrographs of the samples obtained from the LPS group demonstrated decreased mitochondrial membrane integrity with disruptions and breaks in the membrane. This may be indicative of lipid peroxidation or impaired mitochondrial function.

The TEM micrographs of the samples obtained from the LPS and honey group showed possible mitochondrial membrane degradation.

The TEM micrographs obtained from the honey group demonstrated mitochondria with normal shape and size as well as intact membranes.

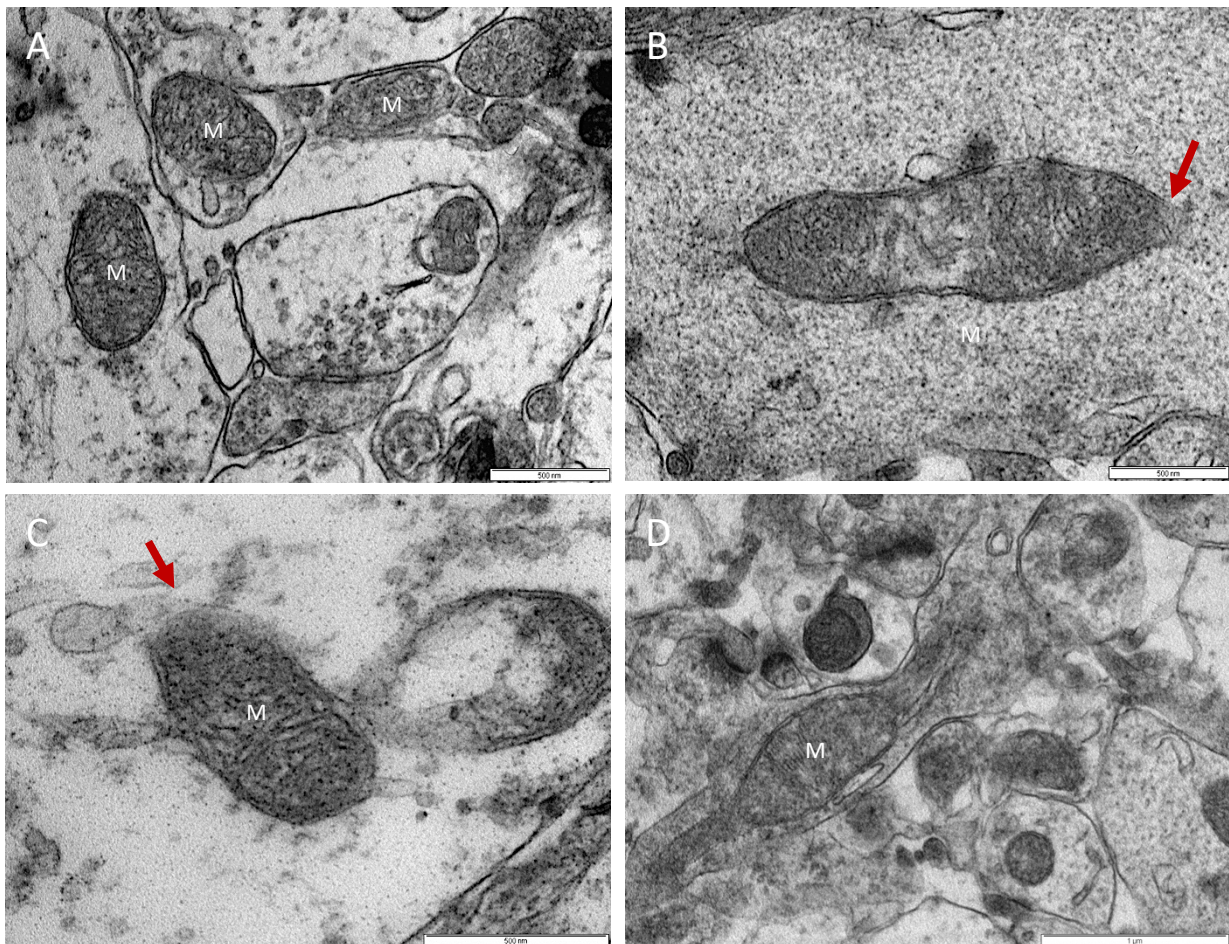


Figure 6.6: TEM micrographs of mitochondrial presence among the groups. Micrograph A indicates the presence of at least three normal mitochondria (M) in close proximity of each other within the control group. Micrograph B indicate a single mitochondrion with elongated and enlarged shape and deteriorating outer membrane (marked by arrow) observed in the LPS group. Micrograph C indicates a slightly enlarged mitochondria with intact inner membrane and possible outer membrane deterioration (arrow) observed in the LPS and honey group. Micrograph D indicates a mitochondrion with normal shape and size as well as intact inner and outer membranes observed in the honey group.

6.3.2 Rough endoplasmic reticulum

The rER observed in the control group was minimal suggesting that abnormal level of protein synthesis was occurring with minimal protein accumulation. However, this group did not demonstrate the same level of organisation within the rER.

By comparison, the LPS exposed group had extensive rER presence with increase space between the cisternae. This is indicative of increased protein synthesis or protein accumulation due to misfolding. There was also a mild level of dilation observed in the rER of this group. This is indicative of some low level of ER stress.

The rER present in the LPS and honey group demonstrated an increased size compared to the control but a decreased size compared to the LPS group. This is indicative that there was an increased level of protein synthesis but not to the extent of that present in the LPS group.

The rER observed in the honey exposed group was similar in extent to that of the control group. This is indicative of undisturbed cellular metabolism of the hippocampal tissue of this group.

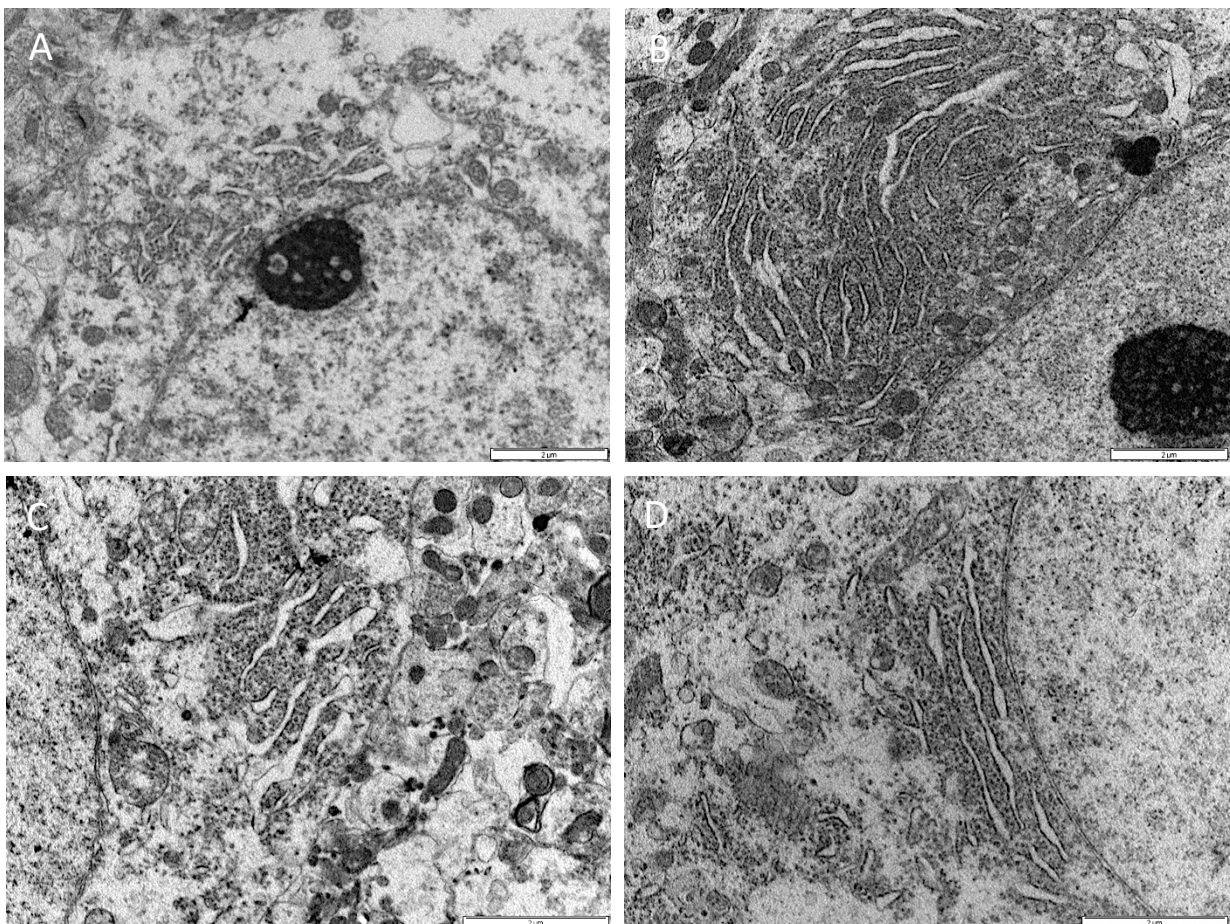


Figure 6.7: TEM micrographs of the rough endoplasmic reticulum observed surrounding the pyramidal neuron nucleus. Micrograph A shows a smaller endoplasmic reticulum observed in the control group. Micrograph B shows a more extensive, more organised rER observed in the LPS group. Micrograph C shows an intermediate rER observed in the LPS and honey group. Micrograph D shows a similar size rER observed in the honey group.

6.4 Discussion

The effect of systemic LPS on the nervous tissue ultrastructure seen in this study may be cause for concern due to the possible presence of LPS in the brain of AD patients compared to controls as well as the increased presence of LPS containing pathogens, such as *E. coli*, in a South African context.⁶ In this chapter, the ultrastructural effects of LPS and honey administration alone and in combination were evaluated by observing the mitochondria and rough endoplasmic reticulum in the CA1 region of the dorsal hippocampus using TEM. The criteria observed included mitochondrial membrane disruption, mitochondrial matrix swelling, nuclear membrane disruption, rough endoplasmic reticulum size and dilation and the presence of secretory vesicles around the endoplasmic reticulum.

Although, the neuronal accumulation of both abnormal tau protein and A β form the pathological hallmarks in those affected by AD, the detailed pathogenic mechanism of the disease is widely unknown. However, there is growing evidence that suggests the presence of damaged or impaired mitochondria plays a fundamental role in the pathogenic mechanism of the disease.⁶² The mitochondria plays a central role in regulating cell survival and cell death under the influence of various stressors. Therefore, the decrease in membrane integrity in the LPS exposed group is of special relevance when explaining the increased neuronal cell death observed in the LPS exposed group during the morphology analysis.

The difference observed in the mitochondrial shape, abundance and membrane integrity observed in the LPS exposed group and the control group aligns with research that indicates differences in mitochondria in AD patients compared to non-AD individuals.⁶³ It is unknown, in clinical circumstance, whether the mitochondrial dysfunction is a by-product of the fundamental pathological events of AD or whether they play a relatively upstream role in the disease with evidence supporting both hypotheses.^{62,63} Therefore, although the

mitochondrial impairment is evident in the groups exposed to LPS, it is unclear whether, in clinical circumstance, this would predate or postdate clinical presentation thus not contradicting the results obtained in the behavioural memory testing performed in chapter 4.

Additionally, symptomatic presentation aside, the mitochondrial dysfunction observed has been established as one of the intracellular processes severely compromised in the early stages of the disease.^{64,65} Since this observed alteration in the mitochondrial membrane is present with no observed difference in the behavioural memory testing of chapter 4, this mitochondrial dysfunction may also be seen as an early feature and predate clinical presentation specifically in the LPS model of the disease.

There is presence of the decreased membrane integrity in the LPS exposed group whereas the mitochondrial membrane appears normal in the control and honey groups. Additionally, the LPS and honey group displays some intermediary mitochondrial membrane integrity loss. This demonstrates that the LPS exposure results in some sort of altered mitochondrial activity and that honey may play an important protective function against the mechanism that causes this alteration. This is an important observation in this study as the mitochondria has been marked as a potential target in AD therapeutic strategies.⁶⁵

The ER plays a role in multiple crucial cellular functions by being an important organelle in the intracellular process of protein synthesis. However, since only properly folded proteins are transported to the golgi apparatus, when misfolded or unfolded proteins are produced they accumulate and induce stress in the ER. Additionally, another intracellular signalling network, known as the unfolded protein response, is activated. This ER stress has been reported in post mortem, *in vitro* and *in vivo* studies of AD and has been implicated in the pathogenesis of the disease.^{66,67}

Additionally, under normal circumstance, there is normal production of specific proteins that are able to bind to APP and prevent the formation of A β .⁶⁶ However, when ER stress is induced the production of these proteins is inhibited which leads to the increased production of A β . Therefore, the possible low-level ER stress due to increased protein accumulation and rER dilation observed in the LPS exposed group may be linked to the increased amyloid deposition observed in this group in the morphology analysis.

The ER stress and accumulation of misfolded proteins triggers a cascade of events that aim to clear unfolded proteins and restore the homeostasis of the ER.⁶⁸ However, under circumstances where the severity of this stress is too extreme, it cannot be reversed and apoptotic cell death of the neuron occurs. This may further increase the strength of the link between the low-level ER stress observed in the LPS exposed group and the observation made in the morphology analysis as it may link the ER stress to the increased neuronal cell death observed.

The intermediary change in the LPS and honey group compared to that of the control and LPS exposed group may demonstrate the possibility of targeting ER stress in therapeutic strategies. This is substantiated by various *in vivo* and *in vitro* studies conducted that demonstrate targeting ER stress and ER stress-mediated apoptosis may contribute to a therapeutic method of recovery from AD.^{69–72}

6.5 Conclusion

Although there were alterations observed between the groups, these alterations were minor and not wide spread. These alterations may lead to subclinical changes that do not yet impact the general behaviour of the animal; however, the long-term effect of these changes may induce AD associated pathology.

From the ultrastructural findings of the current chapter, it can be concluded that LPS and honey exposure alone and in combination had some effect on the ultrastructure and integrity of different organelles within the hippocampal CA1 region of the brain. This effect was not widespread, nor was it severe. This may be due to the low-level exposure or the short duration of exposure.

In order to demonstrate whether this exposure may cause a widespread, severe effect on function and ultrastructure of this region, a higher concentration of LPS or an increased exposure period would be of special interest.

However, these observations are important as the importance of stress induced in subcellular organelles as a pathological mechanism of the disease is an important field of research in both the pathogenesis of AD and possible therapeutic strategies.

CONCLUSION

Much research has been conducted on the pathophysiology of AD mainly due to the high and increasing prevalence worldwide as well as its debilitating symptoms. Many scientific models have been formulated in order to study the progression and possible pathophysiology of the disease, with the LPS-induced neuroinflammatory model being of significant interest. The importance of this model is further heightened in the South African context due to the increased prevalence of infection by certain gram-negative bacteria such as *E. coli*. This model suggests that LPS found in the outer membrane of such bacteria enters the body through the increasingly 'leaky' gut of the aged individual resulting in chronic systemic inflammation and eventually chronic neuro-inflammation. This chronic level of neuro-inflammation results in increased amyloid β deposition and thus increased Alzheimer's pathology.

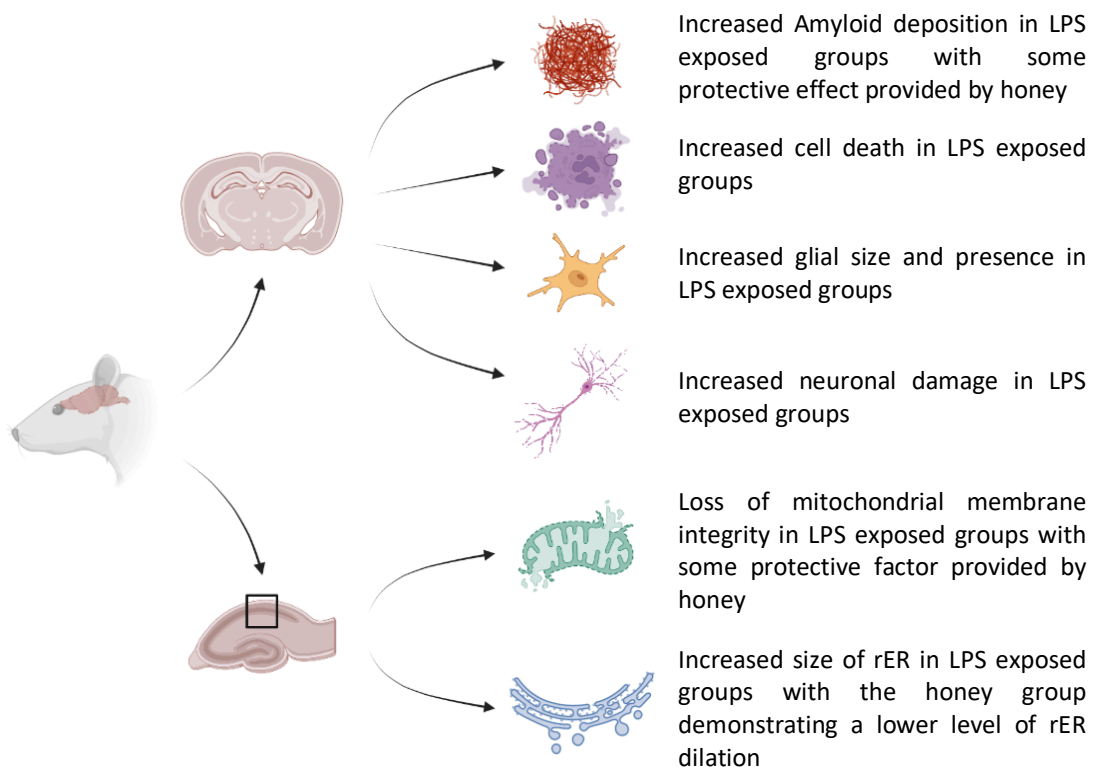
In this study, the Sprague Dawley rat model was used to investigate the effects of low-level exposure to systemic LPS on the dorsal hippocampal region of the brain. Based on existing research, small concentrations of LPS were administered to Sprague Dawley rats in order to produce low level systemic and neuro-inflammatory response. Additionally, Manuka honey was administered as a possible protective factor against this inflammatory response. This predicted response as well as the possible presence of Alzheimer's like pathology was investigated by antemortem behavioural studies that examined the alterations in sickness behaviour, anxiety levels, object recognition memory, and spatial memory. In addition to this, post-mortem histological analysis was carried out. This included both light microscopy techniques to observe changes in general morphology, amyloid beta deposition and Nissl body formation as well as transmission electron microscopy techniques to examine mitochondrial and rER alterations. The Sprague Dawley model was successfully implemented over a thirteen-day period during which the animals were exposed, tested and terminated. As indicated in chapter 3, there was no significant change in animal weight or sickness behaviour throughout the duration of the study, nor was there a significant difference in the brain weight to body weight ratio between the groups. Additionally, chapter 4 demonstrated that there was no significant difference between the performance of the animals in the behavioural testing. Therefore, the low-level exposure to LPS or the

duration used in this study was not sufficient to result in symptomatic presentation of Alzheimer related behaviour or significant nervous atrophy.

The histological analyses produced limited results of significance with the main finding demonstrating a higher level of amyloid deposition in the LPS exposed groups. This deposition occurred to a lesser extent in the group also exposed honey. This amyloid deposition was not sufficient to result in symptomatic presentation but did cause subclinical changes to the tissue.

The ultrastructural analysis also produced results of limited significance as only subtle changes were observed in the mitochondrial membrane integrity, mitochondrial shape and size and features of the rER. Although alterations were present, there was either not a sufficient amount of time to cause a metabolic change in the nervous tissue resulting in symptomatic presentation or a great enough extent of change to result in symptomatic alteration.

The overall observations obtained from the histology and ultrastructural analysis can be



summarised in figure 7.1.

Figure 7.1: Summary of results obtained from the histological and ultrastructural analysis. (Image created using Biorender.com⁷³)

Therefore, a common theme and great limitation of this study was either the duration of exposure or the concentration of LPS administered, or a combination of both. Although the research suggested that the concentration used and exposure period was sufficient to result in low levels of inflammation and some type of neuro-inflammatory response, this response was not sufficient to produce significant results in this study.

However, as presented in the literature review, there does exist a preclinical stage of Alzheimer's disease where biochemical alterations, amyloid deposition and metabolic changes occur in the nervous tissue without sufficient severity to cause clinical presentation. Therefore, although this study was not able to produce clinical presentation in the behavioural tests or widespread alteration in the histology or ultrastructural analysis, it may have demonstrated the beginnings of a preclinical stage of the progression of AD.

In conclusion, this study suggests that LPS and honey exposure alone and in combination does produce some level of response in the dorsal hippocampal region of the Sprague Dawley brain. This response was not sufficient to produce statistically significant differences in behaviour amongst the groups but was sufficient to cause mild alteration in amyloid deposition as well as ultrastructural alteration in the integrity of different organelles within the hippocampal CA1 region of the brain.

The research reported in this thesis, may contribute to the pool of knowledge regarding the neuro-inflammatory response that results from LPS exposure. However, since the main focus of this study was to examine the possible contribution of LPS to AD and the possible neuroprotective effect of Manuka honey on this contribution, more extensive research needs to be conducted, possibly by implementing a longer exposure period or increased exposure concentration.

BIBLIOGRAPHY

1. Prince M, Comas-Herrera A, Knapp M, Guerchet M, Karagiannidou M. World Alzheimer Report 2016: Improving healthcare for people living with dementia. *Alzheimer's Dis Int.* 2016;96–100. Available from: <https://www.alz.co.uk/research/world-report-2016>
2. Prince M, Bryce R, Albanese E, Wimo A, Ribeiro W, Ferri CP. The global prevalence of dementia: A systematic review and meta-analysis. *Alzheimer's Dement.* 2013;9(1):63–75.
3. Keene CD, Montine TJ, Kuller LH. Epidemiology, pathology, and pathogenesis of Alzheimer disease [Internet]. UpToDate. 2018. Available from: https://www-uptodate-com.uplib.idm.oclc.org/contents/epidemiology-pathology-and-pathogenesis-of-alzheimer-disease/print?search=alzheimer+dementia&source=search_result&selectedTitle=2~150&usage_type=default&display_rank=2
4. Zakaria R, Yaacob WMHWAN, Othman Z, Long I, Ahmad AH. Lipopolysaccharide-Induced Memory Impairment in Rats: a Model of Alzheimer's Disease. *Physiol Res.* 2017;66:553–65.
5. Scott KA, Ida M, Peterson VL, Prenderville JA, Moloney GM, Izumo T, Murphy K, Murphy A, Paul R, Stanton C, Dinan TG, Cryan JF. Revisiting Metchnikoff: Age-related Alterations in Microbiota-Gut- Brain Axis in the Mouse. *Brain, Behav Immun.* 2017;65:20–32.
6. Zhan X, Decarli C, Phinney B, Sharp FR. Gram-negative bacterial molecules associate with Alzheimer disease pathology. *Neurology.* 2016;87(22):2324–32.
7. Benedikz E, Kloskowska E, Winblad B. The rat as an animal model of Alzheimer's disease. *J Cell Mol Med.* 2009;13(6):1034–42.
8. Leong X, Ng C, Jaarin K. Animal Models in Cardiovascular Research: Hypertension and Atherosclerosis. *Biomed Res Int.* 2015;2015.

9. Sherwin E, Dinan TG, Cryan JF. Recent developments in understanding the role of the gut microbiota in brain health and disease. *Ann N Y Acad Sci.* 2017;1420(Special Issue: The Year in Neurology and Psychiatry):5–25.
10. Erejuwa OO, Sulaiman SA, Wahab MSA. Honey: A Novel Antioxidant. *Molecules.* 2012;17:4400–23.
11. Sawikr Y, Yarla NS, Peluso I. Neuroinflammation in Alzheimer ' s Disease : The Preventive and Therapeutic Potential of Polyphenolic Nutraceuticals. 1st ed. Vol. 108, Stress and Inflammation in Disorders. Elsevier Inc.; 2017. 33–57 p.
12. Agronin ME. Alzheimer's disease and other dementias: A practical guide. 3rd ed. New York: Routledge; 2014. 39–149 p.
13. Heneka MT, Carson MJ, Khoury JE, Landreth GE, Brosseron F, Feinstein DL, Jacobs AH, Wyss-Coray T, Vitorica J, Ransohoff RM, Herrup K, Frautschy SA, Finsen B, Brown GC, Verkhratsky A, Yamanaka K, Koistinaho J, Latz E, Halle A, Petzold GC, Town T, Morgan D, Shinohara ML, Perry VH, Holmes CA, Breitner JC, Cole GM, Golenbock DT, Kummer MP. Neuroinflammation in Alzheimer's disease. *Lancet Neurol.* 2015;14(April):388–405.
14. van Praag H. Lifestyle Factors and Alzheimer's Disease. *Brain Plast.* 2018;4(1):1–2.
15. Möller HJ, Graeber MB. The case described by Alois Alzheimer in 1911. *Eur Arch Psychiatry Clin Neurosci.* 1998;248(3):111–22.
16. Patterson C. World Alzheimer Report 2018 The state of the art of dementia research: New frontiers. *Alzheimer's Dis Int.* 2018;4–15. Available from: <https://www.alz.co.uk/research/world-report-2018>
17. Sherva R, Kowall NW. Genetics of Alzheimer disease [Internet]. UpToDate. 2018. Available from: https://www-uptodate-com.uplib.idm.oclc.org/contents/genetics-of-alzheimer-disease?sectionName=Othercandidategenes&search=alzheimerdementia&topicRef=16575&anchor=H899456&source=see_link#H899456
18. Jager CA De, Msemburi W, Pepper K, Combrinck MI. Dementia Prevalence in a Rural

- Region of South Africa : A Cross-Sectional Community Study. *J Alzheimer's Dis.* 2017;60:1087–96.
19. Anand KS, Dhikav V. Hippocampus in health and disease: An overview. *Ann Indian Acad Neurol.* 2012;15(4):239–46.
 20. Fogwe LA, Reddy V, Mesfin FB. Neuroanatomy, Hippocampus. *StatPearls.* 2021.
 21. Albert MS, DeKosky ST, Dickson D, Dubois B, Feldman HH, Fox NC, Gamst A, Holtzman DM, Jagust WJ, Petersen RC, Snyder PJ, Carrillo MC, Thies B, Phelps CH. The diagnosis of mild cognitive impairment due to Alzheimer's disease: Recommendations from the National Institute on Aging-Alzheimer's Association workgroups on diagnostic guidelines for Alzheimer's disease. *Alzheimer's Dement.* 2011;7(3):270–9.
 22. Thal DR, Griffin WST, de Vos RAI, Ghebremedhin E. Cerebral amyloid angiopathy and its relationship to Alzheimer's disease. *Acta Neuropathol.* 2008;115(6):599–609.
 23. Sperling RA, Aisen PS, Beckett LA, Bennett DA, Craft S, Fagan AM, Iwatsubo T, Jack CR, Kaye J, Montine TJ, Park DC, Reiman EM, Rowe CC, Siemers E, Stern Y, Yaffe K, Carrillo MC, Thies B, Morrison-Bogorad M, Wagster M V., Phelps CH. Toward defining the preclinical stages of Alzheimer's disease: Recommendations from the National Institute on Aging-Alzheimer's Association workgroups on diagnostic guidelines for Alzheimer's disease. *Alzheimer's Dement.* 2011;7(3):280–92.
 24. Anthon L, Blohm L, Brown B, Christman E, Davis T, Ernstmeyer K, Nicol A, Palarski V, Rastall L, Sigler J. *Nursing Fundamentals: Open resource for nursing.* 2019. 378–402 p.
 25. Johnson KA, Fox NC, Sperling RA, Klunk WE. Brain Imaging in Alzheimer Disease. *Cold Spring Harb Perspect Med.* 2012;2(a006213):1–23.
 26. Klunk WE, Engler H, Nordberg A, Wang Y, Blomqvist G, Holt DP, Bergstro M, Savitcheva I, Debnath ML, Barletta J, Price JC, Sandell J, Lopresti BJ, Wall A, Koivisto P, Antoni G, Mathis CA, Långstro B. Imaging Brain Amyloid in Alzheimer ' s Disease with Pittsburgh Compound-B. *Ann Neurol.* 2004;55(3):306–19.
 27. Budson AE, Solomon PR. Alzheimer's Disease Dementia and Mild Cognitive Impairment Due to Alzheimer's Disease. In: *Memory Loss, Alzheimer's Disease and*

- Dementia. Second Edi. Elsevier Inc.; 2016. p. 47–69.
28. Kitazawa M. M.I.N.D. Project: Alzheimer disease (AD) [Internet]. University of California, Merced. Available from: http://ucmkitazawa.web.fc2.com/mind_project.html
 29. Candiracci M, Piatti E, Dominquez-Barragán M, García-Antrás D, Morgado B, Ruano D, Gutiérrez JF, Parrado J, Castaño A. Anti-inflammatory Activity of a Honey Flavonoid Extract on Lipopolysaccharide-Activated N13 Microglial cells. *J Agric Food Chem.* 2012;60:12304–11.
 30. Perry VH, Teeling J. Microglia and macrophages of the central nervous system: The contribution of microglia priming and systemic inflammation to chronic neurodegeneration. *Semin Immunopathol.* 2013;35(5):601–12.
 31. Keep Memory Alive. Normal vs. Alzheimer’s Brain [Internet]. Available from: <https://www.keepmemoryalive.org/brain-science/alzheimers-brain>
 32. Li Z, Zhu H, Zhang, Ling, Qin C. The intestinal microbiome and Alzheimer’s disease: A review. *Anim Model Exp Med.* 2018;1(August):180–8.
 33. Sherwin E, Sandhu K V, Dinan TG, Cryan JF. May the Force Be With You: The Light and Dark Sides of the Microbiota – Gut – Brain Axis in Neuropsychiatry. *CNS Drugs.* 2016;30:1019–41.
 34. Nazem A, Sankowski R, Bacher M, Al-abed Y. Rodent models of neuroinflammation for Alzheimer’s disease. *J Neuroinflammation.* 2015;12(74):1–15.
 35. Budson AE, Solomon PR. Non-pharmacological Treatment of the Behavioural and Psychological Symptoms of Dementia. In: *Memory Loss, Alzheimer’s Disease and Dementia.* Second Edi. Elsevier Inc.; 2016. p. 218–25.
 36. Budson AE, Solomon PR. Pharmacological Treatment of the Behavioral and Psychological Symptoms of Dementia. In: *Memory Loss, Alzheimer’s Disease and Dementia.* Second Edi. Elsevier Inc.; 2016. p. 226–34.
 37. Bogdanov S, Jurendic T, Sieber R, Gallmann P, Bogdanov S, Jurendic T, Sieber R,

- Gallmann P. Honey for Nutrition and Health: A Review. *J Am Coll Nutr.* 2013;27(6):677–89.
38. Sairazi NSM, Sirajudeen KNS, Asari MA, Mummedy S, Muzaimi M, Sulaiman SA. Effect of tualang honey against KA-induced oxidative stress and neurodegeneration in the cortex of rats. *BMC Complement Altern Med.* 2017;17(31):1–12.
39. Moore A, Wu M, Shaftel S, Graham K, O'Banion M. Sustained expression of interleukin-1B in mouse hippocampus impairs spatial memory. *Neuroscience.* 2009;164(4):1484–95. Available from: <http://dx.doi.org/10.1016/j.neuroscience.2009.08.073>
40. Czerniawski J, Miyashita T, Lewandowski G, Guzowski JF. Systemic lipopolysaccharide administration impairs retrieval of context–object discrimination, but not spatial, memory: Evidence for selective disruption of specific hippocampus-dependent memory functions during acute neuroinflammation. *Brain Behav Immun.* 2015;44:159–66. Available from: <http://dx.doi.org/10.1016/j.bbi.2014.09.014>
41. Donovan J, Brown P. Blood Collection. *Curr Protoc Neurosci.* 2005;33(1):4.
42. McCutcheon JE, Marinelli M. Age matters. *Eur J Neurosci.* 2009;29(5):997–1014.
43. NCD Risk Factor Collaboration (NCD-RisC). Height and body-mass index trajectories of school-aged children and adolescents from 1985 to 2019 in 200 countries and territories: a pooled analysis of 2181 population-based studies with 65 million participants. *Lancet.* 2020;396(10261):1511–24.
44. Kinoshita D, Wagner D, Cohn H, Costa-pinto FA, Sá-rocha LC De. Behavioral effects of LPS in adult , middle-aged and aged mice. *Physiol Behav.* 2009;96(2):328–32. Available from: <http://dx.doi.org/10.1016/j.physbeh.2008.10.018>
45. Marmendal M, Eriksson CJP, Fahlke C. Early deprivation increases exploration and locomotion in adult male Wistar offspring. *Pharmacol Biochem Behav.* 2006;85:535–44.
46. Dantzer R. Innate immunity at the forefront of psychoneuroimmunology. *Brain Behav Immun.* 2004;18:1–6.


47. Yirmiya R, Rosen H, Donchin O, Ovadia H. Behavioral effects of lipopolysaccharide in rats: involvement of endogenous opioids. *Brain Res.* 1994;648:80–6.
48. Stanford Behavioral and Functional Neuroscience Laboratory. Y-maze Standard Operating Procedure.
49. Biala MAG. The novel object recognition memory: neurobiology, test procedure, and its modifications. 2012;93–110.
50. Solomon N, Salvador F. Hippocampus: Anatomy and functions. KenHub. 2020.
51. Zhanmu O, Yang X, Gong H, Li X. Paraffin-embedding for large volume bio-tissue. *Sci Rep.* 2020;(0123456789):1–8. Available from: <https://doi.org/10.1038/s41598-020-68876-5>
52. Papp E, Leergaard T, Calabrese E, Johnson G, Bjaalie J. Waxholm Space atlas of the Sprague Dawley rat brain [Internet]. *NeuroImage.* 2014 [cited 2019 Jul 13]. Available from: <https://scalablebrainatlas.incf.org/rat/PLCJB14>
53. Llorens-Martin M, Blazquez-Llorca L, Benavides-Piccione R, Rabano A, Hernandez F, Avila J, DeFelipe J. Selective alterations of neurons and circuits related to early memory loss in Alzheimer's disease. *Front Neuroanat.* 2014;8(38).
54. Garman RH. Histology of the Central Nervous System. *Toxicol Pathol.* 2011;39(22–35).
55. Lakhan SE. Alzheimer Disease. *Medscape.* 2021.
56. Cai Z, Hussain MD, Yan L-J. Microglia, neuroinflammation, and beta-amyloid protein in Alzheimer's Disease. *Int J Neurosci.* 2014;124(5):307–21.
57. Wang L-M, Wu Q, Kirk RA, Horn KP, Ebada Salem AH, Hoffman JM, Yap JT, Sonnen JA, Towner RA, Bozza FA, Rodrigues RS, Morton KA. Lipopolysaccharide endotoxemia induces amyloid- β and p-tau formation in the rat brain. *Am J Nucl Med Mol Imaging.* 2018;8(2):86–99. Available from: <http://www.ncbi.nlm.nih.gov/pubmed/29755842>
<http://www.pubmedcentral.nih.gov/articlerender.fcgi?artid=PMC5944824>
58. Morley JE, Farr SA, Nguyen AD, Xu F. What is the physiological function of Amyloid-

- Beta Protein? *J Nutr Health Aging*. 2019;23:225–6.
59. Angevin Jr JB. *Encyclopedia of the Human Brain*. 2002. 313–371 p.
 60. François A, Terro F, Quellerd N, Fernandez B, Chassaing D, Janet T, Bilan AR, Paccalin M, Page G. Impairment of autophagy in the central nervous system during lipopolysaccharide-induced inflammatory stress in mice. *Mol Brain*. 2014;7(56).
 61. Savage J, St-Pierre M-K, Hui CW, Tremblay M-E. Microglial Ultrastructure in Hippocampus of a Lipopolysaccharide-Induced Sickness Mouse Model. *Front Neurophysiol*. 2019;13(1340).
 62. Wang W, Zhao F, Ma X, Perry G, Zhu X. Mitochondria dysfunction in the pathogenesis of Alzheimer's disease: recent advances. *Mol Neurodegener*. 2020;15:30.
 63. Swerdlow RH. Mitochondria and Mitochondrial Cascades in Alzheimer's Disease. *J Alzheimer's Dis*. 2018;62(3):1403–16.
 64. Wang X, Wang W, Li L, Perry G, Lee H, Zhu X. Oxidative stress and mitochondrial dysfunction in Alzheimer's disease. *Biochim Biophys Acta - Mol Basis Dis*. 2014;1842(8):1240–7.
 65. Cenini G, Voos W. Mitochondria as Potential Targets in Alzheimer Disease Therapy: An update. *Front Pharmacol*. 2019;10(902).
 66. Li J-Q, Yu J-T, Jiang T, Tan L. Endoplasmic reticulum dysfunction in Alzheimer's disease. *Mol Neurobiol*. 2015;51(1):385–95.
 67. Hashimoto S, Saido TC. Critical review: involvement of endoplasmic reticulum stress in the aetiology of Alzheimer's disease. *Open Biol*. 2018;8(4).
 68. Roussel BD, Kruppa AJ, Miranda E, Crowther DC, Lomas DA, Marciniak SJ. Endoplasmic reticulum dysfunction in neurological disease. *Lancet Neurol*. 2013;12(1):105–18.
 69. Xu TT, Zhang Y, He JY, Luo D, Luo Y, Wang YJ, Liu W, Wu J, Zhao W, Fang J, Guan L, Huang S, Wang H, Lin L, Zhang SJ, Wang Q. Bajijiasu Ameliorates β -Amyloid-Triggered Endoplasmic Reticulum Stress and Related Pathologies in an Alzheimer's Disease

- Model. *Cell Physiol Biochem*. 2018;46(1):107–17.
70. Zhu P, Li J, Fu X, Yu Z. Schisandra fruits for the management of drug-induced liver injury in China: A review. *Phytomedicine*. 2019;59(November 2018):152760. Available from: <https://doi.org/10.1016/j.phymed.2018.11.020>
71. Song L, Piao Z, Yao L, Zhang L, Lu Y. Schisandrin ameliorates cognitive deficits, endoplasmic reticulum stress and neuroinflammation in streptozotocin (Stz)-induced alzheimer's disease rats. *Exp Anim*. 2020;69(3):363–73.
72. Oliveira MM, Lourenco M V., Longo F, Kasica NP, Yang W, Ureta G, Ferreira DDP, Mendonça PHJ, Bernales S, Ma T, De Felice FG, Klann E, Ferreira ST. Correction of eIF2-dependent defects in brain protein synthesis, synaptic plasticity, and memory in mouse models of Alzheimer's disease. *Sci Signal*. 2021;14(668).
73. Biorender.

Appendix 1

Ethical Clearance



UNIVERSITEIT VAN PRETORIA
UNIVERSITY OF PRETORIA
YUNIBESITHI YA PRETORIA

Faculty of Health Sciences

Institution: The Research Ethics Committee, Faculty Health Sciences, University of Pretoria complies with ICH-GCP guidelines and has US Federal wide Assurance.

- FWA 00002567, Approved dd 22 May 2002 and Expires 03/20/2022.
- IORG #: IORG0001762 OMB No. 0990-0279 Approved for use through February 28, 2022 and Expires: 03/04/2023.

29 May 2020

**Approval Certificate
New Application**

Ethics Reference No.: 182/2020
Title: The potential neuroprotective effect of Manuka honey in Sprague-Dawley rats with lipopolysaccharide induced neuro-inflammation

Dear Miss VS Verrall

The **New Application** as supported by documents received between 2020-03-16 and 2020-05-27 for your research, was approved by the Faculty of Health Sciences Research Ethics Committee on its quorate meeting of 2020-05-27.

Please note the following about your ethics approval:

- Ethics Approval is valid for 1 year and needs to be renewed annually by 2021-05-29.
- Please remember to use your protocol number (182/2020) on any documents or correspondence with the Research Ethics Committee regarding your research.
- Please note that the Research Ethics Committee may ask further questions, seek additional information, require further modification, monitor the conduct of your research, or suspend or withdraw ethics approval.

Ethics approval is subject to the following:


- The ethics approval is conditional on the research being conducted as stipulated by the details of all documents submitted to the Committee. In the event that a further need arises to change who the investigators are, the methods or any other aspect, such changes must be submitted as an Amendment for approval by the Committee.

Additional Conditions:

- Approval is conditional upon the Research Ethics Committee receiving approval from AEC.

We wish you the best with your research.

Yours sincerely



Dr R Sommers
MBChB MMed (Int) MPharmMed PhD
Deputy Chairperson of the Faculty of Health Sciences Research Ethics Committee, University of Pretoria

The Faculty of Health Sciences Research Ethics Committee complies with the SA National Act 61 of 2003 as it pertains to health research and the United States Code of Federal Regulations Title 45 and 46. This committee abides by the ethical norms and principles for research, established by the Declaration of Helsinki, the South African Medical Research Council Guidelines as well as the Guidelines for Ethical Research: Principles Structures and Processes, Second Edition 2015 (Department of Health).

Research Ethics Committee
Room 4-80, Level 4, Tavelopele Building
University of Pretoria, Private Bag x323
Gezina 0031, South Africa
Tel +27 (0)12 358 3084
Email: deepika.behari@up.ac.za
www.up.ac.za

Fakulteit Gesondheidswetenskappe
Lefapha la Disaense tsa Maphelo

Appendix 2

MSC committee Approval Letter



MSc Committee
School of Medicine
Faculty of Health Sciences

MSc Committee
7 May 2019

Dr J Bester
Department of Physiology
Faculty of Health Sciences

Dear Dr,

Ms V Verrall, Student no 15048200

Please receive the following comments with reference to the MSc Committee submission of the abovementioned student:

Student name	Ms Victoria Verrall	Student number	15048200
Name of study leader	Dr Janette Bester		
Department	Physiology		
Title of MSc	The potential neuroprotective effect of Fynbos honey in aged Sprague Dawley rats with lipopolysaccharide induced neuro-inflammation		
Date of first submission	April 2019		
Comments to study leader April 2019	<ul style="list-style-type: none"> • Please revise the aim and objectives. It should link on to the title. The objectives need to be reduced, focused and linked to the study and include how it will be done. • Please remove referencing from the executive summary. • The standardized model for Alzheimer's disease needs to be clarified. Is this a recognized model? • Please remove the hypothesis. • Referencing needs correction and consistency. • Please expand on the statistical analysis. • Please correct all grammar errors. • Consider another route of administration as peritoneal route can be problematic. • Please also be advised to submit an application to the Animal Ethics committee. 		
May 2019	<ul style="list-style-type: none"> • Thank you for submitting the revised protocol. 		

MSc Committee, School of Medicine
Faculty of Health Sciences
University of Pretoria,
Private Bag X323
Pretoria 0001, South Africa
Tel +27 (0)12 319 2325
Fax +27 (0)12 323 0732

Fakulteit Gesondheidswetenskappe
Lefapha la Disaense tša Maphelo

Appendix 3

University of Witwatersrand Ethical Clearance

Central Animal Services

Faculty of Health Sciences, 7 York Road, Parktown, 2193, South Africa • Tel: +27 11 717 1300 • Fax: +27 11 717 2199



20 February 2020

To whom it may concern,

Victoria Verrall, under the supervision of Dr Janette Bester, has been given ethical clearance (clearance number 2109/07/44/C) through the Animal Ethics Committee of the University of Witwatersrand to carry out her study on SD rats in the Central Animal Service unit in the medical school of the university.

Any further questions regarding this study may be addressed to Dr K Jardine or Sr A Rammekwa of the Central Animal Service.

Regards

Dr K Jardine



Director: Central Animal Service

011 71701301

Kimberly.jardine@wits.ac.za

Appendix 4

Central Animal Services Competency certificate

<p>UNIVERSITY OF THE WITWATERSRAND, JOHANNESBURG</p> 	<p>ANIMAL RESEARCH ETHICS COMMITTEE Registration number: AREC-101210-002</p>
<p>CERTIFICATE OF ATTENDANCE Researcher Orientation Course</p>	
<p>Course Contents:</p> <ul style="list-style-type: none">• Legislation and Regulations• Ethics• Welfare• Responsibilities in Research• Habituation and Handling• Bio-Security• Security	
<p>Victoria Verrall attended the course held on 22/10/2019 at Central Animal Service.</p>	
 Geoffrey Candy Chair : Animal Research Ethics Committee University of the Witwatersrand	 Dr. Kimberley Jardine Director: Central Animal Service University of the Witwatersrand

Appendix 5

Ethics Renewal



**Faculty of Veterinary Science
Animal Ethics Committee**

6 October 2021

**Approval Certificate
Annual Renewal
(EXT1)**

AEC Reference No.: 182/2020
Title: The potential neuroprotective effect of Manuka honey in Sprague-Dawley rats with lipopolysaccharide induced neuro-inflammation
Researcher: Miss VS Verrall
Student's Supervisor: Dr J Bester

Dear Miss VS Verrall,

The **Annual Renewal** as supported by documents received between 2021-09-13 and 2021-10-01 for your research, was approved by the Animal Ethics Committee on its quorate meeting of 2021-10-01.

Please note the following about your ethics approval:

1. The use of species is approved:

Species and Samples	Number Available
Rats (Sprague Dawley)	60

2. Ethics Approval is valid for 1 year and needs to be renewed annually by 2022-10-06.
3. Please remember to use your protocol number (182/2020) on any documents or correspondence with the AEC regarding your research.
4. Please note that the AEC may ask further questions, seek additional information, require further modification, monitor the conduct of your research, or suspend or withdraw ethics approval.
5. **All incidents** must be reported by the PI by email to Ms Marleze Rheeder (AEC Coordinator) within 3 days, and must be subsequently submitted electronically on the application system within 14 days.
6. The committee also requests that you record major procedures undertaken during your study for own-archiving, using any available digital recording system that captures in adequate quality, as it may be required if the committee needs to evaluate a complaint. However, if the committee has monitored the procedure previously or if it is generally can be considered routine, such recording will not be required.

Ethics approval is subject to the following:

- The ethics approval is conditional on the research being conducted as stipulated by the details of all documents submitted to the Committee. In the event that a further need arises to change who the investigators are, the methods or any other aspect, such changes must be submitted as an Amendment for approval by the Committee.

Room 6-13, Arnold Theiler Building, Onderstepoort
Private Bag X04, Onderstepoort 0110, South Africa
Tel +27 12 529 8434
Fax +27 12 529 8321
Email: marleze.rheeder@up.ac.za

Fakulteit Veeartsenykunde
Lefapha la Diseanse tsa Bongakadiruiwa

Appendix 6

Animal Welfare Monitoring Sheet

Central Animal Service		Forms and Records #: FR-SL.WM003:Cgroup STUDY LOG: WELFARE MONITORING Category C: Group						UNIVERSITY OF THE WITWATERSRAND. JOHANNESBURG	
PI NAME:		AREC#:							
PROCEDURE/ INTERVENTION		DATE:							
	Day: AM	PM	ID#:	Day: AM	PM	ID#:	Day: AM	PM	ID#:
UNDISTURBED OBSERVATION	comment								
Eating and drinking: Yes, No									
Posture: Normal, Huddled									
Mood: Calm, Restless, Lethargic, Depressed									
Movement: Normal, Hunched									
Fur: Groomed, Ruffled									
Breathing: Normal, Laboured, gasping									
Face: See Grimace scale									
Vocalisation: None, whimper									
CAGE OPEN/ HANDLING	comment								
Alert/ Inquisitive, Avoidance									
Approachable, Aggressive, Fear									
Diarrhoea, Blood on bedding									
CLINICAL SIGNS	comment								
Eyes: Bright, Red rimmed, Dim									
Nose: Clean, Discharge									
Skin: Firm elastic, Tented dry									
Intervention site: Clean, Inflamed, oozing, blood									
Self- Mutilation: Chew, bite, scratch self									
Body mass: Same, Gain, Loss									
OTHER OBSERVATION/ COMMENT									

Observations TWICE per day: Record animal ID in line when recording of abnormality/ concern

Score: 0 Normal; 1 Mild 2 Moderate; 3 Severe

Actions to take: 0- 1 Record
2 Record, REPORT and observe more often
3 Record, REPORT and evaluate for humane termination

Developed by: M Costello
Checked by: K Jardine 2018/12/18Version #: 001
AREC Approval: Click or tap to enter a date.

Appendix 7

Plagiarism report

Thesis			
ORIGINALITY REPORT			
14%	10%	9%	%
SIMILARITY INDEX	INTERNET SOURCES	PUBLICATIONS	STUDENT PAPERS
PRIMARY SOURCES			
1	repository.up.ac.za Internet Source		3%
2	pamstories.weebly.com Internet Source		1%
3	Yousef Sawikr, Nagendra Sastry Yarla, Ilaria Peluso, Mohammad Amjad Kamal, Gjumrakch Aliev, Anupam Bishayee. "Neuroinflammation in Alzheimer's Disease", Elsevier BV, 2017 Publication		1%
4	Andrew E. Budson, Paul R. Solomon. "Alzheimer's Disease Dementia and Mild Cognitive Impairment Due to Alzheimer's Disease", Elsevier BV, 2016 Publication		1%
5	link.springer.com Internet Source		1%
6	www.ncbi.nlm.nih.gov Internet Source		<1%
7	worldwidescience.org Internet Source		<1%